PhD Thesis 2019

Beatriz Sobradillo Benguría

eman ta zabal zazu
Universidad del País Vasco
Euskal Herriko Unibertsitatea

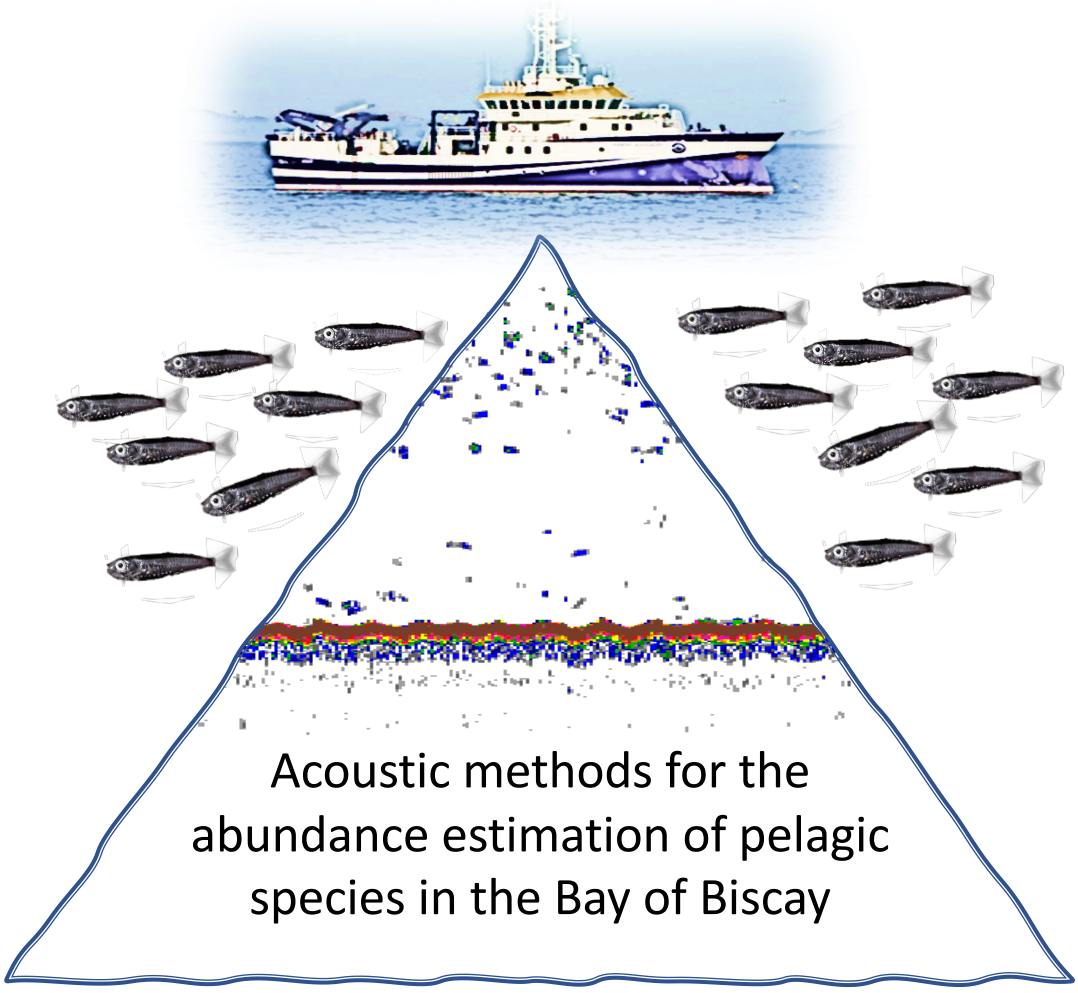

Acoustic methods for the abundance estimation of pelagic species in the Bay of Biscay

eman ta zabal zazu
Universidad del País Vasco
Euskal Herriko Unibertsitatea
azti tecnalia

Acoustic methods for the abundance estimation of pelagic species in the Bay of Biscay

Presented by

Beatriz Sobradillo Benguría

Thesis directors

Dr. Guillermo Boyra Eizaguirre

Dr. Xabier Irigoien Larrazabal

Department

Zoology and Animal Cell Biology

PhD Program

Marine Environment and Resources (MER-EHU)

December 2019

A Noa

TABLE OF CONTENTS

Acknowledgements - Agradecimientos

Quiero dedicar las primeras líneas de mi agradecimiento al responsable de que haya llegado a la meta de esta carrera de fondo y que, además de mi gran guía durante toda la tesis, ha acabado siendo un gran compañero y amigo. Gracias Guillermo. Gracias por haber tenido confianza en mí desde la primera vez que entré en AZTI, por haberme introducido en el mundo de la acústica de manera que no se me atragantase, y por haberme enseñado a pensar y trabajar como una científica, ya sea en tierra o en la mar. Todo ello ha sido inmejorable gracias a tu paciencia y buen humor, pero sobre todo gracias a tu pasión por lo que haces y a tu facilidad para contagiarla.

Poco antes de sumergirme en esta etapa compartí un café muy fructífero y decisivo con Unai Cotano, quien me animó a aprovechar esta oportunidad de meterme en el mundo de la ciencia, y "apretarme el cinturón durante un tiempo". Gracias Unai, sin duda ha sido todo un reto (ahora puedo decir), logrado.

Gracias a la Fundación AZTI por haberme concedido la beca predoctoral para empezar mi carrera como científica. A la Universidad del País Vasco, en especial a Ionan Marigómez y Manu Soto, ya que desde vuestro *txokito* en la playa de Plentzia nos dais a muchos las primeras bases para mojarnos en el mundo de la ciencia.

También quiero agradecer a Xabier Irigoien que, como director, siempre ha estado disponible para aportar ideas, dar consejos y transmitirme apoyo. A Paula Álvarez y María Santos, por llevarme a vuestras campañas y enseñarme tantas cosas, no sólo sobre la caballa o huevos de anchoa, sino también sobre cómo los niños sobreviven cuando su madre se va a la mar.

Ésto me lleva a agradecer a todos los *juvenos* por los buenos momentos que me habéis hecho pasar tanto en la sala de acústica, como en cubierta o en el salón viendo pelis (¡aunque algunas fueran malísimas!): a Deniz, con quien compartí camarote en mi primer embarque, y mis sucesivas compañeras: Carlota Pérez, Amaia Astarloa, Carmen Abaroa, Marian Peña, Silvia Rodríguez y Esther Velasco. A Toño por hacernos reír a todos cuando la rutina ya se apoderaba de nuestro ser, a Gaizka Bidegain, Xiker, Ainhoa Arévalo, Bea Beldarrain, Inma Martín, María Korta, Iñaki Rico, Arkaitz Pedrajas, Iñaki Oyarzabal, Maite Cuesta… a todos los que habéis compartido ratitos conmigo en el barco, ¡gracias!

No me olvido de una parte importantísima en los embarques: la tripulación, desde el piso arriba donde se preparaban unos cafés muy bienvenidos, pasando por los marineros y cocineros, siempre con una sonrisa o una canción con la que alegrar los pasillos.

Y día a día, gracias a todos los doctorandos que habéis compartido conmigo sala (Kemal, Miren, Aitor, Igor, Blanca, Sarai, Iraide, Ainhoa, Unai, Ruairi, Oihane(s), Maite…) o zona naranja (Isa, Amaia, Iván), además de algún que otro baile. Sin olvidarme de lo bien que me acogían en Derio y Sukarrieta las veces que he pasado por ahí. A Andrés Uriarte que, por extensión, sería el abuelo de esta tesis, Pablo Carrera, Enrique Nogueira y Marian Peña, por esas charlas acústicas tanto en el barco como en los grupos de trabajo.

Un gracias especial al equipo de la A8, por compartir ojeras, batallitas, risas, buena música… y kilómetros: Javi, Ainhize, Iratxe, Joana, Maddi, Oihane, María… ¡aún me queda invitaros al desayuno de despedida! Ah, y repito gracias a María Calvo por donarme una silla para trabajar en casa sin romperme la espalda, y por tantas otras cosas con las que llenaría hojas y hojas de palabras.

A Udane Martínez, la jefa secreta del equipo de acústica, y a Jon Uranga por haberme ayudado con mis dudas e incertidumbres siempre que lo he necesitado. Ha sido un placer formar parte del equipo de AZTI durante este tiempo y cruzarme con un montón de gente estupenda a quien me alegro de haber conocido.

Quiero agradecer también a unos cuantos revisores anónimos que (no tras poca batalla) han hecho que mejorara la calidad de mi trabajo. A Matthias Schindler por sus sabios consejos y valiosos comentarios en esta última etapa de la tesis.

Sin duda estos 4 años han tenido muy buenos momentos, pero también los ha habido regulares en los que he necesitado una dosis extra de apoyo y consejos. Y ahí estabais siempre vosotros, mi familia: Laura y Carlos, Iñigo e Izaskun, María y Boki, y todos los pequeños duendecillos que rondan a nuestro alrededor. A mis tías, Clara y Nieves y, por supuesto, detrás de todo, mis padres: gracias por estar **siempre** ahí y ayudarme a mantener el equilibrio. Habéis sido una pieza clave en todo ésto.

A mis gurús, Asun y Ana, y a las que en algún momento me habéis recordado que *todos los días sale el sol* (Alex, Gaby, Ipi, Patron, Chopo y Jess). A mis hermanas *turmarinas* por tirarme siempre "pal sur" en busca de sol, viento y buenos momentos para recargar pilas (Maibe, Belén, Lucía y Lena). A mis grandes vecinos (Giuli y Carlos, Elena, Ainhoa, Gix, Jose, Ane, Jimena, Leire y Eduardo) por compartir pizzas y noches de cine conmigo, aunque me quedase dormida.

A tí Iru, por hacerme viajar sin moverme del sitio y recordarme que “en el peor de los casos, siempre se puede publicar en *Jara y Sedal*”. Menos mal, no me ha hecho falta.

Y guardo estas últimas líneas para tí, NOA, que has tenido que vivir muy de cerca los días de nervios, pero que siempre me has hecho mantener el rumbo y valorar el tiempo juntas.

GRACIAS POR TUS SONRISAS.

Es un placer mirar atrás y hacer recuento de toda la gente que de alguna manera me ha aportado su granito de arena.

Eso que me llevo.

Scientific contributions

Publications

This thesis is based on five scientific works published or in the process to be published in scientific peer-reviewed journals:

1. Boyra, G., Moreno, G., **Sobradillo, B.**, Pérez-Arjona, I., Sancristobal, I. and Demer, D. A., (2018). Target strength of skipjack tuna (*Katsuwanus pelamis*) associated with fish aggregating devices (FADs). ICES Journal of Marine Science, 75: 1790–1802. https://doi.org/10.1093/icesjms/fsy041

In this first work I contributed to create, develop and maintain the R scripts containing the *TS* analysis methodology and multiple *TS* filtering analyses that were applied on a tuna species (skipjack) but were afterwards tested and applied in this thesis.

2. Boyra, G., Moreno, G., Orue, B., **Sobradillo, B**., and Sancristobal, I. (2019). In situ target strength of bigeye tuna (*Thunnus obesus*) associated with fish aggregating devices. ICES Journal of Marine Science. https://doi.org/10.1093/icesjms/fsz131

In the second paper, we further improved the *TS* analysis and *TS* filtering methodology developed for skipjack tuna, now applied to a different tuna species (bigeye) and using further refined analysis where multiple targets filtering was based on an improve HD filtering rather process rather than multifrequency simultaneity.

3. **Sobradillo, B**., G. Boyra, U. Martinez, P. Carrera, M. Peña, and X. Irigoien, (2019). Target Strength and Swimbladder Morphology of Mueller's Pearlside (Maurolicus Muelleri). *Scientific Reports* 9, no. 1: 1–14. https://doi.org/10.1038/s41598-019-53819-6

This third work contains analyses involving *TS* measurements, processing and interpretation on Mueller's pearlside. Concerning *TS* processing, we applied the methodology developed for tuna, adapted to better suit the smaller size of this species. It also included the exhaustive determination of the morphology of pearlside swimbladder based on X-Rays, and the development of a set of scripts to simulate pearlside backscattering using a prolate spheroid model.

4. **Sobradillo, B**., and Boyra, G. (*submitted*). *In situ* and ex *situ* target strength (TS) measurements of European anchovy (*Engraulis encrasicolus)* in the Bay of Biscay.

In this work, in addition to apply the *TS* analysis methodology developed in the previous works to an extensive number of in situ and ex situ set of acoustic recording of anchovy, a nouvelle backscattering model was also applied to be able to accurately simulate the particular morphology of anchovy's swimbladder.

5. Alvarez, P., **Sobradillo, B.,** Aldanondo, N., Boyra, G., Iñarra, B., Martinez, U. (*in prep*). Biology, distribution, acoustic abundance and vertical diel of pearlside *Maurolicus muelleri* (Gmelin, 1789).

The last paper focuses on the application of the *TS* measurements done on Mueller's pearlside by computing tentative abundance, spatial distribution and nictemeral migrations of pearlside in the Bay of Biscay.

<u>Oral communications</u>

During this thesis, the work done was periodically presented in various national and international working groups and congresses:

- ICES Working Group on Acoustic and Egg Surveys (WGACEGG, 2018) *Ex situ TS* measurements of European anchovy in a harbor cage.
- ISOBAY XVI International Symposium on Oceanography of the Bay of Biscay (2018) Acoustic methods for estimating biomass of mesopelagic species *Maurolicus muelleri.*
- 11th International Postgraduate Course Research in Marine Environment & Resources (2017) Understanding frequency response of *Maurolicus muelleri* in the Bay of Biscay. **Sobradillo B.**
- ICES Working Group on Acoustic and Egg Surveys (WGACEGG; 2017, Cádiz) Análisis de *TS* y respuesta en frecuencia de *Maurolicus muelleri* y *Engraulis encrasicholus*. **Sobradillo B**., Boyra G, Pérez-Arjona I.
- WGFAST (2016, Vigo) Working Group on Fisheries Acoustics Science and

Technology

Acoustic estimation of the nycthemeral variability, of pelagic ichthyofauna and plankton abundance in the Bay of Biscay. **Sobradillo B.,** Santos M., Uriarte A., Boyra G

- SEA-Tecniacústica (2015, Valencia) Sociedad Española de Acústica

  Estimación acústica de las abundancias de plancton e ictiofauna pelágicos en el Golfo de Bizkaia. **Sobradillo B.,** Santos M., Uriarte A., Boyra G

- 9th International Postgraduate Course Research in Marine Environment & Resources (2015) Acoustic methods for biomass estimation of pelagic species in the Bay of Biscay. **Sobradillo B.**

List of tables

List of figures

Summary

The Bay of Biscay shelters a large and diverse pelagic community of exploited species that require of direct assessment methods to determine the Total Allowable Catch (TAC) fishing quotas. Particularly, European anchovy (*Engraulis encrasicolus)* supports profitable fisheries for both the Spanish and French fleets, making it one of the most valuable commercial species of the area. Other species such as Mueller´s pearlside (*Maurolicus muelleri)* have arisen increasing interest in their commercial exploitation, urging the development of assessment methods focused on their future potential exploitation.

Acoustic surveys are particularly well suited for quantification of distribution and abundance of pelagic species. They have become one of the most widely used methods for fish stock abundance estimation, and now form an important part of routine stock management all over the world. The main acoustic parameter needed to convert the acoustic energy into numerical abundance is the target strength (*TS*; [dB re 1 m^2]), which is based on species-specific single target detections.

Generally, *in situ TS* measurements are assumed to deliver the most accurate results, if collected with concurrent reliable biological samples and tilt angle information. However, measuring *TS* of fish in their natural environment implies dealing with some difficulties, some of which derive from their small size and densely packed aggregative distribution. To allow more control of the abundance and ensure isolation of target species, *ex situ* experiments can be conducted under controlled environmental conditions. Unfortunately, these experiments pose some concerns that can introduce bias in the *TS* measurements. One of them is that the fish behavior may be altered due to the unnatural conditions in which they are immersed, resulting in biased *TS* measurements. Another issue is related to the short-range measurements that are commonly obtained from cage experiments. At distances too close from the signal source (i.e. inside the near-field), the wave front is not completely formed leading to biased measurements of target strength.

Finally, when the biological properties of the targets are known, the acoustic properties of the whole fish or body components can be estimated using theoretical models to verify or extend the empirical *TS* measurements.

The elaboration of this thesis was motivated by the lack of unbiased *TS* values for European anchovy and Muller´s pearlside, necessary to deliver accurate estimates of abundance by means of acoustic methods.

In the case of anchovy, there are some methodological inconsistencies related to the target strength value currently used for the estimation of anchovy abundance in the Bay of Biscay. First, different values are used by different surveys, and second, none of these values is specific for anchovy. A combination of *ex situ* and *in situ* measurements were utilised at three frequently used acoustic frequencies, including the one used for assessment. *In situ* data were collected during night pelagic trawls in two different seasons along 7 years of study. A backscattering model for physostome fish, where the swimbladder was simulated as a two chambered prolate spheroid, was used to help interpret the results. The obtained *TS* values were -44.6 (±2.3), -46.9 (±3) and -48.4 (±2.7) dB at 38, 120 and 200 kHz respectively, which, for the 3.5-19.5 cm long anchovies studied, yielded b_{20} values of -66.5, -68.7 and -70.4 dB. The results were rather consistent among seasons and among *in situ* and *ex situ* conditions, obtaining significant *TS*-length positive relationships for all frequencies. This research is part of a series of efforts planned to obtain a comprehensive *TS* versus length relationship to update the acoustic assessment methodology of European anchovy in the Bay of Biscay.

The target strength of pearlside was estimated for the first time at five frequencies commonly used in acoustic surveys. Its relationship with fish length (b_{20}) was also determined. Biomass estimates of pearlside in the Bay of Biscay during the four years of study (2014–2017) are given using the 38 kHz frequency. Morphological measurements of the swimbladder were obtained from soft X-ray images and used in the backscattering simulation of a gas-filled ellipsoid. Pearlside is a physoclist species, which means that they can compensate the swimbadder volume against pressure changes. However, the best fit between the model and the experimental data showed that they lose that capacity during the trawling process, when the swimbladder volume is affected by Boyle´s law.

I organised this research work following the traditional monograph structure, divided into the following five chapters:

In **Chapter 1**, *Introduction*, I first present the general context of the research, describing the state of the art of the fisheries in the Bay of Biscay with specific focus on European anchovy and Muller´s pearlside. Then, I described the aim and specific objectives of the thesis, which are divided into the following sections: *TS* measurements, *TS* processing, *TS* interpretation and *TS* application.

In **Chapter 2**, *Background*, I included a general overview on how acoustic methods are applied to fisheries management, followed by a description of the main acoustic principles and definitions, necessary to understand the content of this research.

Chapter 3*, Material and methods,* includes a methodological description of the *in situ, ex situ* and modelling techniques, including all the experiments performed to reduce potential biases associated to sampling, analysis and post-processing procedures. This chapter has been structured following the sections described in Chapter 1.

Chapter 4, *Results,* presents the results of this thesis grouped by species: Mueller´s pearlside and European anchovy, respectively.

In **Chapter 5***, Discussion and conclusions,* I present a general discussion on the results obtained, following the structure presented in chapters 1 and 3. Strengths and weaknesses of the methodologies are discussed, focussing on their contribution to a sustainable stock assessment of two pelagic species in the Bay of Biscay. Finally, I summarized the main conclusions derived from this thesis.

Resumen

El Golfo de Bizkaia alberga una gran variedad de especies pelágicas de gran interés comercial, que han de ser gestionadas mediante métodos directos para determinar la captura total permitida (TAC por sus siglas en inglés; total allowable catch) y las cuotas de esfuerzo. En concreto, la anchoa europea (*Engraulis encrasicolus)* supone una pesca rentable para las flotas española y francesa, convirtiéndola en una de las especies comerciales más valiosas de la zona. Otras especies como la anchoa de fondo (*Maurolicus muelleri)* han despertado un interés creciente en su explotación comercial, instando al desarrollo de métodos de evaluación centrados en su potencial explotación.

Las campañas acústico-pesqueras son particularmente adecuadas para la cuantificación de la distribución y abundancia de especies pelágicas. En los últimos años se han convertido en uno de los métodos más utilizados para la estimación de la abundancia de las poblaciones de peces, y ahora forman una parte importante de la gestión rutinaria de los *stocks* en todo el mundo.

El parámetro acústico que se necesita para convertir la energía acústica en abundancia numérica es la fuerza del blanco (*TS* por sus siglas en inglés; target strength [dB re 1 m^2]), que se basa en detecciones de blancos individuales y es específico para cada especie.

El *TS* se puede determinar tanto teórica como empíricamente. El *TS* determinado empíricamente puede ser medido en condiciones naturales (*in situ*) o en un ambiente controlado (*ex situ).* En general, se supone que las mediciones de *TS in situ* proporcionan los resultados más precisos, sin embargo, medir el *TS* de peces en su entorno natural implica lidiar con algunas dificultades mayormente derivadas de su pequeño tamaño y de su tendencia a agregarse en densidades altas. Las condiciones ideales para estimar el valor del *TS in situ* son:

- Que la agregación sea monoespecífica con peces de tamaño y condición parecida.
- Que la densidad promedio de la agregación sea baja (menos de 1 individuo por volumen de reverberación) y sigan una distribución aleatoria para poder ser detectados como ecos individuales.

- Que la distancia entre la plataforma y la agregación muestreada sea pequeña para poder minimizar el volumen de muestreo y la longitud del pulso.
- Que la distancia entre la plataforma y la agregación muestreada sea mayor que el campo cercano para que los frentes de onda sean paralelos y la intensidad de la onda varíe proporcionalmente al cuadrado de la distancia, según la regla de la presión inversa.
- Que el haz de la ecosonda sea estrecho y la longitud del pulso corta para minimizar el volumen de muestreo.
- Que se recojan evidencias alternativas a las detecciones acústicas (generalmente mediante pescas o registros ópticos).
- Que las condiciones ambientales se asemejen, en la medida de lo posible, a las que tendrán lugar durante los muestreos acústico-pesqueros destinados a estudios de evaluación.

Los experimentos *ex situ* ofrecen la ventaja de poder tener más control sobre la abundancia y asegurar así, un buen aislamiento de la especie objetivo, sin embargo, estos experimentos se realizan en un entorno que no es el natural para los peces, y su comportamiento puede verse alterado sesgando, en consecuencia, las mediciones de *TS.* Otro problema de los experimentos *ex situ* está relacionado con las mediciones de corto alcance ya que se ven afectadas por el efecto el campo cercano. A distancias demasiado próximas a la fuente de la señal, el frente de onda no está completamente formado, por lo que las mediciones de *TS* no son fiables. Finalmente, cuando se conocen las propiedades biológicas de la especie de interés, se pueden estimar las propiedades acústicas del pez entero o de alguno de sus componentes, utilizando modelos teóricos para verificar o ampliar las mediciones empíricas de *TS*. Durante los últimos años, se han desarrollado una gran variedad de modelos numéricos y analíticos, por lo que es imprescindible valorar las ventajas y limitaciones de cada modelo antes de hacer una selección.

En esta tesis, la determinación del *TS* de la anchoa de fondo y anchoa europea se ha realizado mitigando previamente los errores derivados de las mediciones de *TS* en condiciones no ideales, mediante los siguientes procedimientos:

- Se ha reducido el error asociado a la detección de ecos múltiples:
    - Usando datos nocturnos en todos los experimentos
    - Aplicando un filtro de densidades altas en los datos registrados *in situ*
    - Controlando la variación del *TS* promedio a distintos volúmenes del pulso de sonido en las mediciones *ex situ*
- Se ha corregido el sesgo derivado de las mediciones de corto alcance de las mediciones *ex situ*
- Se ha comprobado la capturabilidad de todo el rango de tallas de anchoa de fondo usando distintos tamaños de malla
- Se ha determinado la morfología de la vejiga natatoria de las dos especies objetivo para aplicarla en los modelos teóricos
- Se ha descrito el comportamiento de la vejiga natatoria de la anchoa de fondo durante el proceso de pesca, comparándolo con el comportamiento derivado de los modelos teóricos, bajo distintas asunciones de ángulo de inclinación de la vejiga y tasas de contracción.

La elaboración de esta tesis fue motivada por la falta de valores de *TS* específicos, no sesgados necesarios para proporcionar estimas precisas de abundancia de la anchoa de fondo y la anchoa europea, mediante métodos acústicos. Los análisis se han realizado a partir de datos obtenidos de dos campañas enfocadas a la evaluación de la anchoa en el Golfo de Bizkaia: BIOMAN, basada en el método de la producción diaria de huevos, y JUVENA, enfocada a la estima de abundancia de la anchoa juvenil mediante métodos acústicos.

En esta tesis se ha estimado por primera vez el *TS* de la anchoa de fondo, en 5 frecuencias comúnmente utilizadas en estudios acústicos, además de su b_{20} para cada una de las cinco frecuencias (-65.9 ± 2, -69.2 ± 3, -69.2 ± 2, -69.5 ± 2.5 and -71.5 ± 2.5 dB at 18, 38, 70, 120 and 200 kHz, respectivamente). También se proporcionan estimas de abundancia realizadas para los años de estudio (2014-2017) utilizando la frecuencia de 38 kHz. Las mediciones morfológicas de la vejiga natatoria se obtuvieron a partir de imágenes de rayos X y se utilizaron en la simulación de la retrodispersión de un elipsoide lleno de gas. La anchoa de fondo es una especie fisoclista, lo que significa que pueden compensar el volumen de la vejiga frente a cambios de presión. Sin embargo, el mejor

ajuste entre el modelo y los datos experimentales mostró que pierden esa capacidad durante el proceso de pesca, cuando el volumen de la vejiga natatoria se ve afectado por la ley de Boyle.

En el caso de la anchoa europea, hay algunas inconsistencias metodológicas en cuanto al *TS* empleado para la estimación de abundancia en el Golfo de Bizkaia. En primer lugar, se usan distintos valores en las distintas campañas acústicas de evaluación y, en segundo lugar, ninguno de estos valores es específico de la anchoa. En esta tesis se combinaron datos de mediciones *in situ* y *ex situ* en las tres frecuencias acústicas que se usan normalmente, incluyendo la que se usa típicamente para la evaluación. Se recogieron los datos *in situ* durante pescas nocturnas de arrastre pelágico en dos estaciones diferentes (primavera y otoño) a lo largo de 7 años de estudio. Se usó un modelo de retrodispersión para peces fisóstomos, para ayudar a interpretar los resultados, donde la vejiga natatoria se simplificó a un esferoide prolado de dos cámaras. Los valores de *TS* obtenidos fueron -44.6 (±2.3), -46.9 (±3) y -48.4 (±2.7) dB a 38, 120 y 200 kHz respectivamente que, para las anchoas de 3.5-19.5 cm de largo estudiadas, arrojaron valores de relación *TS*-talla *(b_{20})* de -66.5, -68.7 y -70.4 dB. Los resultados fueron bastante consistentes entre estaciones y entre condiciones *in situ* y *ex situ*, obteniendo relaciones positivas de *TS*-talla, significativas para todas las frecuencias. Este estudio forma parte de una serie de esfuerzos para obtener una relación *TS*-talla que permita actualizar la metodología de evaluación acústica de la anchoa europea en el Golfo de Bizkaia.

He organizado este trabajo de investigación siguiendo la estructura clásica de monografía, dividiéndola en los siguientes cinco capítulos:

En el **capítulo 1***, Introducción,* presento el contexto general de la investigación, describiendo el estado del arte de la pesca en el Golfo de Bizkaia con un enfoque específico hacia la anchoa de fondo y la anchoa europea. En la última parte de este capítulo resumo los objetivos específicos de la tesis, divididos que las siguientes secciones: mediciones de TS, procesado de TS, interpretación del *TS* y aplicaciones del TS.

En el **capítulo 2**, *Contexto*, incluyo una descripción general sobre cómo se aplican los métodos acústicos a la gestión pesquera, seguida de una descripción de los principales principios y definiciones acústicas, necesarios para comprender el contenido de esta investigación.

El **capítulo 3,** *Material y métodos*, incluye una descripción metodológica de las técnicas *in situ*, *ex situ* y de modelado teórico, incluyendo todos los experimentos realizados para reducir los posibles sesgos asociados con los procedimientos de muestreo, análisis y posterior procesamiento. Este capítulo lo he dividido siguiendo la estructura presentada en el capítulo 1.

He dividido el **capítulo 4***, Resultados,* en dos grandes secciones correspondientes a cada especie estudiada. En primer lugar, presento los resultados de la anchoa de fondo: primero, describo los resultados del experimento de capturabilidad, seguido de la variación de su respuesta acústica en función de la frecuencia operacional. A continuación, presento los resultados de las estimas de *TS* obtenidas para cada frecuencia, que son usados para calcular las relaciones *TS*-talla y hacer las estimas de abundancia para los años de estudio. Finalmente, la última parte de la sección de la anchoa de fondo la enfoco a los resultados de la morfología de la vejiga natatoria y del modelo teórico. En la sección dedicada a la anchoa europea describo primeramente los resultados del experimento *ex situ* para la corrección de los datos registrados dentro del campo cercano. A continuación, presento las distribuciones de *TS* y tallas de los datos *in situ* y *ex situ* filtrados, con los que determino las relaciones *TS*-talla en las tres frecuencias usadas para el estudio. Por último, se muestra una predicción de los patrones directividad obtenidos a partir del modelo teórico basado en el método de las soluciones fundamentales.

En el **capítulo 5**, *Discusión y conclusiones*, hago una discusión general sobre los resultados obtenidos, incluyendo las ventajas y desventajas de las metodologías aplicadas para producirlos, y su contribución a las metodologías acústicas de evaluación de *stock*. Para un mejor seguimiento de la discusión, he seguido el orden de las secciones descritas en los capítulos 1 y 3. Finalmente he resumido las principales conclusiones derivadas de esta tesis.

En resumen, esta tesis supone un gran avance en el estado del arte de la gestión de dos especies pelágicas en el Golfo de Bizkaia:

- Los resultados obtenidos a partir del estudio de la anchoa de fondo suponen una contribución esencial para futuras estimas de abundancia y simulaciones teóricas, claves para evaluar el impacto que pueda tener su potencial explotación, permitiendo así establecer las medidas necesarias para su gestión.
- Los resultados para la anchoa europea forman parte de una serie de esfuerzos realizados para obtener una relación *TS*-talla específica, que permita actualizar la metodología para su gestión en el Golfo de Bizkaia.

1. INTRODUCTION

1.1. Fisheries management in the Bay of Biscay

The Bay of Biscay is a gulf in the southern region of the northeast Atlantic that covers a total area of 225,000 km^2 with a maximum depth of 4,375 m. It stretches from Cape Ortegal in Galicia (43°46´N 7°52´W) to Penmarc´h Point in Brittany (47°48´N 4°22´W) (**Figure 1.1**). It shelters a large and diverse community of commercial species including hake (*Merluccius merluccius*), anchovy (*Engraulis encrasicolus)*, mackerel (*Scomber scombrus*), sardine (*Sardina pilchardus*), horse mackerel (*Trachurus trachurus*), anglerfish (*Lophius sp*) or megrims (*Lepidorhombus sp*). Fishery management in general mainly depends on estimating the size of the exploited population (Gulland, 1983) to determine the Total Allowable Catch (TAC) and effort quotas (Latour *et al.*, 2003; Pikitch, E. K. *et al.*, 2004; Smith *et al.*, 2007).

Figure 1.1 *Map illustrating the location of the Bay of Biscay (adapted from Wikipedia). Black dots located in Cape Ortegal (Southwest) and Penmarc´h Point (Northeast), and dashed line determines the western limit of the Bay of Biscay.*

To provide assessment and management advice on fish stocks from the Bay of Biscay, estimates of abundance are currently provided by expert groups (ICES., 2014). More specifically, the assessment of small pelagic fishes requires of direct assessment methods of biomass or population abundance, typically either from acoustic or from egg production methods (Barange *et al.*, 2009). Even though the survey indexes of biomass are usually taken as relative indexes of abundance in the integrated assessments, the estimates are generally given in tons as originally these methods were designed to produce absolute levels of biomass. For this reason, controversies are occasionally generated when absolute levels of assessment biomass diverge largely from the absolute numbers provided by the indexes. For standardization purposes, the methods and their associated parameters are routinely revised to achieve more reliable abundance indices and to approach as much as possible unbiased estimates of biomass.

Acoustic surveys are considered effective methods to quantify the distribution and abundance of many pelagic marine fauna (Simmonds and Maclennan, 2005). To convert the acoustic data into biomass estimates, it is necessary to estimate the target strength (TS; dB re 1 m^2), which is a measure of the amount of incident wave reflected by a single target (Simmonds and MacLennan, 2005) , and determine its relationship with the fish length. Generally, measurements of *TS* done on fish in their natural environment (e.g. *in situ*) are assumed to deliver the most accurate results, if collected with concurrent reliable biological samples and tilt angle information (Torgersen and Kaartvedt, 2001; Madirolas *et al.*, 2016; Zare *et al.*, 2017). However, measuring *TS* of fish in their natural environment implies dealing with difficulties that may lead to biased *TS* values and should, therefore, be carefully considered. When targeting small pelagic species, probably the most important source of *in situ TS* bias is the inability of the single target detection algorithm to resolve multiple echoes (Soule *et al.*, 1996). Hence, it is a critic aspect of the *TS* measurement process to apply procedures to mitigate this potential bias.

In parallel to the process of analyzing *TS* measurements, is often useful to run fish backscattering simulations, which help interpreting and generalizing the observed results. As up to 95% of the level of acoustic response of a gas-filled swimbladder-bearing fish is attributable to the swimbladder (Foote, K.G., 1980), many backscattering

models derive from the swimbladder morphology. Changes in the volume or surface area of the swimbladder can influence the *TS* significantly (Blaxter and Batty, 1990; Horne, 2000) and lead to considerable differences in abundance estimates.

Gas-filled bladdered fish can be classified into two classes: physoclists, which are able to compensate the swimbladder volume to pressure changes, and physostomous, which are not. Among the small pelagic species that can be found in the Bay of Biscay, in this work we will focus on two species that have a different type of swimbladder: Mueller's pearlside, a physoclist, and European anchovy, a physostome. Each of these species is in a completely different state of exploitation: the former is a potentially exploitable resource while the latter is a fully exploited one.

1.1.1. A potentially exploitable resource: Mueller´s pearlside

Mesopelagic fishes constitute an important component of the food web in the ocean and form the sound scattering layers (SSLs) (Williams *et al.*, 2001; Cherel *et al.*, 2008). Despite their small size, they are numerically important in temperate and tropical oceanic waters (Gjøsaeter and Kawaguchi, 1980; Sassa, C. *et al.*, 2002; Irigoien *et al.*, 2014), constituting major forage food for various commercially-fished species (Prosch, R.M *et al.*, 1989; O'Driscoll *et al.*, 2009). Due to the increasing interest in their commercial exploitation (Savinykh, V.F. and Baytalyuk, A.A., 2010; Directorate-General for Maritime Affairs and Fisheries, 2018; Prellezo, 2018; Springmann *et al.*, 2018; Hidalgo and Browman, 2019), accurate estimates of its abundance are key to evaluate the impact of their potential exploitation and establish the necessary management measures (Prellezo, 2018; Hidalgo and Browman, 2019).

The total abundance of mesopelagic fish in the world oceans is unknown. Biomass estimates published in the last 20 years range between 2 and 20 Gt. New acoustic estimates are over one order of magnitude above historic estimates based on net sampling (Irigoien *et al.*, 2014; Jennings and Collingridge, 2015; Proud *et al.*, 2017, 2018; Anderson *et al.*, 2018), challenging our understanding of gross ocean carbon production, major food chains and ecosystem carbon flow in these deep-water systems. Two main reasons leading to this uncertainty have been identified. First, mesopelagic fish species

are difficult to fish due to high avoidance to experimental pelagic trawls (Kaartvedt *et al.*, 2012; Peña, 2019), potentially leading to an underestimation of their biomass. Second, the composition of the acoustic scatterers in the deep scattering layers may include other species than fish (e.g. siphonophores), potentially leading to an overestimation of their biomass (Proud *et al.*, 2018). To overcome this, a combination of trawl and multifrequency acoustic methodologies has been recommended for the estimation of mesopelagic fish abundance (Koslow *et al.*, 1997; Kloser *et al.*, 2009; Pakhomov *et al.*, 2010).

Among the mesopelagic species, Mueller's pearlside (*Maurolicus muelleri,* Gmelin, 1789; pearlside hereafter) is one of the most abundant and potentially accessible species to commercial fisheries, as it often resides closer to the surface than other mesopelagic species (Godø *et al.*, 2009). However, to date there are no scientific surveys focused on the biomass estimation of mesopelagic species in the Bay of Biscay. There are particular difficulties to accomplish acoustic-based biomass estimations for this species. Firstly, for mesopelagic species in general and pearlside in particular, the small size of the swimbladder might cause the appearance of resonance-induced maxima inside the range of the operative frequencies most common in acoustic surveys, hence inducing non-linear relationships between *TS* and length (Davison *et al.*, 2015b) and thus hampering, or at least complicating, their estimation of abundance. Secondly, even if pearlside is considered a physoclist species, its actual swimbladder volume compensation performance during the trawling process is not clear, making difficult to know whether the observed swimbladder size at the surface was representative of the actual size at the depth of capture. In fact, when modelling the swimbladder, there is lack of consensus in literature on whether to consider pearlside as a physostome (Godø *et al.*, 2009; Scoulding *et al.*, 2015; Proud *et al.*, 2018) or as a physoclist (Fujino, T. *et al.*, 2009; Peña *et al.*, 2014; Kloser *et al.*, 2016; Peña and Calise, 2016) species, which generates confusion on the most basic application of the empirically measured *TS* values to estimate abundance: are the *TS* values valid for all the depth range, or, if not, how should they be changed according to depth?

1.1.2. Stock assessment of an exploited species: European anchovy

European anchovy (*Engraulis encrasicolus*; Linnaeus, 1758) is one of the main commercial species in the Bay of Biscay, supporting profitable fisheries for both the Spanish and French fleets. The internationally coordinated scientific advice relies on the stock assessment of this resource, following the so-called Catch-Bayesian Biomass-Based Model (CBBM) (Ibaibarriaga *et al.*, 2008; ICES, 2015), which integrates the information coming from commercial fleets and scientific surveys, providing estimates of the adult stock abundance and recruits. The scientific surveys contributing to the assessment are BIOMAN (Santos, M. *et al.*, 2018), based on the Daily Egg Production Method in spring and two trawl-acoustic surveys, PELGAS (Massé, J. *et al.*, 2018) in spring and JUVENA (Boyra *et al.*, 2013) in autumn.

The methodologies of the surveys are discussed and evaluated annually at the ICES Working Group of Acoustics and Eggs ('WGACEGG', n.d.) and the results are synthetized at the ICES Working Group on Southern Horse Mackerel, Anchovy and Sardine (WGHANSA) (ICES., 2017) to produce the CBBM assessment. Fortunately, the different surveys used as input for the CBBM assessment of anchovy are significantly correlated with each other ('WGACEGG', n.d.), showing crossed-consistency, as expected.

However, there are still some methodological inconsistencies requiring revisions, especially concerning the trawl-acoustic methodology part of the assessment. The two acoustic surveys use different TS-length relationships for the estimation of anchovy abundance, none of which has been obtained from anchovies. This hampers the harmonization of the results of both surveys into a single abundance estimation in absolute terms, as has been acknowledged by ICES WGACEGG, being the achievement of a common *TS*-length relationship for the region considered one of the key objectives of the working group (ICES, 2013).

1.2. Hypothesis, aim and objectives

After presenting the general context and motivation of this research work, the following **hypothesis** has been defined:

Acoustic techniques can be used to determine the individual acoustic signal of small, densely-aggregated pelagic fish in order to determine the basic elements necessary to deliver unbiased acoustic estimates of abundance, to be used for resource monitoring, scientific advice and ultimately, fishery management of these resources.

The **aim** of this thesis is to obtain unbiased *TS* estimates and *TS*-length relationships of two pelagic species in the Bay of Biscay: European anchovy and Muller´s pearlside. To achieve this aim, *in situ* and *ex situ* measurements were done at multiple frequencies, using several procedures to address the main sources of bias associated to these techniques. In addition, swimbladder morphological measurements and backscattering simulations were carried out to help the interpretation and the proper application of the obtained results. Given the difference between both species, distinct backscattering models were applied for each. To achieve this aim, this thesis work has been divided into the following individual **objectives**:

TS measurement and processing

- To estimate *TS* values of Muller´s pearlside at 18, 38, 70, 120 and 200 kHz frequencies using acoustic data collected from *in situ* measurements.
- To estimate *TS* values of European anchovy at 38, 120 and 200 kHz frequencies, using acoustic data collected from both *in situ* and *ex situ* measurements.
- To reduce the potential multiple target bias from the *TS* measurements:
    - working during the nighttime
    - applying a high-density filter to the *in situ* measured data
    - controlling the incidence of the volume of the sound pulse on the mean *ex situ* measured *TS*.
- To correct the bias derived from the short-range measurements of the *ex situ* experiments.

- To test the catchability of small length classes of pearlside using different mesh size codends

TS interpretation and application

- To determine the morphology of the swimbladder of both species and use it to model the acoustic backscatter using appropriate theoretical models for each species.
- To describe the swimbladder behaviour of pearlside during the trawling process by comparing the model behaviour under different swimbladder tilt angle and contraction rate values.
- To provide estimates of biomass of pearlside for the years of study.

2. BACKGROUND

2.1. The role of acoustics in fisheries management

The utility of underwater sound to detect and identify aquatic lifeforms has been considered of great potential for almost a century now, when the first successful experiment on the acoustic detection of fish in a tank was published (Kimura, 1929). Progressive advances in the development of technology (Sund, 1935; Wood *et al.*, 1935), together with the important contributions evidenced after World War II (Hodgson, 1950; Hodgson and Fridriksson, 1955), were essential milestones on the progress in acoustic identification methods. It was not until then that the first investigations on the application of acoustic methods to fish abundance estimation were published (Tungate, 1958; Mitson and Wood, 1961), and not until the 70s and 80s that a broader perspective on the potential of the acoustic techniques was achieved.

The increasingly sophisticated acoustic technologies offered the possibility of registering information of fish populations at high spatio-temporal resolution, over wide scales (Trenkel *et al.*, 2011; Godø *et al.*, 2014), becoming an important application of acoustics in fisheries research (Gunderson, 1993).

2.2. Acoustic surveys and calibration

Acoustic surveys are often conducted to estimate the abundance of pelagic fish populations (Gunderson, 1993): a certain area is covered following transects while acoustic echoes from fish are registered. These echoes may be observed anywhere in the water column, but this technique will only be useful when the fish of interest are away from the seabed and not too close to the surface. This makes acoustic survey techniques particularly suitable for pelagic species such as anchovies (Engraulidae) (Simmonds and MacLennan, 2005) and pearlsides (Sternoptychidae).

For a survey to provide reliable results, the echosounders have to be calibrated following standard procedures (Demer *et al.*, 2015). Calibration of acoustic instruments is crucial when used for quantitative purposes such as biomass estimation and should be performed with exhaustive attention to detail. During the first acoustic surveys, before the first protocol was published (Foote K.G. *et al.*, 1987), calibration was a major source

of error of fish abundance estimates (Blue, 1984). The ICES Fisheries Acoustics, Science and Technology Working Group (WGFAST), has promoted the methodological developments for a good performance of the calibration procedures, guiding the acoustic community to uniformly apply the same methods to calibrate the acoustic equipment. Technological innovation and development made it necessary to create a new practical guide for calibration (Demer *et al.*, 2015), however, due to the continuous progress in the field, new updates should be incorporated regularly to achieve the best quality results.

In modern practice, a standard target is commonly used for calibration. A tungsten carbide or copper sphere is suspended below the transducer while the echosounder transmits and receives signals as it would during the survey, measuring the echo produced by the target and the time delay between the echo and the transmitted pulse **(Figure 2.1)**. To determine the acoustic parameters correctly, factors such as the environmental conditions (i.e. the speed of sound in water or the absorption coefficient) and the echosounder frequency must be known. Details on the particular types of spheres that are commonly used with the typical frequencies of study can be found in Demer *et al* (Demer *et al.*, 2015).

All data obtained for the elaboration of this thesis was collected from multi-vessel surveys, which required an additional inter-ship calibration procedure to be carried out after the independent calibration of each vessel. This is a necessary measure to check if there are no significant differences in their respective measurement capabilities (Simmonds and MacLennan, 2005).

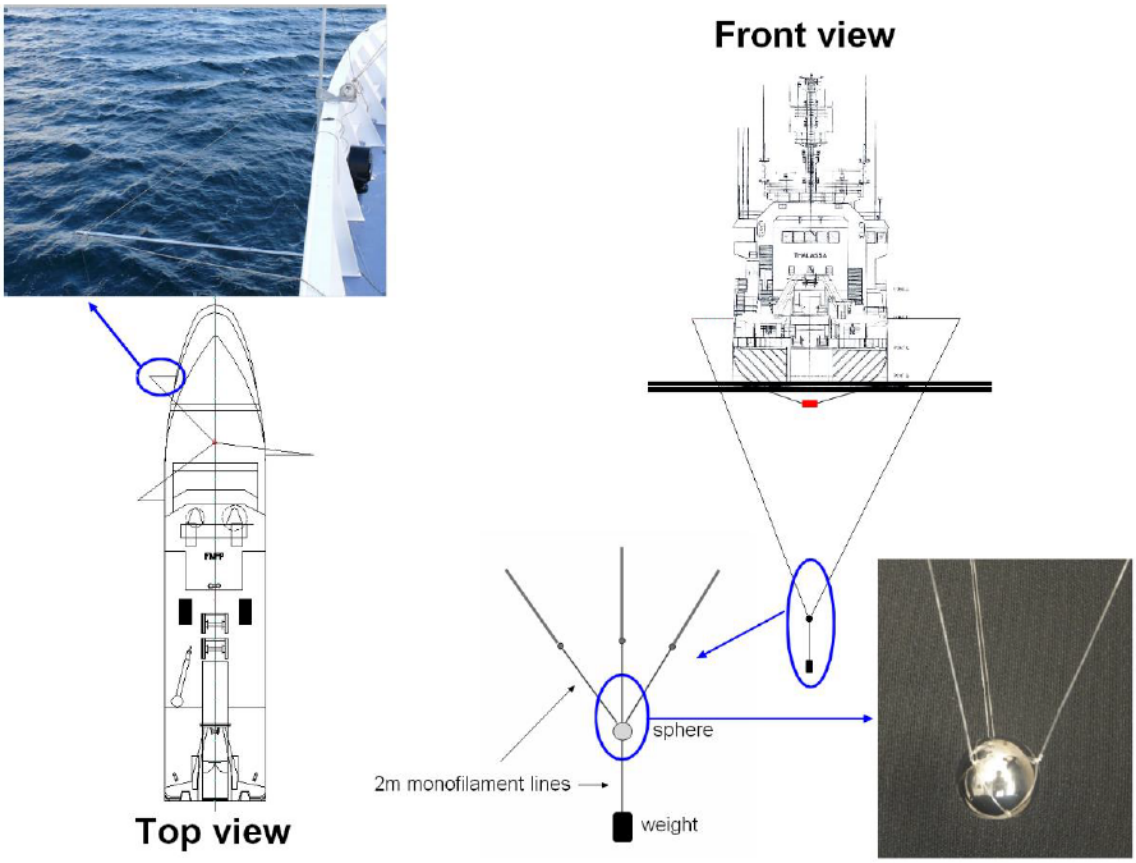

Figure 2.1 *Calibration method using a sphere as standard target suspended by three monofilament lines (Demer et al., 2015).*

2.3. Acoustic principles

Sound is a mechanical disturbance that propagates as a pressure wave in an elastic medium, decreasing its intensity with the increase of range. Any device that uses sound to detect targets in water is defined as sonar. The **echosounder** is a kind of sonar that projects the sound in a directional beam in the form of a main lobe oriented vertically downwards, and several sidelobes of reduced intensity. It consists of a transceiver (that generates electrical energy) and a transducer (converts the electrical energy into mechanical sound energy) (Simmonds and MacLennan, 2005) **(Figure 2.2)**. They are typically made from piezoelectric elements that generate electric energy when an oscillating external voltage is applied (Simmonds and MacLennan, 2005). In fisheries acoustics, the most commonly used frequencies at which the electrical energy is produced are 18, 38, 70, 120, 200 and 333 kHz.

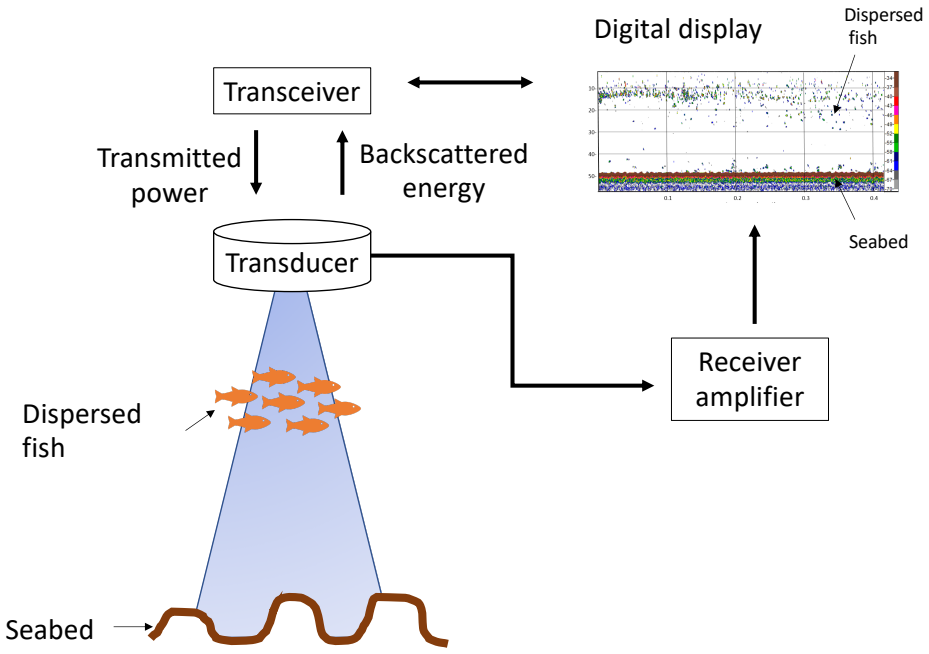

Figure 2.2 *Scheme illustrating the concept of echosounding. The transmitted pulse is reflected by the targets and seabed as an echo that is displayed on an echogram.*

When the pulse of sound encounters a target, a proportion of the incident energy is scattered back towards the transducer, amplified and converted to electrical energy that is displayed on a two-dimensional picture, or **echogram**, showing the ensonified volume of water in the vertical (depth or range) and horizontal (space or time) domain **(Figure 2.3)**.

The echo or backscattered sound is generally quantified in the linear domain as the **backscattering cross-section** ($\boldsymbol{\sigma}_{bs,\,[m^2]}$), or in the logarithmic space as ***TS*** expressed in decibels as:

$$TS = 10log_{10}(\sigma_{bs})$$

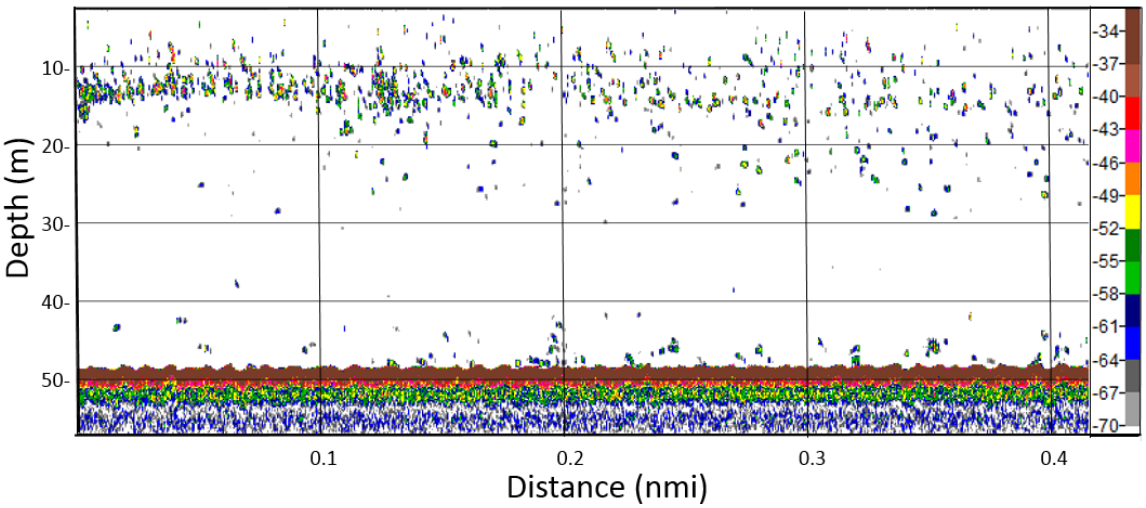

Figure 2.3 *Example of an echogram showing juvenile anchovy dispersed at 15 m depth, in autumn at 38 kHz. The colour scale on the right shows the echo intensity (s_v [dB re 1m2]). The seabed is at 49 m depth represented in brown.*

The maximum detection range of an echosounder is limited by the absorption of sound in water that increases with the operational frequency. The intensity of the marks in the echogram is proportional to the difference in the acoustic impedance (difference in density and sound speed) between the target and the water (Love, 1971), and can be used as a measure of biomass in the water column. **Split-beam echosounders** such as the EK60 scientific echosounder, use transducers divided into four quadrants, and can determine the direction and location of the targets in the beam by comparing the time-of-arrival difference of the signals received by each quadrant (Demer *et al.*, 1999). The accuracy of the output makes it possible to count individual fish or measure the density of fish aggregations, however, to resolve individual echoes, they must be at least half the pulse length ($c\boldsymbol{\tau}$) separated from each other, where $\boldsymbol{\tau}$ is the pulse duration [s] and c in the speed of sound [ms^{-1}]. When the individual targets are small and in high packing densities, the echoes form a continuous received signal with varying amplitude, and it is no longer possible to resolve individual echoes. The sum of all the discrete targets that contribute to echoes from the sampled volume (V_0) is the **volume backscattering coefficient** (s_v) (MacLennan *et al.*, 2002):

$$s_v = \sum \sigma_{bs}/V_0 \,,$$

where:

$$V_0 = c\tau\psi R^2/2,$$

with $\boldsymbol{\psi}$ being the equivalent beam angle of the transducer in steradians.

The **volume backscattering strength** (S_v) is the equivalent logarithmic measure:

$$S_v = 10log_{10}(s_v)$$

If the backscattering volume strength is integrated over bigger volumes, it can then be expressed as the **mean volume backscattering strength** (MVBS or $\widehat{S_v}$).

The **area backscattering coefficient** (s_a; [m^2 m^2]) is more commonly used in acoustic surveys as it is the acoustic energy integrated over a layer between two depths. One of the scaled versions used for fisheries surveys is known as the **nautical area scattering coefficient** (NASC or s_A; [m^2nmi^2), which is s_a integrated over one nautical mile, defined as:

$$s_A = 4\pi(1852)^2 s_a$$

2.3.1. Target strength

The number of fish per unit volume can be deduced by knowing the target strength of the fish that contribute to the acoustic signal. The target strength is a measure of the

proportion of the incident energy that is backscattered by the target (MacLennan *et al.*, 2002), expressed as a log-linear function of fish standard length (SL; cm) of the form:

$$TS = a\log_{10}(SL) + b,$$

where the slope, *a,* and the intercept, *b*, are species-specific constants. This equation is used on *TS* of fish from the same species over a range of sizes ensonified at the same frequency (McClatchie, 2003). As stated by MacLennan and Simmonds (2002), in the absence of data evidencing the contrary, *a* value can be assumed to be 20. In the case of clupeoids, such as anchovy, *a* is normally close to 20 (Love, 1977; Foote, K.G., 1980) and the *TS* equation is often replaced by:

$$TS = 20\log_{10}(SL) + b_{20},$$

However, when the amount of data available is sufficient to determine a species-specific *TS*-length relationship, this value should not be used without first determining whether it is the most suitable one (McClatchie, 2003).

2.3.1.1. Target strength measurements

In situ measurements

Generally, *in situ TS* measurements are assumed to deliver the most accurate results, if collected with concurrent reliable biological samples and tilt angle information (Torgersen and Kaartvedt, 2001; Madirolas *et al.*, 2016; Zare *et al.*, 2017). However, measuring *TS* of fish in their natural environment implies dealing with difficulties that may lead to biased *TS* values and should, therefore, be carefully considered. Firstly, during daytime, small pelagic fish such as European anchovy (Massé, 1996) or pearlside, aggregate in schools too densely packed to resolve individual targets. Secondly, the fact that *TS* is a stochastic variable means that it can have a range of values described by a probability distribution. Since *TS* measurements are usually recorded over a period of

time and across a particular layer of fish, a wide range of target strength values might be registered, representing different size-classes or behavioural states (Ona, 2003; Simmonds and MacLennan, 2005).

Ex situ measurements

Another possible strategy is to conduct *ex situ* experiments (Kang and Hwang, D, 2003; Kang *et al.*, 2009), allowing more control of the abundance and assuring isolation of the target species. However, *ex situ* experiments pose some concerns such as possibly altering the behavior of the targets (Nakken and Olsen, 1977; Ona, 1990). Another caveat of this method is derived from the near-field effect derived from short range measurements. Additionally, the backscatter of the cage should be extracted from the fish *TS* measurements. This can be done by previously measuring the empty cage or by using a cage larger than the acoustic beam (Ona, 2003).

Multiple targets

One of the challenges of *TS* measurements is to ensure that the *TS* data is not affected by multiple targets present in the acoustic reverberation volume (Sawada *et al.*, 1993), thus leading to a bias in the *TS* value. Ideally, single-fish detectors are able to detect single echoes when these are well spaced but, in the case of small pelagic fish, their high packing densities are likely to prevent the successful detection of single target echoes (Barange *et al.*, 1996).

There are different strategies to overcome this problem. Lowering the transducers and a camera closer to the fish targets (thus reducing the sampling volume) has often helped mitigate it (Massé, 1996; Ona, 2003; Kang *et al.*, 2009; Murase, H. *et al.*, 2011; Fernandes *et al.*, 2016). In the Bay of Biscay, a variant of this technique has been applied to estimate *TS* of anchovy (Doray *et al.*, 2016), but the methodology caused a change in the fish behavior that probably biased positively the mean *TS* values. Other strategies involve working during nighttime, when most species disperse and migrate near the surface (Misund, 1999), yet these are most useful when the study areas are dominated by the

target species (Foote K.G. *et al.*, 1987; Barange *et al.*, 1996; Peltonen and Balk, 2005; Zhao *et al.*, 2008), but might be problematic in case of mixture of fish species or in presence of high abundances of plankton.

However, when the previous approaches have not succeeded to register well-spaced single targets, there are other strategies developed to reject multiple echo detections under high density conditions. Some of them were tested during the first months of the development of this thesis, on a set of *TS* data of *in situ* skipjack and bigeye tuna collected around drifting Fish Aggregating Devices (FADs) (Boyra *et al.*, 2018, 2019).
The first method consisted in increasing the threshold of the standard deviation of phases between the samples of the received pulse, which are the parameters that should control the acceptance of multiple echoes (Soule, 1997). The second method was a fish tracking analysis (Blackman, 1986), which consists in grouping targets according to their mutual spatial and temporal proximity, considering that they are successive detections of the same fish in a track. Another attempt for multiple target removal was based on the simultaneously detected targets at multiple frequencies (Demer *et al.*, 1999; Conti *et al.*, 2005; Scoulding *et al.*, 2015) which requires that the *TS* values pass the single target criteria in at least two frequencies independently to be considered valid. The last tested method consisted on filtering the areas of the echogram with highest densities of fish individuals, thus with higher probability of failure of the single target detection algorithm (Barange *et al.*, 1996; Massé, 1996; Gauthier and Rose, 2001; Scoulding *et al.*, 2015).

TS-length relationship

Despite the stochastic nature of *TS*, one would expect that the average of many *TS* measurements would follow a systematic dependence on the species, size and behaviour of the fish targets. In fact, standard errors below 5% of the mean are typical when 500 – 1000 measurements are made (Zhao, 1996). However, when several modes are present in the *TS* distributions, the average *TS* value might not be representative of a determined size-class. In the case of well-differentiated size modes of fish obtained from the trawl catches, these can be matched to the modes present in the *TS*

distributions, but, in the case of superimposed modes, other statistical methods should be applied. A common approach (MacLennan and Menz, 1996) is to assume a specific distribution of the probability density function (PDF) (i.e. Gaussian, Rayleigh) and a *TS* function (typically *TS* = 20logL + b), so that *TS* values are calculated for each length in the catch histogram. Then, a least-square fitting procedure is applied to obtain the *b* value that minimises the differences between the calculated and observed *TS* histograms.

Near-field effect

At distances near the face of the transducer, the wave-fronts are not parallel producing unpredictable changes of intensity with range. *TS* measurements done in this area are expected to be biased due to the inherently unstable nature of the acoustic beam. The far-field area is the part of the beam were the wave-fronts are nearly parallel, and where the variations of intensity are more predictable (Simmonds and MacLennan, 2005). To avoid bias derived from the near-field effects, the boundary range (R_b) between the near and the far fields can be calculated using the linear distance across the transducer face (*a)* and the wavelength (λ):

$$R_b = a^2/\lambda$$

It is recommended to perform the acoustic measurements at ranges of at least $2R_b$ to be considered applicable to the far-field conditions. However, *ad hoc* experiments can be designed to determine the spatial variation of the intensity in the near field and calculate the correction values to be applied to the empirical measurements. Such corrections should only be applied at ranges where the intensity variations are predicted by theoretical modelling.

2.3.1.2. Target strength theoretical modelling

For a complete understanding of sound scattering by aquatic organisms, empirical and theoretical methods should be combined (Henderson, M. J. and Horne, J. K., 2007) in order to understand to what extent the experimental findings can be used for biomass estimation in acoustic surveys (Jech *et al.*, 2015). The improvement in the numerical and analytical approaches in the last years has increased the diversity of acoustic scattering models, making it essential to evaluate the effectiveness of a model for each specific species or survey. Since the early 60s, many theoretical models for swimbladder-bearing fish species have been developed focusing on the swimbladder morphology and its acoustical properties, since it accounts for up to 95% of the backscattered energy from gas-filled swimbladder-bearing fish (Foote, K.G., 1980). A comprehensive summary and comparison of the most used ones has recently been published (Macaulay *et al.*, 2013; Jech *et al.*, 2015). There are two main similarities between those models: (1) they evaluate the *TS* assuming the far-field condition (Massé, 1996) and (2) they are based on the approximation of the swimbladder to an idealised shape. Of these, the **Prolate Spheroid Model** (PSM) (Andreeva, 1964; Weston, D. E., 1966; Love, 1978; Furusawa, M., 1988; Ye, 1997) uses an idealized representation of a swimbladder (Simmonds and MacLennan, 2005) and has been applied in several studies (Fujino, T. *et al.*, 2009; Yasuma *et al.*, 2009; Prario *et al.*, 2015; Scoulding *et al.*, 2015; Madirolas *et al.*, 2016; Peña and Calise, 2016; Proud *et al.*, 2018).

More sophisticated models such as the Boundary Element Models (BEM) or Finite Element Models (FEM) (Foote and Francis, 2002; Francis and Foote, 2003; Lilja *et al.*, 2004) use the true shape of scattering objects but they turn out computationally unaffordable for arbitrary close distances (Pérez-Arjona *et al.*, 2018). However, *TS* calculations at a desired finite distance with an important reduction in computational costs, can now be performed using a new class of numerical methods that have emerged in the last decades, the so-called meshless methods (Pérez-Arjona *et al.*, 2018). Making use of fundamental solutions accounting directly for infinite or semi-infinite spaces, the **Method of Fundamental Solution** (MFS) has proven a successful tool for estimating the measurable *TS* of fish and the contribution of the different inner structures of fish to *TS*, with similar, or even more accuracy than FEM or BEM but with a reduction of

computational costs what can be specially important when considering fish models with more fish structures than swimbladder, e.g., fish backbone (Fairweather *et al.*, 2003; Pérez-Arjona *et al.*, 2018).

2.3.2. Biological acoustics

2.3.2.1. The swimbladder

Up to 95% of the backscatter of a gas-filled swimbladder-bearing fish, is attributable to the swimbladder (Foote, K.G., 1980) due to the density contrast between gas and water (Haslett, R. W. G., 1962). Changes in the volume or surface area of the swimbladder can influence the *TS* significantly (Blaxter and Batty, 1990; Horne, 2000) and lead to considerable differences in abundance estimates. Gas-filled bladdered fish can be classified into two classes.

2.3.2.1.1. Physoclists

The physoclistous fish have closed swimbladders. They have glands to extract gas from the water to be secreted into the bladder. They can compensate the swimbladder volume for pressure changes by “pumping up” or removing gas by glandular action. The cod (*Gadus morhua*) and other gadoids belong to this group (Simmonds and MacLennan, 2005) as well as some mesopelagic species such as the pearlside. However, its actual swimbladder volume compensation performance during the trawling process is not clear, hampering the interpretation of the observed swimbladder size at the surface. In fact, when modelling the swimbladder, there is lack of consensus in the literature on whether to consider pearlside as a physostome (Godø *et al.*, 2009; Scoulding *et al.*, 2015; Proud *et al.*, 2018) (the swimbladder volume obeys Boyle´s law) or as a physoclist species (Fujino, T. *et al.*, 2009; Peña *et al.*, 2014; Kloser *et al.*, 2016; Peña and Calise, 2016).

2.3.2.1.2. Physostomes

Physostomous fish have a pneumatic duct that connects the swimbladder to the digestive tube and, therefore, to the surrounding water (Whitehead, P.J.P and Blaxter, J.H.B., 1989). During ascending migrations, the gas is vented through the pneumatic duct. Changes in the ambient pressure induce changes in the swimbladder shape by continuous diffusion through the bladder wall. Many clupeoids such as anchovy, belong to this group and are unable to compensate the swimbladder volume for pressure changes. Because of this, it is expected that *TS* decreases with depth according to the Boyle's law as has been observed in previous measurements of anchovy (Zhao *et al.*, 2008) and other physostomous species (Ona, 2003).

3. MATERIALS AND METHODS

3.1. *Data collection*

3.1.1. Acoustic data

3.1.1.1. Echointegration data

In this work, only the s_A allocated to pearlside was used to produce spatial distribution maps and vertical profiles, since the spatial analyses of anchovy are already part of the annual reports elaborated by ICES WGACEGG. The acoustic backscattering at 38 kHz collected during the transects was echointegrated annually by 0.1 nmi (elementary distance sampling unit or EDSU) per ~50 m bins, to a maximum depth of 500 m. This part of the survey strategy (Boyra *et al.*, 2013) consisted in providing spatial distribution and biomass annual estimates of several species at a single frequency (38 kHz).

3.1.1.2. TS data

In situ data collection

Acoustic-trawl data was collected from years 2010 to 2017, during two scientific surveys that take place in the Bay of Biscay in two different times of year (**Figure 3.1**). JUVENA (Boyra *et al.*, 2013) takes place in September, focusing on the juvenile fraction of the anchovy population while BIOMAN (Santos, M. *et al.*, 2018) is developed in May (during the peak of the spawning season) focusing on the adult component. Since year 2014, JUVENA has adopted a new ecosystemic approach with the scope of assessing a bigger number of target species such as pearlside. Two scientific research vessels were used in each survey: RV *"Ramón Margalef"* (RM, hereafter) and RV "*Emma Bardán*" (EB, hereafter). Both registered continuous acoustic data with an EK60 scientific echosounder (Kongsberg Simrad AS, Kongsberg, Norway) with split-beam transducers of 38, 120 and 200 kHz. Additionally, RM registered data at 18, 70 and 333 kHz frequencies. The transducers were placed in a drop keel that reached a maximum depth of 6.75 m. All nominal beam widths were 7º except for the 18 kHz transducer, with a beam width of 11º. Pulse duration was 1024 μs with a ping rate of 0.7 s^{-1}. The scientific echosounders of each research vessel were calibrated at least once a year, typically at the beginning of the survey, following standard procedures (Demer *et al.*, 2015), using a tungsten

carbide sphere of 38.1 mm of diameter. Intercalibration exercises were carried out each year between the two vessels following standard methodologies (Simmonds and MacLennan, 2005). The most relevant calibration parameters of the *in situ* and *ex situ* measurements are described in **Table 3.1**.

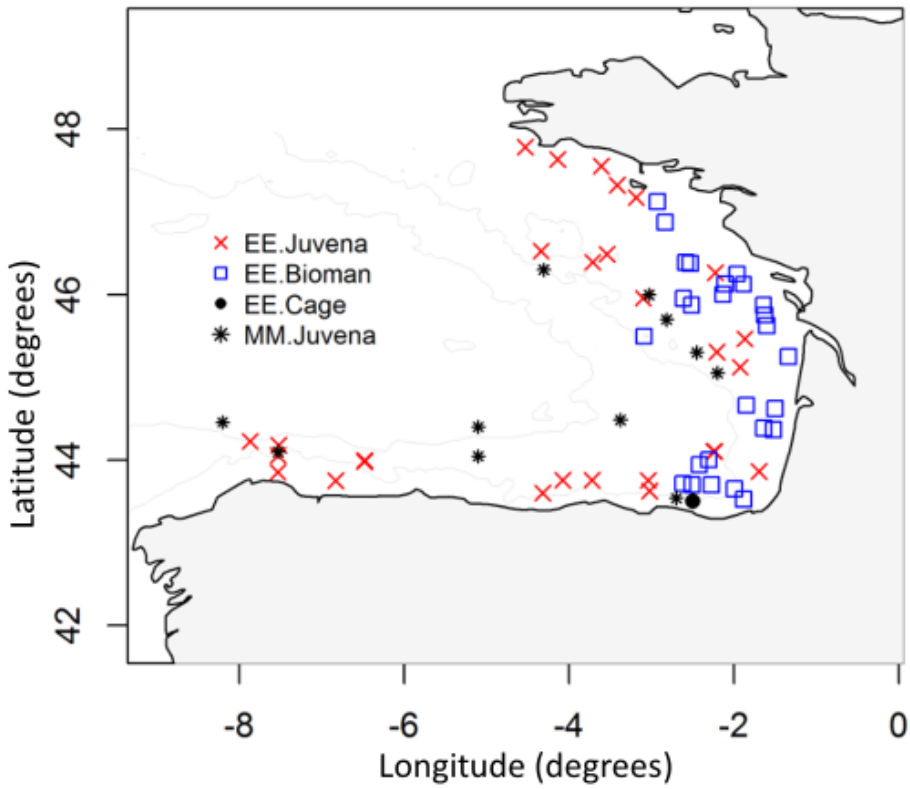

Figure 3.1 *Area of study in the Bay of Biscay, with the sampling locations for EE (European anchovy) and MM (pearlside).*

Table 3.1 *Calibration settings of the* in-situ *data collected from research vessels Ramón Margalef (1) and Emma Bardán (2). Target strength of reference target was -42.3, -40 and -39.9 dB at 38, 120 and 200 kHz, respectively. Allowed TS deviation was 5 dB.*

Year	Survey	Frequency (kHz)	Pulse duration (μs)	Power (W)	Gain (dB)	S_a correction (dB)
2010	JUVENA[1]	38		1200	25.57	-0.66
		120	1024	256	26.77	-0.26
		200		210	25.63	-0.34
2011	BIOMAN	38		1200	23.94	-0.76
		120	1024	250	25.96	-0.43
		200		210	26.51	-0.36
2012	JUVENA[2]	38		1200	23.94	-0.76
		120	1024	250	25.96	-0.43
		200		210	26.51	-0.36
2013	JUVENA[2]	38		1600	22.76	-0.79
		120	1024	250	26.03	-0.43
		200		120	26.45	-0.34
2014	BIOMAN	38		1200	23.94	-0.73
		120	1024	150	26.03	-0.43
		200		120	26.19	-0.25
2014	JUVENA[1]	18		1600	22.76	-0.79
		38		1400	25.46	-0.68
		70	1024	600	26.38	-0.42
		120		200	25.89	-0.40
		200		90	27	-0.23
2014	JUVENA[2]	38		1200	23.94	-0.73
		120	1024	150	26.14	-0.33
		200		120	26.19	-0.25
2015	BIOMAN	38		1200	23.98	-0.70
		120	1024	150	26.14	-0.33
		200		120	26.19	-0.25
2015	JUVENA[2]	38		1200	23.98	-0.70
		70	1024	750	26.86	-0.32
		120		150	26.08	-0.33
		200		120	26.19	-0.25
2016	BIOMAN	38		1200	23.86	-0.73

Year	Survey	Frequency (kHz)	Pulse duration (μs)	Power (W)	Gain (dB)	S_a correction (dB)
		120	1024	150	26.25	-0.29
		200		120	26.13	-0.23
2016	JUVENA[1]	18		1800	22.03	-0.83
		38		1200	25.56	-0.66
		70	1024	600	26.38	-0.40
		120		125	26.58	-0.35
		200		90	25.94	-0.32
2017	BIOMAN	38		1200	23.88	-0.79
		120	1024	150	26.25	-0.29
		200		120	26.13	-0.23
2017	JUVENA[1]	18		1600	22.22	-0.73
		38		1600	23.51	-0.65
		70	1024	600	27.07	-0.33
		120		200	26.78	-0.25
		200		120	26.70	-0.28
2017	JUVENA[2]	38		1200	23.88	-0.79
		120	1024	150	26.25	-0.29
		200		120	26.13	-0.23

Table 3.2 *Details of the pelagic trawls and experiments used for the analysis.*

Trawl	Date	Survey	Lat °	Lon °	Anchovy catch (% gr)	Mean length (cm ± sd)	Mean depth (m)
European anchovy – in situ							
5009	10/05/2011	BIOMAN	46.53	-4.34	100	14 ± 0.2	9.85
5010	10/05/2011	BIOMAN	43.71	-2.62	90	15 ± 0.4	11.79
5011	11/05/2011	BIOMAN	43.70	-2.51	91	15 ± 0.5	18.14
5013	11/05/2011	BIOMAN	43.70	-2.27	95	14 ± 0.9	14.64
5014	11/05/2011	BIOMAN	44.00	-2.31	100	14 ± 0.9	13.56
5040	23/05/2011	BIOMAN	43.94	-2.42	96	13 ±0.4	9.91
5044	24/05/2011	BIOMAN	46.13	2.57	96	10 ± 0.1	7.85

Trawl	**Date**	**Survey**	**Lat** °	**Lon** °	**Anchovy catch** (% gr)	**Mean length** (cm ± sd)	**Mean depth** (m)
5049	27/05/2011	BIOMAN	45.75	-1.63	98	13 ± 0.4	13.85
5014	12/05/2014	BIOMAN	46.39	-2.59	100	13 ± 0.8	9.17
5017	13/05/2014	BIOMAN	43.63	-3.02	100	14 ± 0.1	13.75
5027	16/05/2014	BIOMAN	43.75	-4.08	97	13 ± 0.7	9.42
5031	17/05/2014	BIOMAN	45.12	-1.93	91	15 ± 0.9	9.85
5039	25/05/2014	BIOMAN	46.49	-3.54	100	13 ± 0.7	15.13
5040	25/05/2014	BIOMAN	47.33	-3.42	100	13 ± 0.8	13.96
5043	26/05/2014	BIOMAN	47.56	-3.61	100	13 ± 0.5	13.35
5048	28/05/2014	BIOMAN	47.17	-3.19	100	13 ± 0.9	9.82
5049	28/05/2014	BIOMAN	44.37	-1.52	100	13 ± 0.5	8.36
5046	26/05/2015	BIOMAN	44.62	-1.50	100	12 ± 0.7	10.66
5041	25/05/2016	BIOMAN	45.87	-1.64	97	13 ± 0.8	9.17
5044	26/05/2016	BIOMAN	45.87	-2.52	85	15 ± 0.3	18.65
5011	11/05/2016	BIOMAN	46.13	-1.89	99	13 ± 0.7	10.69
5019	15/05/2016	BIOMAN	46.00	-2.14	92	12 ± 0.8	9.23
5020	15/05/2016	BIOMAN	46.25	-1.96	90	14 ± 0.8	8.93
5034	23/05/2016	BIOMAN	47.13	-2.93	95	13 ± 0.7	8.64
5037	24/05/2016	BIOMAN	46.88	-2.83	99	11 ± 0.8	8.60
5014	11/05/2017	BIOMAN	43.98	-6.48	87	13 ± 0.5	9.10
5032	16/05/2017	BIOMAN	43.76	-3.72	98	11 ± 0.4	10.36
9050	27/09/2010	JUVENA	46.39	-3.71	98	11 ± 0.4	15.96
9205	04/09/2012	JUVENA	44.23	-7.87	93	7 ± 0.4	9.46
9213	11/09/2012	JUVENA	44.10	-2.25	87	8 ± 0.1	13.75
9222	17/09/2012	JUVENA	46.38	-2.53	98	8 ± 0.8	15.15
9230	21/09/2013	JUVENA	44.18	-7.52	100	9 ± 0.9	15.63
9233	23/09/2013	JUVENA	45.46	-1.87	100	16 ± 0.3	7.55
9235	24/09/2013	JUVENA	45.96	-3.10	100	15 ± 0.5	9.65
9236	24/09/2013	JUVENA	43.65	-2.00	100	16 ± 0.6	14.42
9011	09/09/2014	JUVENA	44.39	-1.64	100	8 ± 0.6	16.50
9201	03/09/2014	JUVENA	44.66	-1.85	100	6 ± 0.1	7.79
9222	18/09/2014	JUVENA	46.13	-2.11	87	9 ± 0.8	13.43
9201	30/08/2015	JUVENA	45.63	-1.60	100	6 ± 0.1	13.50
9233	20/09/2015	JUVENA	45.95	-2.62	98	10 ± 0.6	19.63

Trawl	Date	Survey	Lat °	Lon °	Anchovy catch (% gr)	Mean length (cm ± sd)	Mean depth (m)
9240	24/09/2015	JUVENA	45.50	-3.09	99	12 ± 0.1	15.11
9002	01/09/2016	JUVENA	44.00	-6.48	98	6 ± 0.2	13.29
9009	06/09/2016	JUVENA	43.60	-4.32	91	8 ± 0.8	19.17
9015	11/09/2016	JUVENA	43.86	-1.70	90	7 ± 0.3	13.56
9002	03/09/2017	JUVENA	43.52	-1.88	97	9 ± 0.9	13.18
9004	04/09/2017	JUVENA	45.25	-1.34	100	8 ± 0.3	19.32
9005	05/09/2017	JUVENA	43.75	-6.83	97	11 ± 0.1	14.12
9009	15/09/2017	JUVENA	44.06	-7.53	100	8 ± 0.5	14.54
9019	20/09/2017	JUVENA	43.85	-7.53	87	9 ± 0.9	14.77
9215	18/09/2017	JUVENA	43.75	-3.04	100	5 ± 0.8	9.05
9223	21/09/2017	JUVENA	46.27	-2.22	99	9 ± 0.9	13.33
9234	05/10/2017	JUVENA	44.10	-2.24	100	15 ± 0.5	10.20
9236	06/10/2017	JUVENA	45.30	-2.21	99	12 ± 0.4	7.95
European anchovy – ex situ							
n1	11/07/2012	CAGE	47.63	-4.14	100	10 ± 0.1	3.26
n2_1	19/07/2012	CAGE	47.78	-4.53	100	10 ± 0.1	2.61
n2_2	20/07/2012	CAGE	43.50	-2.50	100	10 ± 0.1	2.51
n3_1	20/02/2013	CAGE	43.50	-2.50	98	10 ± 0.9	2.58
n3_2	20/02/2013	CAGE	43.50	-2.50	98	10 ± 0.9	2.55
Muller´s pearlside – in situ							
9010	08/09/2014	JUVENA	44.06	-5.10	91	3.0 ± 0.2	70
9002	31/08/2015	JUVENA	44.46	-8.20	100	4.3 ± 0.6	75
9006	05/09/2016	JUVENA	44.05	-5.10	100	2.6 ± 0.3	153
9012	08/09/2016	JUVENA	43.54	-2.70	97	4.9 ± 0.9	163
9020	22/09/2016	JUVENA	45.70	-2.82	100	4.0 ± 0.5	106
9006	06/09/2017	JUVENA	44.10	-7.52	36*	2.9 ± 0.5	120
9012	16/09/2017	JUVENA	44.48	-3.38	37*	2.7 ± 0.4	51
9013	17/09/2017	JUVENA	45.05	-2.20	100	4.7 ± 0.8	120
9015	18/09/2017	JUVENA	45.21	-2.45	97	3.6 ± 0.6	114
9017	20/09/2017	JUVENA	45.94	-3.03	100	3.8 ± 0.5	105
9031	27/09/2017	JUVENA	46.30	-4.31	97	4.1 ± 0.4	55

Ex situ data collection

TS measurements were made with a three-frequency (38, 120 and 200 kHz) Simrad EK60 split-beam scientific echosounder system installed in a floating 0.6 m x 0.6 m platform ~20 cm below the sea surface. The cage was cylindrical with 7 m depth and 16 m of diameter, with a mesh size of 0.4 cm. The floating platform was placed about halfway (~4 m) between the center and the border of the cage, where the highest abundance of fish was detected (**Figure 3.2**). The raft was connected to a logistic boat that housed the ancillary electronic equipment and the 12 V batteries used as power source. Day and night data were registered during the study but, after preliminary inspection of the data, only night experiments were used in the analysis.

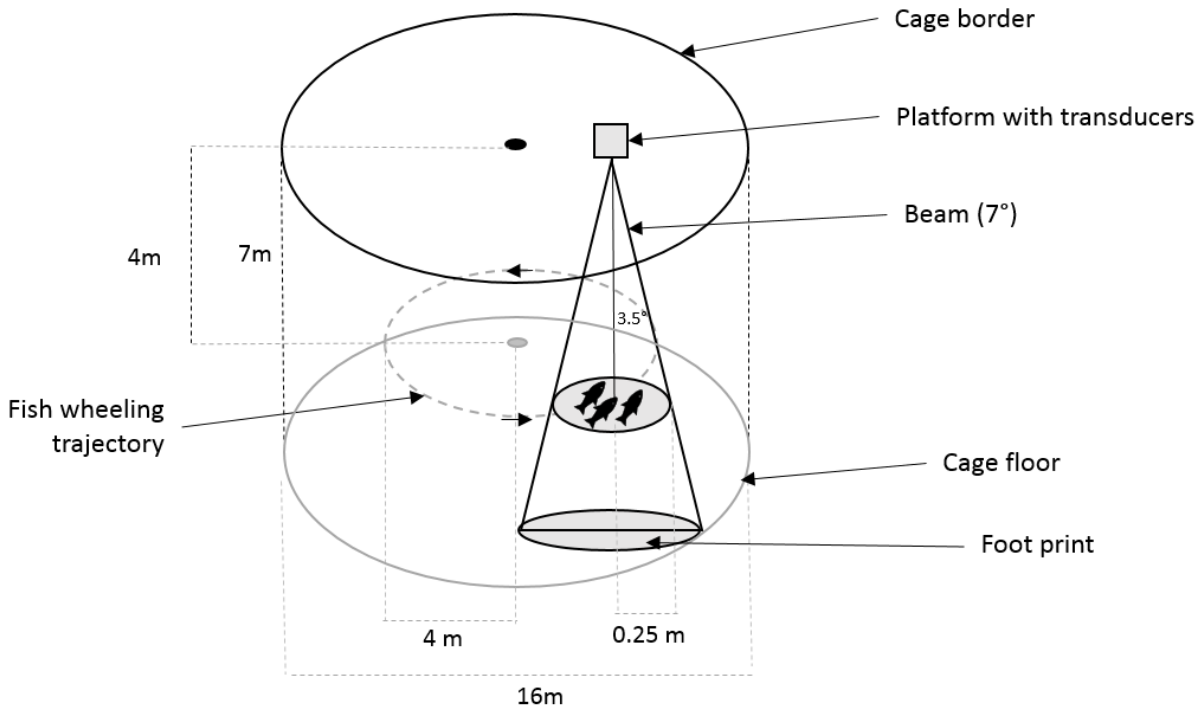

Figure 3.2 *Scheme of the experimental set up in the cage used for the ex situ measurements of European anchovy.*

Daytime data yielded significantly higher *TS* values, probably due to the higher packing densities, as was reported by the diver, hence likely subjected to higher probability of detecting unresolved multiple echoes. According to divers´ report, the presence of mackerel was restricted to the bottom layer, below 6 meters depth. Calibrations were done following the standard procedures (Demer *et al.*, 2015) and were repeated for all pulse durations and power settings (**Table 3.3**).

Table 3.3 Calibration settings of the *ex-situ* data. Note that the 200 kHz gain values differ from the expected increasing trend with time, because there were 2 different 200 kHz transducers used.

Year	Experiment (code)	Frequency (kHz)	Pulse duration (μs)	Power (W)	Gain (dB)	S_a correction (dB)
2012	**N1**	38	256	800	23.62	-0.66
		120	256	200	23.55	-0.59
		200	256	180	25.74	-0.44
2012	**N2**	38	256	800	23.51	-0.65
		120	64	200	25.23	-0.58
		200	64	180	24.74	-0.67
2013	**N3**	38	512	800	25.40	-0.75
		120	256	200	26.63	-0.61
		200	128	180	26.07	-0.76

Near-field experiment

Due to the cage dimensions (**Figure 3.2**) the ex situ acoustic measurements were unavoidably performed inside the near-field of the 38 kHz transducer (the critical range calculated to be 4.5 m) (Medwin and Clay, 1998). To test the validity of these data, an *ad hoc* calibration experiment was carried out, in which a reference target (a tungsten carbide sphere of 38.1 mm of diameter) was measured at different distances (2, 3, 4, 6 and 12 m) from a horizontally oriented 38 kHz transducer. The experiment was repeated

with the 200 kHz transducer (whose critical range is 1.33 m) for comparison. The transducers were first calibrated at 12 m, where the near-field effect was not biasing the target detections and were consecutively approached to the energy source. The gain differences between measures inside and outside the near-field were used to apply the corrections to the ex situ anchovy *TS* measurements.

3.1.2. Biological data

3.1.2.1. Pelagic trawls

Ground truth trawl hauls were performed based on the interpretation of the echograms, aiming to determine the species size distribution across the whole area of study. Both vessels performed trawl hauls during JUVENA surveys but only EB performed trawl hauls during BIOMAN due to the regular activities that take place in the RM during the latter one, related to the Daily Egg Production Method. Trawl samplings were done with a Gloria HOD 352 pelagic trawl of 15 m of vertical opening, provided with a 10-mm mesh size (bar length) at the cod end. Fishing trawls were performed during day and night, between 5 and 300 m depth at a mean speed of 4 knots. Acoustic data recorded during trawl hauls with predominance (>85%) of the target species in the catch (either anchovy or pearlside) were selected for the *TS* analysis (**Table 3.2**). Lengths were obtained from a random sample of >50 individuals of each haul and measured to 0.5-cm standard length classes (*SL*; cm) onboard the research vessel.

Catchability of small length classes of pearlside

Due to the high avoidance of mesopelagic fish to experimental pelagic trawls (Kaartvedt *et al.*, 2012; Peña, 2019), an *ad hoc* experiment was performed to test whether the mesh size codend was able to efficiently capture the whole length distribution of the pearlside population. For this, we used two different codends on the same model of pelagic trawl: one codend had the 10 mm minimum mesh used for the samples involved in the *TS* analyses and the other codend had a gradual mesh size, ranging from 8 to 2 mm, specially designed to target micronekton species. In total there were 21 positive hauls of pearlside for the experiment; from these, 13 were done with the small mesh and 9

with the large one. The experimental procedure consisted of measuring the length of 100 individuals from each trawl to compare the length distributions obtained with both gears using statistical analysis of variance (ANOVA).

3.1.2.2. Experimental cage

Ex situ *TS* measurements were obtained from two sets of anchovy individuals, captured in September 2012 (Set 1) and July 2013 (Set 2) in the Bay of Biscay**.** Both were captured by the purse seiner *Itsas Lagunak* and transported in the life bait fishing tanks onboard the vessel. The first set was composed of 120 anchovies that were kept in water tanks (1 m depth x 3 m diameter) in the Aquaculture School of Mutriku for eight months before being moved to the sea culture cage at the mouth of Mutriku harbor (Gipuzkoa, Spain; 43°18´N, 02°22´W) **(Figure 3.1).** The second set consisted of ~5,000 anchovy individuals mixed with ~100 horse mackerels and was transported directly from the purse seiner tanks to the harbor cage. After being moved to the cage, anchovies were left at least two days to settle before starting the experiments. A diver visually inspected the cage periodically for maintenance, feeding and monitoring the fish. Two groups of measurements (N1, N2) were carried out using the first set of anchovies and one (N3) using the second one. At the end of each set of measurements, 50 specimens were weighed and measured for standard length *SL*.

3.2. Data analysis

3.2.1. Echointegration data

3.2.1.1. Single frequency analysis

Acoustic energy was first cleaned from unwanted signals and then echointegrated using a threshold of -60 dB. The software used for this purpose was Movies+ (developed by Ifremer, France). The nautical area scattering coefficient (s_A; $m^2\,nmi^{-2}$) was allocated by species and size according to the hauls and the echogram typology. It was then used to obtain the mixed species echointegrator conversion factor (Simmonds and MacLennan,

2005). The s_A allocated to pearlside at a given time was used to examine the effects of the daily vertical migration (DVM). Finally, the abundance in numbers was obtained after dividing s_A by the mean backscattering coefficient of pearlside and multiplying by the mean weight and EDSU to obtain the annual biomass in the studied area.

3.2.1.2. Multifrequency analysis

Multifrequency analysis was done on acoustic data collected from hauls with more than 85% of the catch being one of the target species (***Figure 3.3A***) using Echoview software (*Echoview Software*, 2013). The deepest trawls were performed at mean depths of 163 m and 19.6 m in the case of pearlside and anchovy, respectively **(Table 3.2).** Due to the range limitation of the high frequencies, background noise that registered below 100 m at 200 kHz was removed **(*Figure 3.3*B)** following the techniques described by De Robertis and Higginbottom (De Robertis and Higginbottom, 2007) (cells of 20 pings by 5 samples, smoothed via 5 x 5 convolution into the background noise removal operator, with maximum noise of -125 dB and minimum signal-to-noise ratio (SNR) = 1.

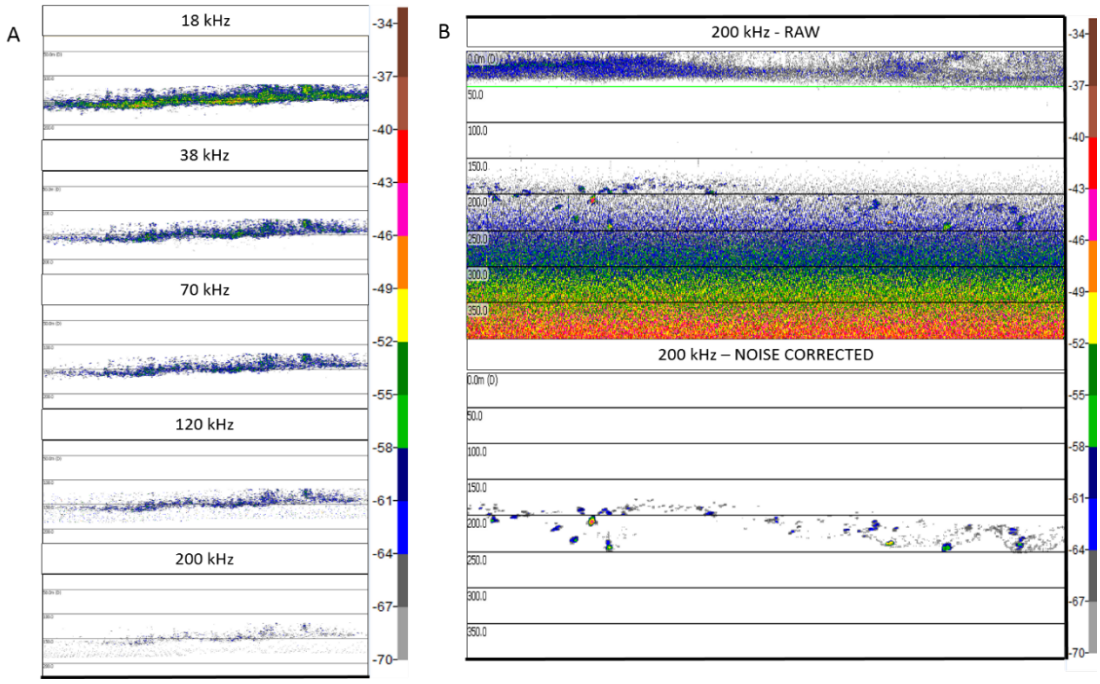

Figure 3.3 *Example echograms showing the typical pearlside multifrequency scattering layer (A) and the background noise correction applied to the 200 kHz frequency, at depths greater than 100 m (B).*

Frequency-dependent dB difference

Echointegrations were done using Echoview Software Pty Ltd, 2013, version 5.2 (*Echoview Software*, 2013) over cells of 50 m vertical x 0.1 nautical mile with a -70 dB minimum threshold; subsequent analyses were performed in R software (*R: A language and environment for statistical computing*, 2017). ΔMVBS between frequencies is often used to discriminate between scattering groups (Madureira *et al.*, 1993; Massé, 1996; Murase *et al.*, 2009; Lezama-Ochoa *et al.*, 2011; Gastauer *et al.*, 2017). In this thesis, a bi-frequency algorithm (Ballón *et al.*, 2011; Lezama-Ochoa *et al.*, 2011) was used on the in situ experiments, based on the differences in mean volume backscattering strength (S_v [dB re 1 m^2 m^{-3}]) at 38 and 120 kHz, to separate swimbladdered fish from fluid-like organisms or macro-zooplankton. A binary matrix was created from the data selected by the algorithm, and applied as a mask to the three frequencies of study using Echoview (*Echoview Software*, 2013). All the echograms were visually inspected to cross-check the correct performance of the algorithm. ΔMVBS was calculated using 38 kHz as the reference frequency and all averaging was performed in the linear domain and converted back to the logarithmic scale.

3.2.2. TS analysis

3.2.2.1. Single target detection

TS values were derived from echosounder data using the Echoview single target detection algorithm for split beam echosounders (Soule, 1997). A -70 dB minimum threshold was applied with a pulse determination level of 6 dB. The minimum and maximum normalised pulse lengths were 0.7 and 1.5, respectively, the maximum beam compensation applied was 6 dB and the maximum standard deviation of minor and major axis angles was 0.6 degrees.

Multiple targets

To reduce the expected bias derived from the multiple targets´ detection, all measurements were made at night to facilitate the detection of single fish targets.

Measurements at the cage were performed using different pulse durations (64, 128, 256 and 512 μs) to check whether the values obtained varied at increasing sampling volumes (*i.e.*, decreasing vertical resolutions) due to higher failure probability of the single target discrimination algorithm for larger volumes.

The preliminary analysis performed on the four methods described in the methodology section: *Multiple targets*, was used to discard the methods that were not effective in removing multiple target detections. The standard phase deviation did not affect mean *TS* values (varied less than 0.5 dB) and was thus discarded. The multiple frequency and the high-density filtering methods provided rather similar results (differing in 2, 0.8, ~3, ~3 and 2.5 dB at 18, 38, 70, 120 and 200 kHz frequencies, respectively). However, since the maximum distance between the spatial coordinates of the detections at different frequencies was larger than the typical size of the target species, the multiple frequency method was not considered reliable. This thesis, therefore focused on the high-density filtering method.

This approach consisted in filtering the areas of the echogram with highest densities of fish individuals, thus with higher probability of failure of the single target detection algorithm. The number of fish per echo-integrated volume was determined by (Sawada *et al.*, 1993) as:

$$N_V = \frac{c\tau\Psi R^2 s_V}{2\sigma_{bs}},$$

where c is the speed of sound in water in ms^{-1}, τ is the transmit pulse duration in seconds, Ψ is the equivalent beam angle in steradians, *R* is the target range in meters, s_v is the volume backscattering coefficient and σ_{bs} a preliminary value for the backscattering cross section (Maclennan et al., 2002), i.e., the linearized *TS* value, which is normally obtained from the length distribution of the target fish and a *TS*-length model.

In general, the high fish density filtering procedures were able to reduce the bias considerably (Foote K.G. *et al.*, 1986; Soule *et al.*, 1996; Scoulding *et al.*, 2015). The difficulty relied on determining the appropriate density threshold, because, it was observed in our case, that the smaller the threshold applied, the lower were the obtained *TS* values in an endless progression. In order to provide a valid criterion for

establishing a fish density threshold, the diagnostic tools for unbiased *TS* estimation by (Gauthier and Rose, 2001) was applied. According to it, the high fish density threshold was obtained from the comparison of the fish density in a given volume N_V and the number of single targets detected by the algorithm in the same volume:

$$T_V = \frac{c\tau\Psi R^2 \mathrm{target}_\Omega}{2V_\Omega},$$

where V_Ω is the volume at the cutoff angle omega and $target_\Omega$ is the mean number of targets per ping. The threshold was identified when the number of single targets reached saturation due to higher probability of detecting multiple targets (Gauthier and Rose, 2001). Thus, the echogram was divided in a grid of regular cells and calculated T_V and N_V at each cell. We represented T_V against N_V and the threshold was chosen at the inflection point, if any. A windowing smoothing process was applied by grouping the fish densities by ranges to allow the appearance of the pattern. Also, as the sharpness of the inflection point would depend on the effectiveness of the single target detection algorithm, in order to try to obtain a clearly identifiable peak, a relatively strict single target detection algorithm (in terms of rejection of multiple targets) was applied. Signals were filtered to reject pulses narrower than 70% and wider than 150% than the transmitted pulse, and the maximum standard deviation of the sample angles at each pulse was set to 0.2 degrees in both dimensions, using the full 6 dB beam compensation (corresponding to a beam angle of around 7º). A sensitivity analysis was run to test the applicability and results of the method at different decreasing cell scales: from 10 m x 100 pings, 10 m x 50 pings, 10 m x 25 pings and 10 m x 10, decreasing until 1 ping (which, given that 1 ping ≈ 0.15 m, resulted in grid cells from 1500 to 1.5 m^2). For each resolution, a different threshold was calculated by modifying the parameters that allowed the inflection point representation to be clear (such as the sequence of *Nv* thresholds at which the mean *TS* values are obtained for calculation). Due to the differences in number and spatial distribution of the targets at each cell size, the mean *TS* values were weighted to the number of targets in each cell.

3.2.2.2. TS-length relationship

Based on the amount of data available from each species, the *TS*-length relationship was determined following two different procedures.

TS-L for pearlside

In the case of pearlside, a 20log SL relationship was assumed to produce b_{20} estimates at five frequencies (18, 38, 70, 120 and 200 kHz) by the least-squares fitting procedure (MacLennan and Menz, 1996). The filtered *TS* dataset was fit to a normal distribution derived from the fish size histogram of the catches (modelled *TS* distribution assuming 20 log *SL*) to evaluate the mean, standard deviation (*SD*) and b_{20} of the best fit, given by the coefficient of determination (R^2).

TS-L for European anchovy

In the case of anchovy, the number of acoustic-trawls available for analysis permitted to perform a free-fitting linear relationship of mean *TS* versus mean length values, to determine the most suitable *a* value.

3.2.3. TS *interpretation*

3.2.3.1. Swimbladder morphology

X-ray images

Random subsamples were frozen in liquid nitrogen immediately after being captured and stored in individual plastic bags at -15 ºC onboard the research vessel. Four months after being captured frozen samples (283 pearlside individuals and 12 anchovies) were carefully removed from the plastic bags and set in order by trawls. This was done in the laboratory under a temperature-controlled environment (0° C) to minimise the damaging effect on the biological structures. The three cross-sectional dimensions of the swimbladder length (L_{sb}; cm), height (H_{sb}; cm) and width (W_{sb}; cm) plus the tilt angle (θ_{sb}) were determined based on soft X-ray images (IntechForView CR system) of the lateral and dorsal aspects of the fish **(Figure 3.4)**. Only the specimens with undamaged swimbladders (63 pearlside individuals and 4 anchovies) were considered for the

measurements (i.e. there were some cases in which these were absent or disfigured and bubbles of air were visible elsewhere from the swimbladder). The dimensions of the detector plate were 430 mm x 350 mm with a pixel size of 86 µm. Samples were located at 1 m from the source and exposed to 40 kV per 1.6 mA/sec.

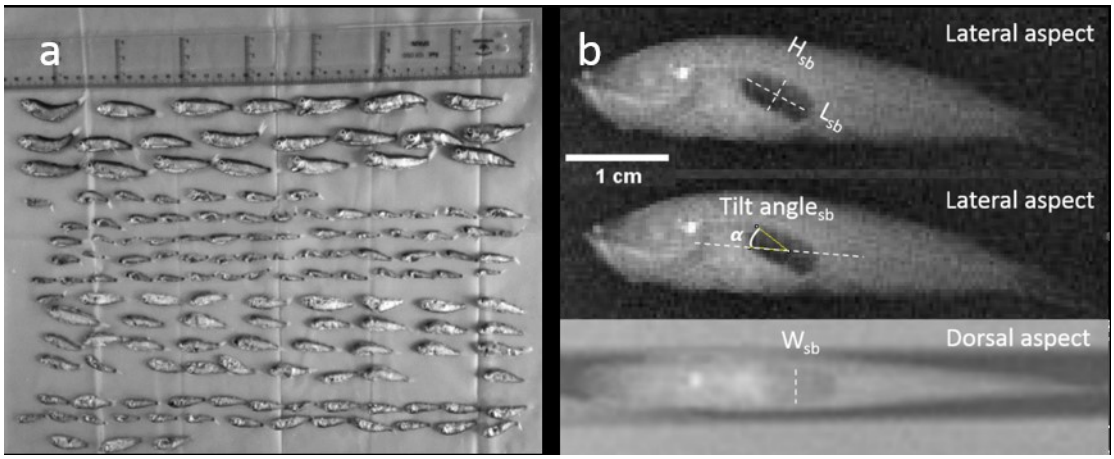

Figure 3.4 *Example showing the spatial arrangement of fish samples for the X-ray session (a). Soft X-ray images of the lateral and dorsal aspects (**b**) of a specimen of M. muelleri (standard length, SL = 47 mm). A 1 cm scale bar was included.*

3.2.3.2. Modelling pearlside - Prolate spheroid model (PSM)

The effects of depth and size on the swimbladder target strength were analysed using a scattering model that applied an ellipsoidal approximation for the swimbladder (Andreeva, 1964; Weston, D. E., 1966; Love, 1978; Furusawa, M., 1988; Ye, 1997).

The semi-major (a = $L_{sb}/2$) and semi-minor axes in the lateral (b = $H_{sb}/2$) and dorsal (c = $W_{sb}/2$) aspects were used to calculate the equivalent sphere radius a_{esr} (Strasberg, M, 1953):

$$a_{\mathrm{esr}} = (a\ b\ c)^{1/3}$$

All the equations used in this study, as well as the environmental and material properties, were adopted from previous studies (Andreeva, 1964; Love, 1978) (**Table**

3.4). The sequence in which the different equations of the model were used followed the same structure as in Scoulding *et al* (Scoulding *et al.*, 2015).

Although pearlside is a physoclist species (Marshall N. B., 1960), different assumptions related to the depth dependence of swimbladder volume were compared. (1) The first assumption implied that the swimbladder dimensions were independent of depth due to volume compensation associated with physoclist species (Kloser *et al.*, 2002; Fujino, T. *et al.*, 2009; Peña *et al.*, 2014; Peña and Calise, 2016); thus, we assumed no effect of Boyle´s law. (2) A pressure-induced volume reduction of the swimbladder was considered according to Boyle´s law (Godø *et al.*, 2009; Scoulding *et al.*, 2015; Proud *et al.*, 2018) by which the dimensions at the fishing depth were expected to be smaller than those observed at the surface. In this case, the following model was used:

$$\sigma_z = \sigma_0(1 + \frac{z}{10})^{\alpha},$$

where σ_z is the backscattering cross-section at depth *z*, σ_0 at the surface and α is the estimated contraction rate parameter (-0.67 for a free ellipsoid) (Ona, 2003). (3) This assumption accounted for the mechanical stress of the fish derived from the trawling process, where α was treated as a floating parameter of values ranging from 0 to -0.67. Values for mean ($\bar{\theta}$) and standard deviation ($\boldsymbol{\sigma}_\theta$) of tilt angle were obtained from the X-ray images. (4) Finally, the whole space of combined parameters was explored, using γ, $\bar{\theta}$ and $\boldsymbol{\sigma}_\theta$ as floating parameters. Except for the third variant of the model, in which the tilt angle parameters were determined from the X-ray images, the other three assumptions explored normal distributions with mean values ranging from 0–70° and standard deviations of 0–30°.

Table 3.4 *Model parameters*

Model parameters	Symbols	Units	Values
Sound speed	c_w	m s^{-1}	1490
Density of sea water	ρ_w	Kg m^{-3}	1026
Density of fish flesh	ρ_f	Kg m^{-3}	1050
Density of air	ρ_a	Kg m^{-3}	1.3

Ratio of specific heat for air (swimbladders)	γ_a	-	1.4
Specific heat at constant pressure for air (swimbladders)	cp_a	Cal kg^{-1} $°C^{-1}$	240
Surface tensión	s	N m^{-1}	200
Thermal conductivity of air	κ_a	Cal m^{-1} s^{-1} $°C^{-1}$	5.5 x 10^{-3}
Real part of complex shear modulus of fish tissue	μ_r	N m^{-2}	1 x 10^6
Complex part of shear modulus of fish tissue	μ_i	N m^{-2}	3 x 10^4

The Akaike information criteria (AIC) was used to select the best variant of the model because it considers the goodness of fit of the model and penalises the use of optimised parameters over the use of parameters with fixed values.

$$AIC = nlog(SS_{res}) + 2(p+1) - nlog(n)$$

where *n* is the number of observations and *p* is the number of floating parameters used. The optimal model was then used to interpret the actual swimbladder behaviour of pearlside.

3.2.3.3. Modelling European anchovy – Method of Fundamental Solutions (MFS)

Anchovy is a physostomous fish with a dual chambered swimbladder, which the simulation simplified as a two chambered prolate spheroids (Andreeva, 1964; Weston, D. E., 1966; Love, 1978; Furusawa, M., 1988; Ye, 1997), PS_1 and PS_2, being the major axis of PS_1 orthogonal with respect to the incident acoustic pulse and the major axis of PS_2 tilted α with respect the major axis of PS_1 (**Figure 3.5**). The model also considered the backbone contribution, expected to attenuate the swimbladder signal (Pérez-Arjona *et al.*, 2018), but discarded the flesh contribution. The prolate spheroids dimensions and the tilt angle were based on soft X-ray images. The calculations were carried out for mean standard length S*L*=10.5 cm, with corresponding PS_1 and PS_2 dimensions given by: length (semi-major axes, a_1= 0.625 cm and a_2=0.5 cm), height (semi-minor axes, b_1=0.2 cm and b_2=0.2cm) and width (semi-minor axes c_1= b_1 and c_2= b_2), and relative angle θ=12 degrees.

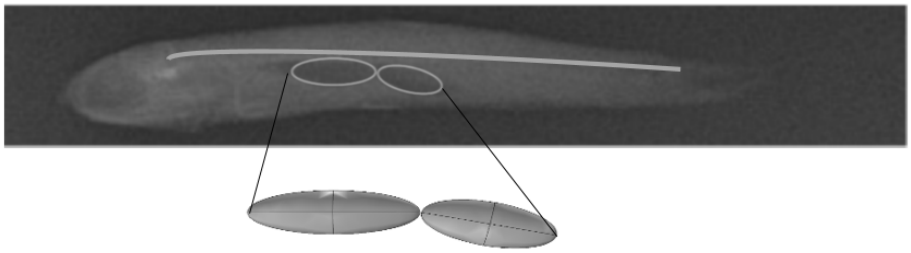

Figure 3.5 *Lateral radiograph of a specimen of Engraulis encrasicolus showing the two connected swimbladder chambers (PS1 and PS2) and the backbone. Fish length = 10.1 cm, fish height = 1.04 cm.*

The method of fundamental solutions was used to solve the three-dimensional Helmholtz equation in the frequency domain (Fairweather *et al.*, 2003). The two chambered swimbladder was considered a pressure-release surface and the fish backbone was modelled as a fluid filled (ρ=1100 kg/m^3, c=2270 m/s) straight cylinder (length=9 cm and radius=1mm) with smooth edges surrounded by homogeneous host medium (sea water with acoustical properties ρ=1026 kg/m^3, c=1490 m/s). The basic principle of the MFS is that the sound field in a homogeneous region can be simulated by the linear superposition of the effects of a number of virtual sources, each one with its own amplitude, and imposing boundary conditions on the scatter surface (Fairweather *et al.*, 2003; Pérez-Arjona *et al.*, 2018). The MFS virtual sources were located with at least 6 sources per wavelength to adequately resolve the acoustic wave. For the sake of comparison with experimental measurements, the acoustic source has been considered the specific case of the far field of a circular piston, as an idealization of a scientific echosounder transducer. Additionally, the MFS was applied on short-range distances to be compared with the near-field experimental results. The transducer size was chosen to produce a half-beam angle at −3 dB of 3.5° following the transducers' specifications of Simrad EK60 scientific echosounders at the working frequencies. The MFS model was solved at the three working frequencies used in measurements 38 kHz, 120 kHz and 200 kHz and convergence tests were carried out for each frequency to guarantee the proper density mesh. The *TS* directivity was considered for incidence angle distribution θ (90±5°) and θ between (90±10°), being θ=90° the backscattering direction.

4. RESULTS

4.1. Mueller´s pearlside

4.1.1. Biological sampling

A total of 11 trawls where *M. muelleri* was the dominant species were used for the analyses (**Table 3.2**). Krill *Meganyctiphanes norvegica* contributed on average 3.6% of the total numbers, while squid (*Loligo vulgaris*), salps (*Salpasalpa*) and jellyfish (*Rhopilema spp.*) contributed to the catches to a lesser extent. Standard length distributions of pearlside ranged from 2.6 ± 0.3 cm to 4.9 ± 0.9 cm. A total of 63 individuals with apparently undamaged swimbladders were finally used for the morphological measurements. The pearlside swimbladder appeared as a regular-shaped single-chamber ellipsoid with a long (a=L_{sb}/2) and short (b=H_{sb}/2) lateral semi-axis and a short dorsal semi-axis (c=W_{sb}/2) and an average tilt angle of 24° ± 7° (**Figure 3.2**, **Table 4.1)**.

Table 4.1 *Results of the morphological measurements of the swimbladder (n = 63).*

	Symbol	Units	Range	Mean ± SD
Standard body length	L_f	cm	1.41 – 5.23	2.87 ± 0.78
Length	L_{sb}	cm	0.25 – 0.98	0.45 ± 0.14
Height	H_{sb}	cm	0.07 – 0.35	0.20 ± 0.07
Width	W_{sb}	cm	0.03 – 0.31	0.12 ± 0.06
Dorsal area	$A_{sb.D}$	cm^2	0.006 – 0.17	0.05 ± 0.03
Lateral area	$A_{sb.L}$	cm^2	0.01 – 0.18	0.06 ± 0.04
Long lateral semi-axis	a	cm	0.13 – 0.49	0.22 ± 0.07
Short lateral semi-axis	b	cm	0.03 – 0.16	0.08 ± 0.02
Short dorsal semi-axis	c	cm	0.01 – 0.15	0.06 ± 0.03
Swimbladder ratio	a/L_f	-	0.05 – 0.12	0.08 ± 0.02
Aspect ratio	Ɛ	-	0.09 – 0.47	0.26 ± 0.09
Tilt angle	θ	°	11.4 – 43.6	24 ± 7

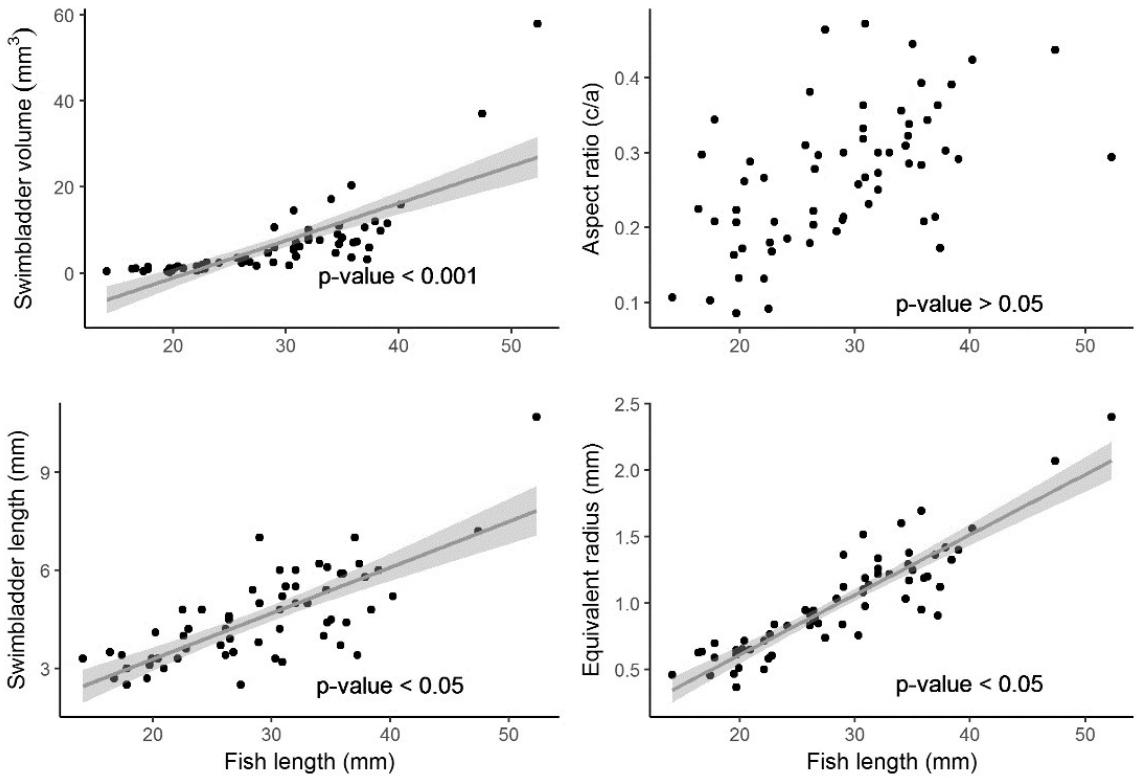

Figure 4.1 *Swimbladder morphological measurements. Relationship between standard length (mm) and the swimbladder volume, aspect ratio (Ɛ=c/a), swimbladder length and equivalent radius of the 63 specimens with gas-filled swimbladders. The shadowed area represents the 95% confidence intervals.*

Results indicate that for an increase in fish length, there is an increase in swimbladder volume (r^2 = 0.6, p < 0.001), length (r^2 = 0.07, p < 0.05) and equivalent radius (r^2 = 0.6, p < 0.05) **(Figure 4.1Error! Reference source not found.**). As for the aspect ratio, data suggested a positive correlation with fish length, although this was not significant (r^2 = 0.02, p > 0.05).

4.1.1.1. Capture efficiency vs mesh size experiment

The mean ± standard deviation body length of the fish captured with the 8 to 2 mm mesh was 3.3 cm ± 0.8 cm whereas for the 10 mm mesh it was 2.7 cm ± 0.7 cm, with the minimum sizes caught being ~1.5 cm in both cases (N=1201). To further assess this, in one site we repeated two trawls consecutively, targeting the same aggregation using

both mesh sizes. In this case, the mean sizes were 3.5 cm ± 0.4 cm and 3.6 cm ± 0.4 cm for the 8-2 mm and 10 mm mesh sizes, respectively, and the statistical tests provided non-significant differences between means ($p > 0.05$). According to this result both trawls seem equally able to perform sampling of small sizes in the range of this study and hence the biological sampling for the *TS* analysis was unbiased and representative of the true pearlside size distribution.

4.1.2. Spatial distribution patterns of Mueller´s pearlside in the Bay of Biscay

Mueller's pearlside was predominantly found off the shelf or at the outer part of the continental shelf, although it reached the 100 m isobath on the French shelf. Its vertical distribution during daytime ranged from 50 m down to the maximum depth sampled in this study (500 m) **(Figure 4.2)**. The location of the acoustic detections of pearlside in the water column varied with time being on average about 50 m shallower during nighttime **(Figure 4.3)**.

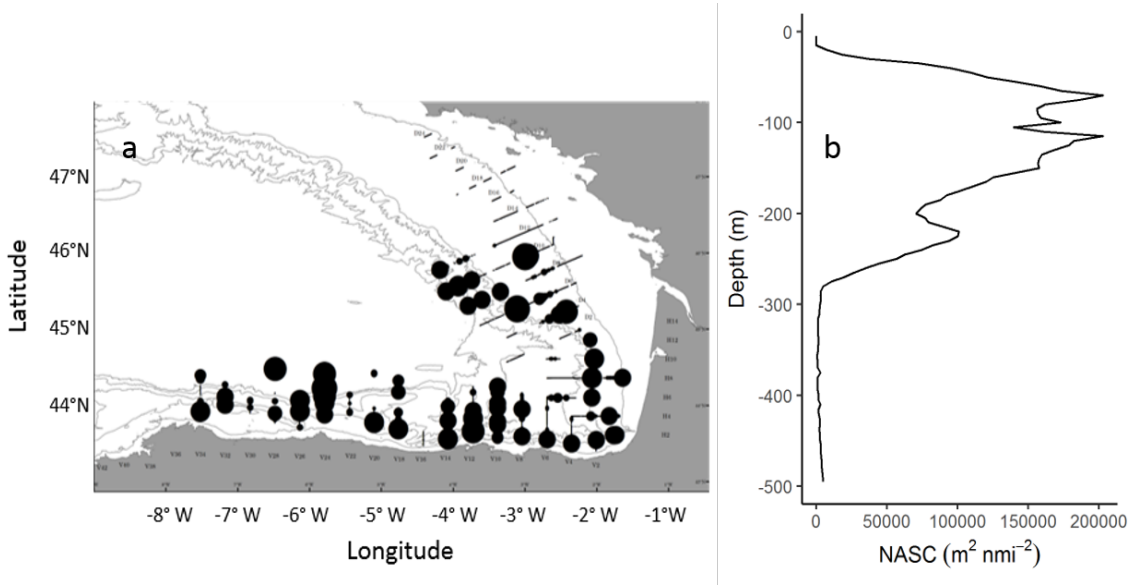

Figure 4.2 *Horizontal (a) and vertical (b) distribution of the Nautical Area Scattering Coefficient (NASC; m^2 nmi^{-2}) of M. muelleri. Bathymetric lines drawn in grey. This map is representative of the spatial distribution of pearlside within the area of study.*

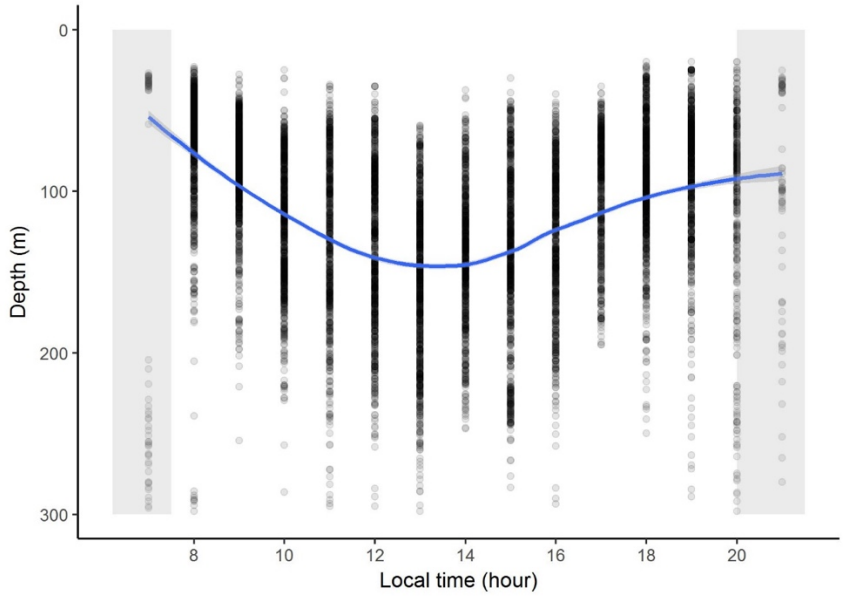

Figure 4.3 *Vertical migration. Diurnal vertical migration patterns of* M. muelleri *with mean depth (m) plotted against local time of day in hours. The density of points is proportional to the nautical area scattering coefficient (s_A; m^2 nmi^{-2}). Loess smoother represented as solid line.*

4.1.3. Frequency dependent dB difference

Pearlside $\Delta MVBS_{38}$ showed a general decreasing trend towards high frequencies. The observed pattern described the highest difference at 18 kHz with a sharp decline towards 38 kHz, consistent with the presence of a resonance peak at frequencies below 38 kHz. There was an approximately similar response at 38 and 70 kHz and a final decay for the 120 and 200 kHz frequencies **(Figure 4.4)**.

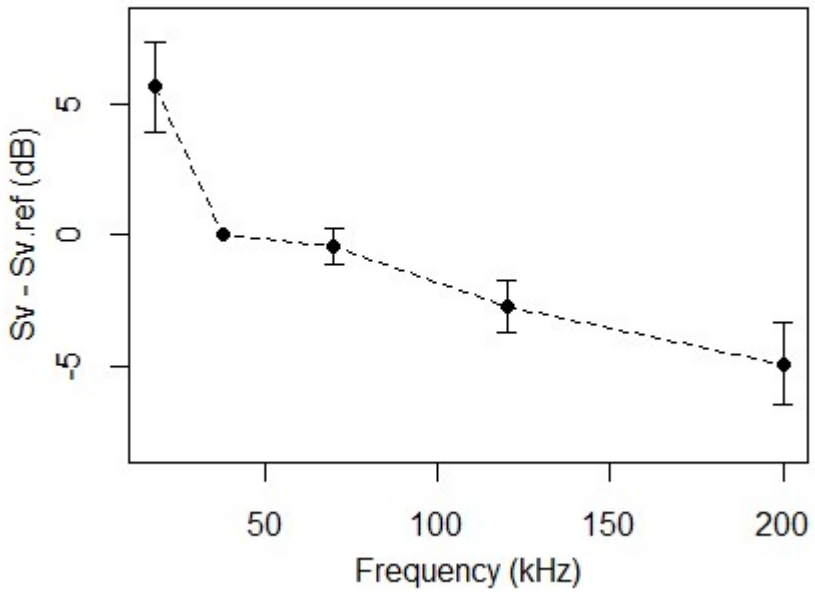

Figure 4.4 *Averaged in situ dB difference $\Delta MVBS_{38}$ of pearlside. A general decreasing trend was observed with increasing frequency. Error bars indicate 95% confidence interval.*

4.1.4. In situ TS

Even if the N_v values varied within the scale of measurement, the averaged *TS* values were constant regardless of the grid size, showing differences of less than 0.2 dB within scales. The smallest scale size (5 pings x 5 meters) was chosen for the N_v threshold determination. The point of inflection of the number of T_v on the fish number N_v **(Figure 4.5)** was observed at threshold values of 0.12, 0.07, 0.16, 0.06 and 0.04 fish per m^3 at 18, 38, 70, 120 and 200 kHz frequencies, respectively, meaning that only cells that passed those thresholds were retained for subsequent analysis. The filtered *TS* datasets consisted of 109, 154, 578, 255 and 158 targets at each respective frequency, on which the b_{20} fitting procedure was based.

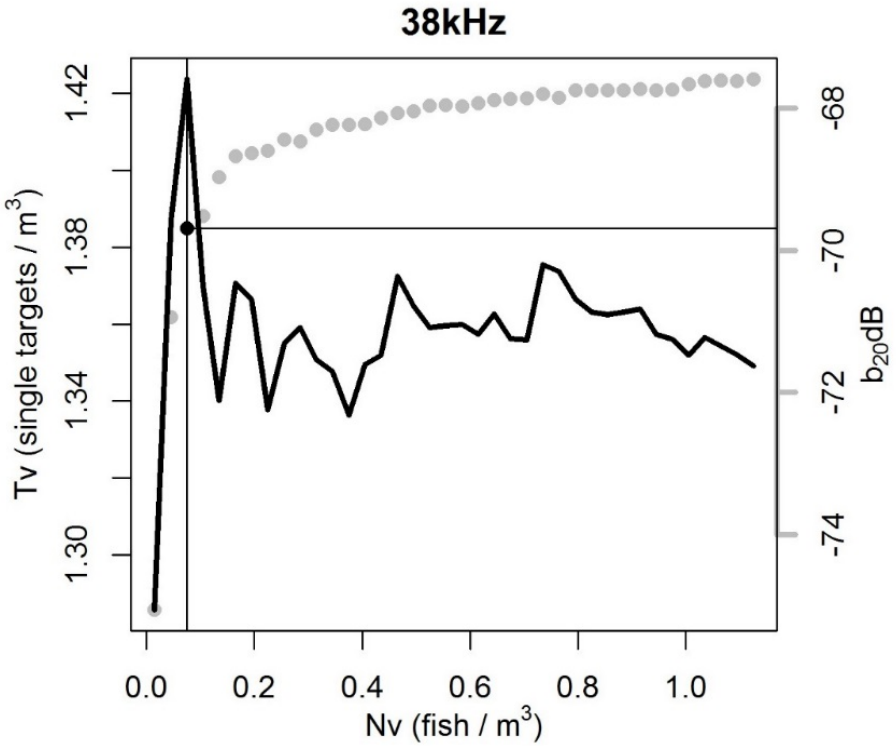

Figure 4.5 Example of the number of targets per sample volume (Tv) against number of fish per acoustic reverberation volume (Nv) at 38 kHz. Grey points are the b_{20} values averaged for every Nv threshold value. Black point indicates filtered b20 value at Tv/Nv inflexion point, that corresponds to a 0.075 Nv threshold.

The best-fit b_{20} values derived from the N_v-filtered *TS* and SL distributions were -65.9, -69.2, -69.2, -69.5 and -71.5 dB for the 18, 38, 70, 120 and 200 kHz, respectively, with coefficients of determination (R^2) ranging from 53 to 73% (**Figure 4.6**). These *TS*-length relationships correspond to the depth range of the filtered dataset (17–143 m) and standard fish length ranging from 2.7 to 4.3 cm.

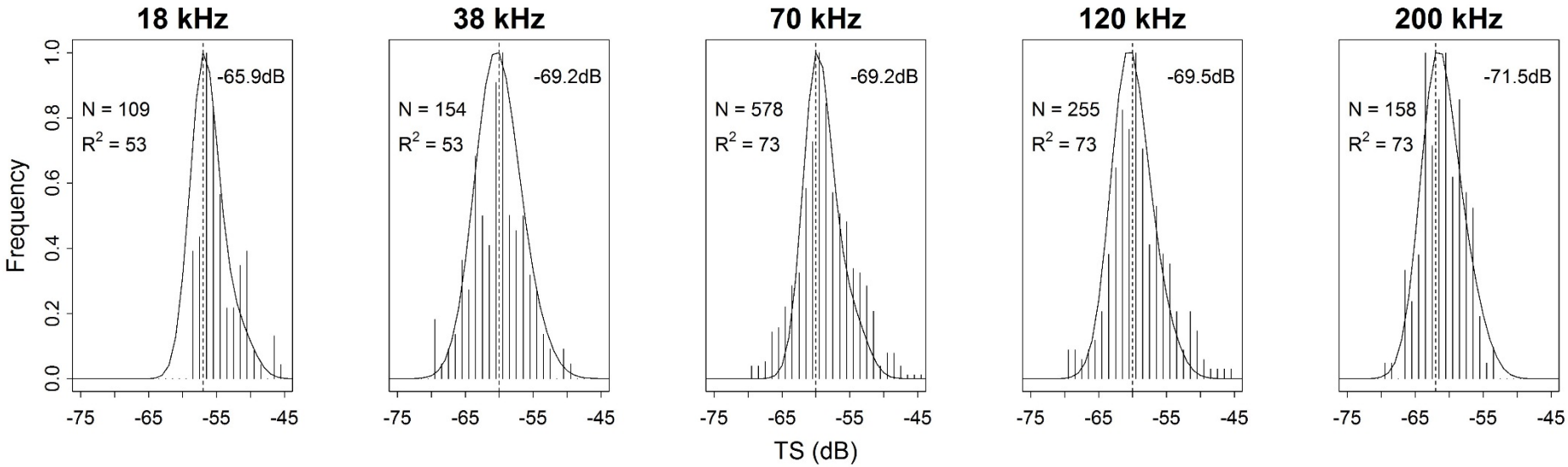

Figure 4.6 *Predicted and observed TS fitting procedure. The filtered TS dataset (black vertical solid lines) was fit with a normalized length distribution (solid curve) to evaluate the mean (dashed vertical line), standard deviation (2, 3, 2, 2.5 and 2.5 for 18, 38, 70, 120 and 200 kHz, respectively) and b_{20} (topright corner of each panel) of the best fit, given by coefficient of determination (R^2) of observed versus modelled TS distributions. N stands for the number of targets that passed the filtering process and were used in the optimization.*

4.1.5. Biomass estimation

The biomass of pearlside in the Bay of Biscay was calculated with single frequency data registered at 38 kHz over the four years analysed in this study. It followed a decreasing trend from 2014 to 2016 but reached maximum numbers in 2017. The minimum and maximum estimates were 70.7 and 161.7 thousand tons in years 2016 and 2017, respectively (**Table 4.2)**.

Table 4.2 *Time series of biomass estimation of pearlside in the Bay of Biscay.*

Year	**<s_A>** (m^2nm^{-2})	**Area** (nm^2)	**Mean weight** (gr)	**Mean length** (cm)	**Biomass @ 38 kHz** (Tn)	**CV** (%)
2014	309.3	21,073	0.51	3.42	142,242	30
2015	630.79	8,663	0.58	3.96	127,447	35.3
2016	348.96	7,189	0.36	3.44	70,784	68.2
2017	511.30	13,313	0.53	3.68	161,713	35.7

4.1.6. Acoustic scattering model

The general behaviour of the backscattering model used was illustrated by simulating the *TS*-length and *TS*-depth relationships for swimbladder contraction rates $\alpha = 0$ and $\alpha = -0.67$ **(Figure 4.7)**. Regarding the size effect, modelled *TS* values decreased with decreasing swimbladder size, but the resonance frequency increased. The effect of size on the resonance frequency was clearly seen when $\alpha = -0.67$, but smaller when $\alpha = 0$ (estimated to be below 50 kHz for all the examined sizes). The effect of depth on the resonance frequency was minimal when $\alpha = 0$, but clearly observed when $\alpha = -0.67$. Maximum *TS* values at resonance decreased with depth, having a major effect when $\alpha = -0.67$. Depth variations produced major changes on smaller swimbladder sizes.

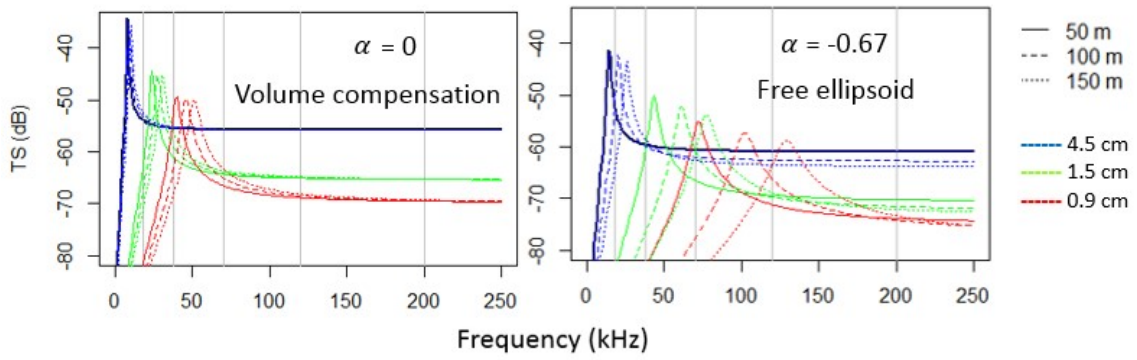

Figure 4.7 *Scattering model simulations. Resonance scattering model behavior for simulations of different sizes and depths, considering swimbladder contraction rates $\alpha = 0$ (left) and $\alpha = -0.67$ (right). In these theoretical simulations, broadside incidence ($\Theta = 0°$) was assumed*

When α was set to 0 (no pressure effect) and the tilt angle was used as a floating parameter, the optimised tilt angle was 70º ± 5 **(Table 4.3a)**. The lowest AIC value was achieved when using a fixed α = -0.67 (Boyle´s law effect), and the mean tilt angle (θ) that minimised the distance between the modelled and experimental *TS* values followed a normal distribution with a mean of 10º ± 5 **(Table 4.3b)**. The model simulation that assumed the measured $\theta \pm \boldsymbol{\sigma}_\theta$ from the X-ray images **(**24° ± 7**)**, produced an optimised contraction rate of -0.66 **(Table 4.3c)**. The highest AIC value was obtained when the three variables were treated as floating parameters, and the whole space of combinations among parameters was evaluated with the ranges defined above **(Table 4.3d)**.

Table 4.3 *Performance comparison (AIC, Akaike Information Criteria) of the different backscattering model variants tested. Mean depth and fish length averaged from filtered dataset:*

	Swimbladder contraction rate (γ)	**Mean tilt angle** (θ)	**SD tilt angle** ($\boldsymbol{\sigma}_\theta$)	**Number of optimized parameters (*)**	**AIC**
(a)	-0.66*	24**	7**	1	16
(b)	0	70*	5*	2	15
(c)	-0.67	10*	5*	2	8
(d)	-0.62*	65*	10*	3	19

The optimal model (α = -0.67 and θ = 10º ± 5) was plotted for a range of frequencies from 0 to 250 kHz, for a mean depth of 84.5 m and mean *SL* of 3.68 cm **(Figure 4.8)**. Additional curves were included using the mean depth and length from all the trawls used in this study (in grey). The *in situ* filtered *TS* data at the five frequencies of study (black points) fit the model curve closely **(Figure 4.8)**.

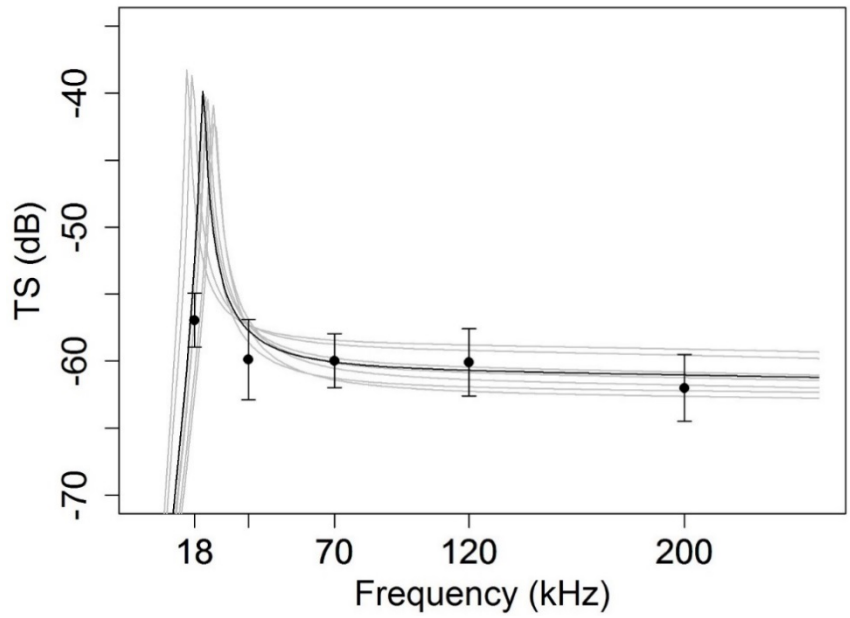

Figure 4.8 *Model vs filtered in situ TS data. Optimal model (α = -0.67 and Θ = 10º ± 5) plotted for frequencies from 0 to 250 kHz using mean depth 84.5 m and mean length 3.68 cm (black line). Additional curves show the model behavior using depths and standard lengths associated to the trawls used in the study (grey lines). Black dots are the in situ filtered TS values with error bars showing the standard deviation from the mean values.*

4.2. European anchovy

4.2.1. Data collection

The *in situ* data selection criteria retained a total of 53 hauls **(Table 3.2)**, 27 of which corresponded to the spring survey BIOMAN and 26 to the autumn one, JUVENA. All of them were performed during nighttime, where anchovy schools were observed (Boyra *et al.*, 2013) to break up into a layer of dispersed fish through the first meters of the water

column. Spring hauls were limited to the eastern part of the Bay of Biscay, covering the French coast, while autumn hauls covered a wider area, reaching 8ºW longitude. The *ex situ* experiments were performed in the inner part of the Bay of Biscay, in a common area for the spring and autumn surveys **(Figure 3.1)**.

4.2.1.1. Near field experiment

The analytical solutions of the on-axis pressure effect and the far field approximation obtained with the MFS model converged at 4.5 m from the source **(Figure 4.9A)**. The *TS* deviation between both curves described a decreasing pattern with distance **(Figure 4.9B)**. The gain differences measured between the near and far field during the experiments converged with the analytical solution at distances > 2.5 m **(Figure 4.9B)**. *Ex situ TS* measurements at depths smaller than 2.5 m were discarded for not being predictable by the model. Since the calibration in the cage was performed at 4 meters, *TS* measurements within 3.5 and 4.5 meters were considered unbiased and no correction was applied. However, measurements within 2.5 to 3.5 meters were corrected by subtracting 0.33 dB and values within 4.5 to 6 meters by adding 0.24 dB.

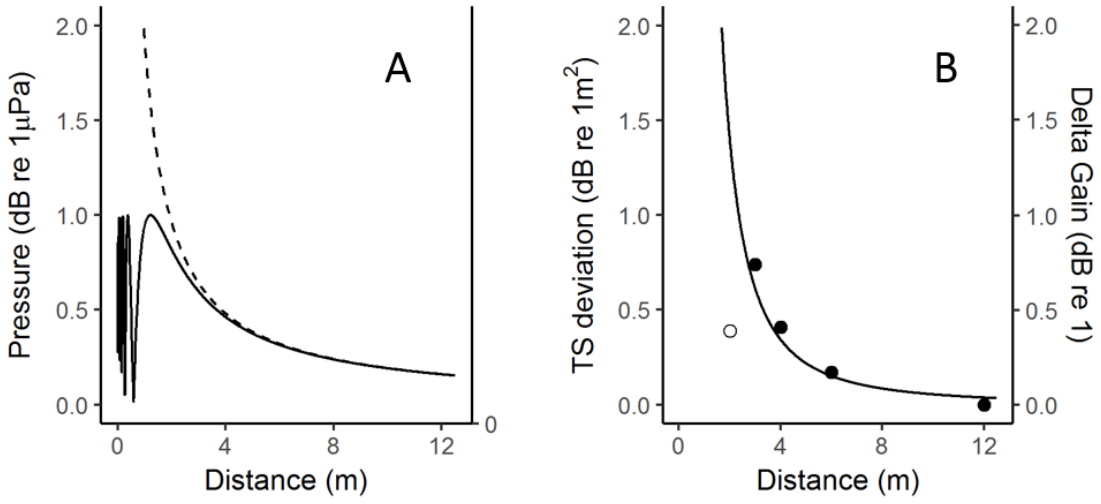

Figure 4.9 *(A) Analytical solution for pressure in the vertical axis (solid line) and the far-field approximation (segmented line). (B) TS deviation between the pressure in the vertical axis and far field analytical approximations (solid curve) at different distances from the source. The black points represent the experimental gain difference between near and far field. Deviation of the experimental and analytical solutions are relevant at distances below 2 m (empty circle).*

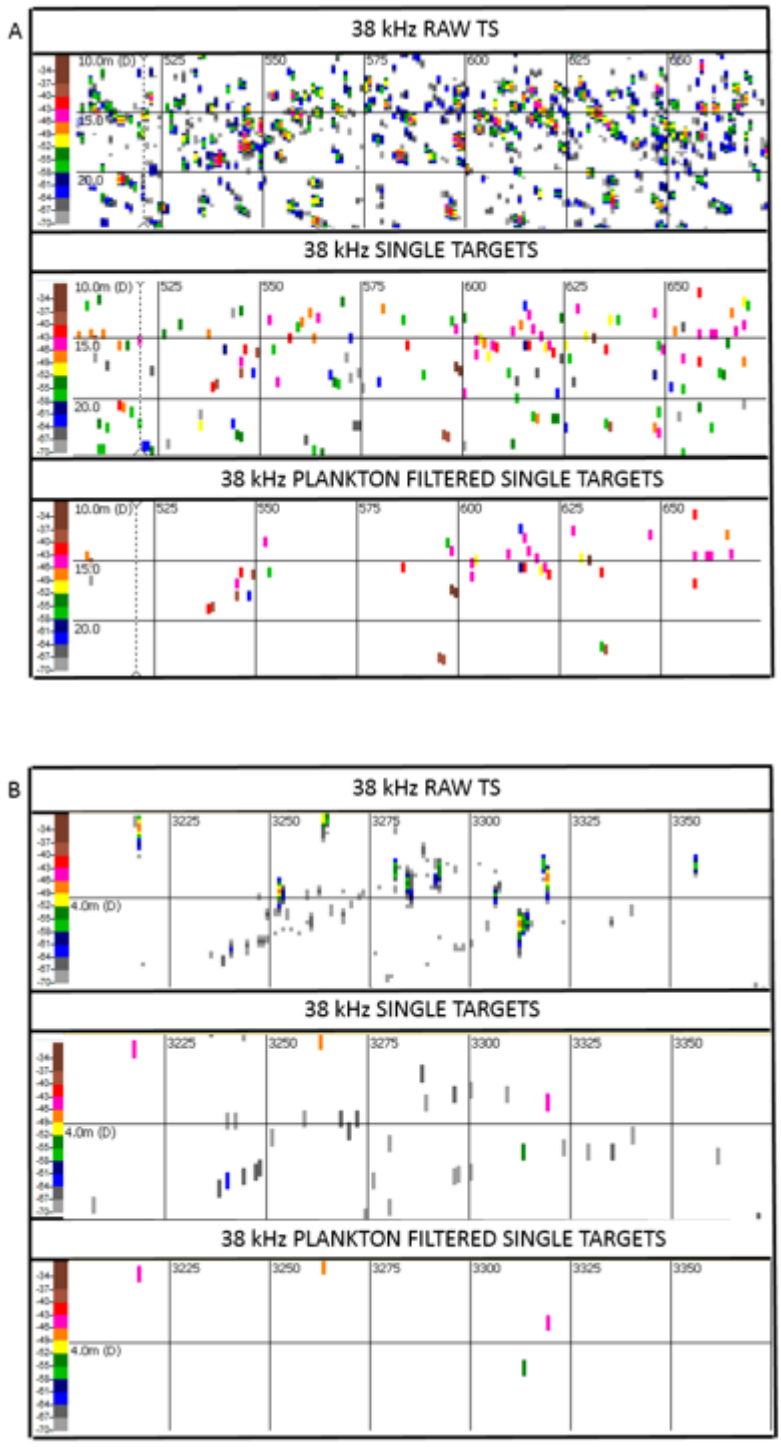

Figure 4.10 Example echograms illustrating the results of the plankton filtering process to the *in situ* (A: haul 179019) and *ex situ* data (B: N1).

4.2.2. Target selection

After the plankton filtering performance (an example is illustrated in **Figure 4.10A, B),** the application of the high-density filter to the *in situ* data retained 30%, 52% and 74% of the

targets at 38, 12 and 200 kHz, respectively. All three *ex situ* experiments were included in the analysis since no significant differences were observed among the mean *TS* values measured at different pulse durations **(Figure 4.11)**. A total of 6388, 15695 and 19012 targets were finally used for the *TS* estimates at 38, 120 and 200 kHz, respectively. The filtered dataset covered a depth range of 2.5 to 27.5 m. The fish length values measured from the different experiments ranged from 3.5 to 19.5 cm, with highest mean (±standard deviation) value obtained in spring 13.4 (±1.5) cm, and smaller mean values in the cage experiments and autumn survey: 10.4 (±1) and 10 (±3.4) cm, respectively. The highest size variability was observed in the autumn survey, with a wider distribution than in the spring and cage measurements (**Figure 4.12A**). The filtered *TS* distributions showed mean values at increasing operative frequencies of -43.3 (±1.5), -45.4 (±2.3) and -47.1 (±2.1) dB in BIOMAN, -45.4 (±0.9), -45.5 (±2.3) and -47.7 (±2.3) dB in the cage experiments, and -46.2 (±2.7), -49.4 (±2.1) and -50.3 (±2.5) dB in JUVENA **(Figure 4.12B).** All *TS* distributions were clearly monomodal except for the 120 and 200 kHz measurements from the cage, where the mode was less pure. The *TS* values, on the other hand, exhibited no clear relationship with depth (slope = 0.1, p-value =0.18, R^2=3%).

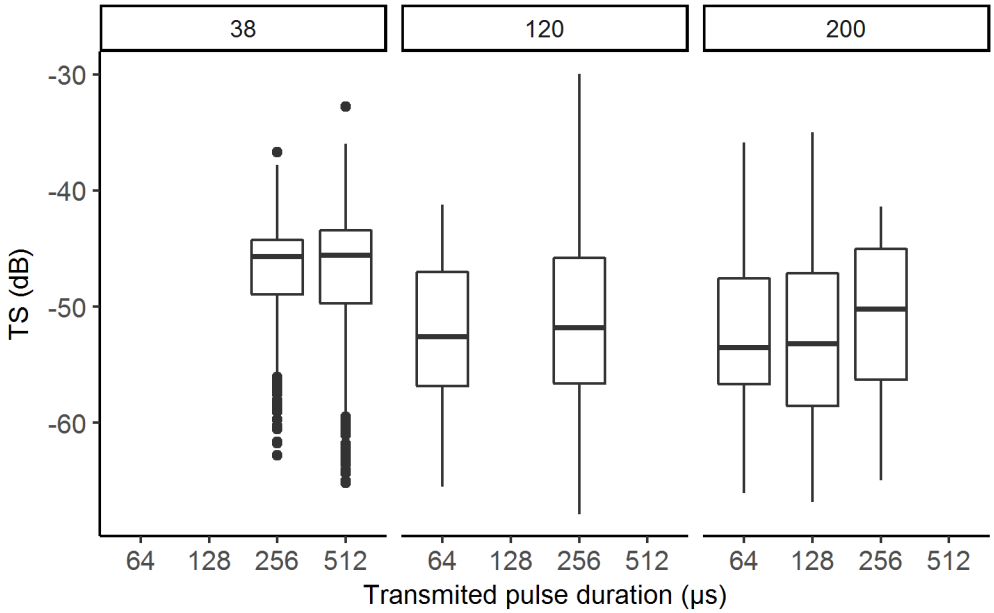

Figure 4.11 Boxplots summarizing *TS* distributions against pulse duration used in the *ex situ* experiments. Pairwise t-test produced p-values > 0.05 within pulse durations.

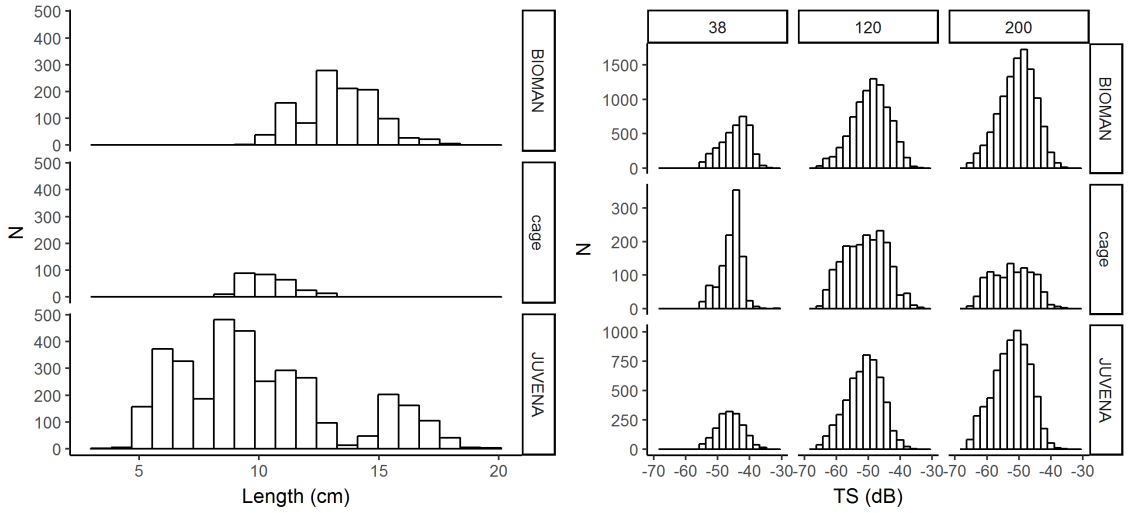

Figure 4.12 Length and filtered *TS* histograms grouped by *in situ* (BIOMAN, JUVENA) and *ex situ* (cage) measurements.

4.2.3. TS-length relationships

Overall, the measured *TS* values increased linearly with the logarithm of the fish length. In agreement with the corresponding mean body lengths, *TS* values are generally higher for the spring hauls, than for the autumn ones and the experimental cage results **(Figure 4.13)**. Overall, the three types of measurements *(ex situ* and *in situ* from both surveys) fitted nicely the same *TS* versus log-length regression. When the slope of the regression was forced to 20, the b_{20} values for the *in-situ* measured data were -66.5, -68.9 and -70.5 dB at 38, 120 and 200 kHz, respectively, and -66.1, -66.4 and -68.7 dB for the *ex-situ* measurements (**Table 4.4**). If the whole dataset was considered, these values were -66.5, -68.7 and -70.4 dB. The free fitting linear model produced significant results *in-situ*, with slopes of 18.2 and 23.5, non-significant results *ex-situ* and, when considering the whole data set, significant slopes slightly over 20 at the three operative frequencies, with intercepts at -68.8, -69 and -72.9 dB, respectively.

Table 4.4 Statistics of the empirical *TS*-L linear regression parameters. Significance codes: 0 `***´; 0.001 `**´; 0.01 `*´

	Frequency (kHz)	*a*	*b*	b_{20}	N
IN SITU	38	22.2***	-68.8***	-66.5***	53
	120	20.5***	-69.5***	-68.9***	53
	200	22.5***	-73.2***	-70.5***	53
EX SITU	38	34.1	-80.5*	-66.1***	3
	120	47.4	-94.3	-66.4***	3
	200	82.1	-131.9	-68.7***	3
IN SITU + EX SITU	38	22.2***	-68.8***	**-66.5*** **	56
	120	20.3***	-69***	**-68.7*** **	56
	200	22.4***	-72.9***	**-70.4*** **	56
THEORETICAL MODEL	38	16.9	-63	-66.2	-
	120	16.3	-65.8	-69.7	-
	200	19.8	-70	-70.3	-

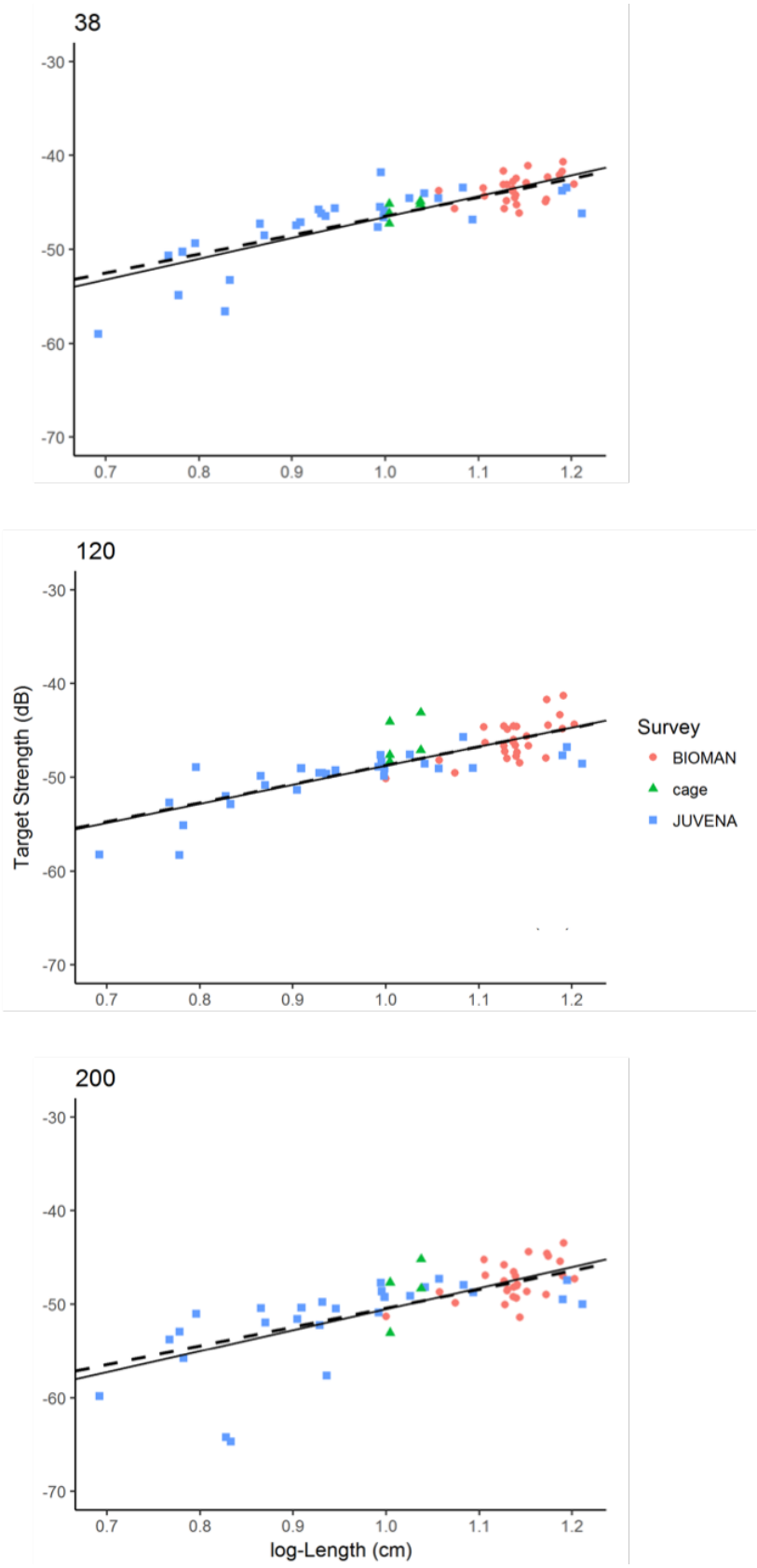

Figure 4.13 *Mean TS against total length (L) relationship. Bold solid line = experimental forced fitting (b_{20}); dashed line = experimental free fitting, and dotted line = numerical fitting (b_{20}). Red circles correspond to BIOMAN hauls, blue squares to JUVENA hauls and green triangles to the cage experiments.*

4.2.4. Acoustic scattering model

The two-chambered swimbladder and backbone simulations **(Figure 4.14)** predicted more directive patterns of *TS* against tilt angle at increasing frequencies, which led to steeper decrease of the *TS* values with beam angles for the first ±10º. Thus, although the maximum *TS* values that occurred at 12º from normal incidence, (i.e., normal to the oblique swimbladder chamber) were similar at all frequencies, the mean values were considerably higher for lower frequencies.

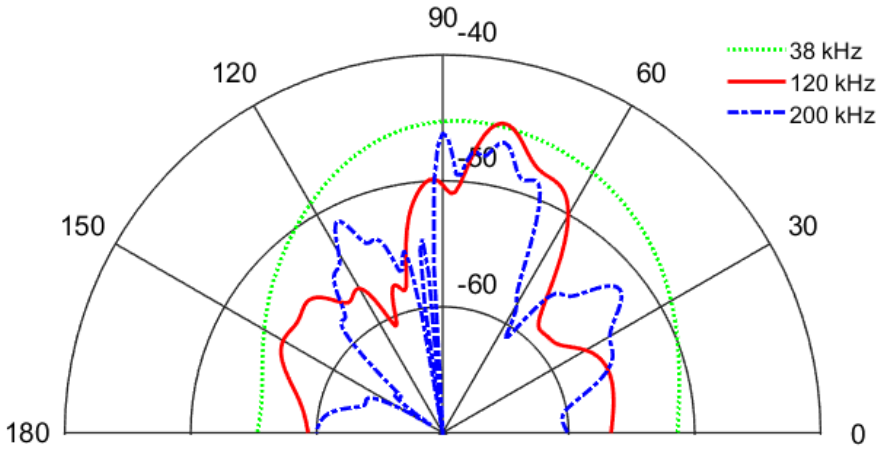

Figure 4.14 Beam directivity patterns obtained with the backscattering simulation of the two-chambered swimbladder plus backbone at the three frequencies of study. The maximum *TS* values are obtained for a tilt angle of 78° (12° from normal incidence). Although these maximum values are similar at all frequencies, the *TS* values averaged for SD ranges of ±5°, ±10° or ±15° are lower for higher frequencies.

5. DISCUSSION

5.1. TS measurements and processing

This thesis presents a comprehensive study aimed at determining the values of target strength (*TS*) and *TS*-length relationships of two important pelagic species in the Bay of Biscay, European anchovy and Muller´s pearlside. These are basic elements necessary to estimate their biomass, thus allowing proper management of both resources.

When measuring *TS* values for small pelagic species, two of the key difficulties are to apply a correct lower threshold (Weimer and Ehrenberg, 1975) and to avoid bias by unresolved multiple targets (Soule *et al.*, 1995). Being both, anchovy and pearlside, small pelagic species and subjected to potential bias due to unresolved multiple targets, they shared some common efforts concerning filtering for bias mitigation. First, all measurements were made at night to facilitate the detection of single fish targets. Then, data exploration would determine whether to apply further filtering or not.

The ex situ measurements´ results were similar at different effective resolutions of the acoustic sensors (**Figure 4.11**), supporting the notion that the relatively low fish density at the cage at night was sufficient to avoid multiple echoes and hence requiring of no additional filtering processes. As mentioned above, mean *TS* values at increasing sampling volumes are expected to increase owing to the higher probability of including multiple targets.

Conversely, measurements obtained from *in situ* experiments for both species were further filtered by removing the areas where fish density was above an empirically determined threshold value (Sawada, K. *et al.*, 1993; Ona, E. and Barange, M., 1999). One of the main issues associated to this method is that the filtered TS value is calculated based on a previous *TS* value used as initial input. However, the empirically determined threshold value (Nv) was proven independent of the horizontal scale at which it was calculated, thus avoiding the circularity-issue of calculating a *TS* value that is dependent on a previous one. The method presented here is based on preliminary tests performed in the early days of the development of this thesis, and published as part of a previous work (Boyra *et al.*, 2018). Even if this method was proven effective for the bias reduction derived from multiple targets, it should be noted that the signal from multiple echoes might not be entirely removed and a certain degree of bias may remain.

Anchovy data were collected during spring and autumn for 7 years, covering a wide range of fish lengths (3.5-19.5 cm) and physiological conditions. The size and TS distributions (**Figure 4.12**) at the different sampling periods reflect this seasonality, as the largest specimens were measured during the spring spawning peak (when only adults are present in the area) and the smallest during the autumn survey (when part of the adult stock is absent due to trophic migrations whereas juveniles predominate) (Boyra *et al.*, 2013). This study has shown significant positive correlations between *TS* and fish length and a good correlation between *in situ* and *ex situ* results. The range of sizes of anchovy used in this work practically covers the full range of sizes observed during the acoustic surveys of anchovy in the Bay of Biscay (4-20 cm). The optimal slope obtained for the whole data set at all frequencies was consistently close to 20 (**Table 4.4**), meaning that the horizontal cross-sectional area of the swimbladder changes proportionally to the square of the fish length, according to expectations (Simmonds and Maclennan, 2005). The non-significant *TS*-length relationship derived from the *ex situ* data was not considered relevant, instead being attributed to the small number of points (only three) available.

Despite the highly significant *TS*-length relation obtained, a few of the smallest anchovy trawls tend to provide lower mean *TS* values than expected by the fitted linear relationship (left part of **Figure 4.13**). Several potential causes were considered as responsible for this effect. For example, it could be a consequence of the tendency of the smallest juveniles of being more associated with plankton, which would tend to negatively bias mean *TS* values. This was checked by further inspecting the echograms and catch composition of those trawls in search of plankton, but neither the echograms nor the catches showed sign of higher than average proportion of plankton. Alternatively, it could be caused by different behavior of the smallest anchovies, which have been reported to change its aggregating patterns with growth, gathering in increasingly larger and denser shoals (Boyra *et al.*, 2016). A larger range of tilt angles caused by a less polarized swimming fashion could lead to a smaller mean *TS* value. This effect should be higher for the highest frequency, due to higher directivity, thus in agreement with our results. Another possible cause could be an allometric growth, or

perhaps a late inflation of the swimbladder, which would tend to produce comparatively lower *TS* values for the smallest size ranges.

At 38 kHz, the most used frequency in fisheries acoustics (Simmonds and Maclennan, 2005), recent studies have provided b_{20} = -68.6 dB on similar species *Engraulis anchoita* (Madirolas *et al.*, 2016), obtained from 11-17 cm specimens during night-time *in situ TS* measurements. Other experiments on *Engraulis japonicus* (Zhao *et al.*, 2008) have yielded *TS*-length relationships with b_{20} = -65.8 dB (Kang *et al.*, 2009) for lengths ranging 4.8-12.2 cm and -66.5 dB (Sawada *et al.*, 2009) for 10.6 cm. Thus, our values for anchovy (b_{20} = -66.5 dB at 38 kHz) are within the range of the latest published *TS* values and *TS*-length relations obtained for engraulid species.

The only previous work to examine the *TS* of European anchovy, obtained by funneling the targets through a net with an open cod-end, yielded a mean b_{20} of -65.2 dB from 12.5 cm anchovies at ~60 m depth at 70 kHz (Doray *et al.*, 2016). This methodology avoided multiple target bias, but at the expense of forcing the anchovies to swim almost horizontally (i.e. with a narrower distribution of tilt angles than expected to be their natural behavior) towards the net mouth. Although the results of that work are not directly comparable with our own due to differences in frequency and behaviour, they can be considered qualitatively consistent. These authors' theoretical 2 dB decrease predicted at 38 kHz is consistent with a reduction in the range of tilt angles illustrated in **Figure 4.14**.

One should take into account that the depths of the anchovies studied (2.5-27.5 m) are in the upper range of the typical 5-120 m of the acoustically sampled depth for assessment, which constitutes a limitation for determining the depth dependence of *TS*. However, given that anchovy is a physostomous species and thus unable to compensate its swimbladder volume against pressure changes, *TS* can be expected to decrease with depth according to Boyle's law, as has been observed in previous measurements of anchovy (Zhao *et al.*, 2008) and other physostomous species (Ona, 2003).

Mesopelagic fish are known to avoid or escape from fishing trawls (Pakhomov *et al.*, 2010; Heino *et al.*, 2011; Kaartvedt *et al.*, 2012; Peña, 2019) biasing the length distribution of the population (Gartner, 1988; Itaya *et al.*, 2007; Davison *et al.*, 2015a).

However, the results of the mesh size experiment (section 4.1.1.1) proved that the used fishing gear was able to sample the whole size range found in our area of study (1.5–6.5 cm). However, it is recommended to test the capture efficiency of each sampling area before performing studies on pearlside and, if significant differences are found, minimise the associated bias by applying a capture efficiency correction factor (Davison *et al.*, 2015a).

The derived *TS* versus length relationships show consistency with the positive and significant correlation found between standard fish length and volume of swimbladder for this species (**Figure 4.1**). This represents a step forward compared to a recent study on the same species (Scoulding *et al.*, 2015) where neither a consistent *TS*-length relationship was achieved nor clear relationships were found between standard fish length and swimbladder volume. The *TS* estimates of pearlside presented in this thesis agree with *TS* estimates of pearlside from previous studies (**Table 5.1**): values ranging from -60.4 to -52.5 dB at 38 kHz were reported for a total length of 4.5–5.7 cm at 10–50 m depth (Yoon, G-D. *et al.*, 1999), -70 to -50 dB was estimated for 2–4 cm specimens between 10–60 m depth (Torgersen and Kaartvedt, 2001). Reported target strength estimates for 2.3 and 3.5 cm specimens at 20–64 m depth varied from -60.3 to -60.8 dB at 38 kHz (Scoulding *et al.*, 2015). This is 0.5–1 dB higher than our results. In comparison with the reported multifrequency *TS* estimates of that study, our results were inside their range at 18 kHz, but 2–4.5 dB higher at high frequencies. One possible explanation for this discrepancy could be the effect of tilt angle on high frequencies (Fujino, T. *et al.*, 2009; Scoulding *et al.*, 2015). Variable fish behaviours during the *TS* measurement process could result in high variability of the tilt angles. However, our results imply a smaller difference than studies analysing other similar species (Benoit-Bird and Au, 2001).

Table 5.1 *Summary table with relevant TS estimates published in the last 20 years.*

Reference	Specie	Depth (m)	Length (cm)	TS (dB)				
				18 kHz	38 kHz	70 kHz	120 kHz	200 kHz
This study	*M. muelleri*	**17 - 137**	**2.7 - 4.3**	**-56.9**	**-59.8**	**-59.9**	**-60**	**-62**
Scoulding *et al* (2015)	*M. muelleri*	20 - 64	3.5	-53.6	-60.8	-	-62.9	-66.4
Scoulding *et al* (2015)	*M. muelleri*	20 - 64	2.3	-57.1	-60.3	-	-62	-65
Benoit-Bird and Au (2001)	*Myctophids*	0-200	3.7-6.1	-	-	-	-	-58.8
Sawada *et al* (2011)	*D. Theta*	150	5.4-5.5	-	-	-55.8	-	-
Torgersen and Kaartvedt (2001)	*M. muelleri*	10-60	2-4	-	-70 to -50	-	-	-
Yoon *et al* (1999)	*M. Muelleri*	10-30	4.5-5.7	-	-60.4 to -52.7	-	-	-
Yoon *et al* (1999)	*M. muelleri*	30-50	4.5-5.7	-	-59.2 to -52.5	-	-	-

5.2. Interpretation of the obtained TS values

To help interpret the obtained empirical results, the acoustic response of both species was modelled using specific theoretical approaches according to their swimbladder morphology. In the case of anchovy, the morphological parameters obtained here are in line with previously published values for the same (Doray et al., 2016) and similar species (Madirolas et al., 2016), corroborating the dual-chambered morphology of the swimbladder (**Figure 3.5**). Conversely, a comprehensive morphological description of pearlside swimbladder, unpublished for this species, was presented in this thesis based on 63 X-ray images. Given the smaller size and simpler shape of the swimbladder of pearlside, a gas-filled prolate spheroid approximation was used to simulate the acoustic response of this species.

In the case of anchovy, given its particular swimbladder morphology, a specific backscattering model was utilized to simulate its acoustic backscattering, based on the method of fundamental solutions (MFS) (Fairweather *et al.*, 2003; Pérez-Arjona *et al.*, 2018) for physostomous fish, simulating the swimbladder as two-chambered prolate spheroids (Andreeva, 1964; Weston, D. E., 1966; Love, 1978; Furusawa, M., 1988; Ye, 1997) plus the backbone. The MFS is a meshless method that has been proven useful in

estimating the measurable *TS* of fish and the contributions of the different inner structures of fish to *TS*, with similar or even greater accuracy than FEM or BEM, yet with reduced computational costs, a consideration that is especially important when examining fish models with additional fish structures to a swim bladder (e.g. a fish backbone) (Pérez-Arjona *et al.*, 2018). Moreover, in the specific case of the *ex situ* measurements of fish located inside the near-field, the use of the MFS permitted to increase the number of valid measurements by predicting the acoustic response of targets located at distances above 2.5 meters, instead of being limited by the critical range (4.5 meters). Most of the methods considered for the numerical evaluation of *TS* are solely valid when estimating *TS* in the far field (Jech *et al.*, 2015). Only the finite element method (FEM) (Lilja *et al.*, 2004) and the boundary element method (BEM) (Foote and Francis, 2002) provide alternatives at arbitrarily close distances, but they (especially FEM) have a high, and in some cases even unaffordable, computational cost.

The backscattering model also provided some rough explanation of the *TS* frequency response. According to the model, despite the similarity between the highest *TS* values across frequencies, the greater directivity of the higher frequencies (**Figure 4.14**) produced lower mean *TS* values when averaged over a range of tilt angles. In general terms, a rather good general agreement was obtained between the simulations and the empirical results (**Table 5.1**). The obtained *TS* trend with frequency, with slightly higher responses at lower frequencies (**Figure 4.13**), was typical of the beginning of the geometric region of a bladder-bearing fish species (Simmonds and Maclennan, 2005; Fernandes *et al.*, 2006). This pattern may prove useful in developing multi-frequency masks to discriminate anchovy from plankton and other (bladderless) pelagic species (Lezama-Ochoa *et al.*, 2011).

In the case of pearlside, there were no previous knowledge about its swimbladder morphology and thus, a comprehensive study was conducted to describe morphology of this species for a wide range of fish lengths. This study showed significant positive correlations between the length of pearlside and three of the studied morphological parameters (swimbladder length, volume and equivalent sphere radius) (**Figure 4.1**). The swimbladder volume relationship with fish length was already studied in a previous work (Scoulding *et al.*, 2015), although no clear relationship was reported. The positive

correlation between aspect ratio and fish length obtained here means that the swimbladder tends to be more elongated for smaller individuals. On a study focused on similar species (*M. japonicus*) (Fujino, T. *et al.*, 2009), positive correlations were described for swimbladder length and equivalent radius with fish length. However, no correlation between the aspect ratio and fish length was reported. The mean tilt angle of the swimbladder measured from the X-ray images (24º ± 7) agrees with the range of values published for similar (Fujino, T. *et al.*, 2009) and same species (Scoulding *et al.*, 2015), being 0–24.8º and 0–55º, respectively.

One of the remaining uncertainties for this species before this work was the effect that changes in depth associated with capture may have on swimbladder size. It is commonly assumed that pearlside, being a physoclist species, can absorb and secrete gas from the swimbladder to maintain a constant buoyancy while moving through the water column (Simmonds and MacLennan, 2005). However, it remained unclear whether pearlside can compensate the swimbladder volume during the trawling process. The swimbladder can be overexpanded and even damaged due to decompression (Nichol, D. G. and Chilton, E. A., 2006) or mechanical stress. When modelling swimbladder backscattering for this species, some studies used smaller sizes than those measured at the surface, compressed according to Boyle´s law, treating pearlside as a physostomous fish (Godø *et al.*, 2009; Scoulding *et al.*, 2015; Proud *et al.*, 2018). However, other studies used swimbladder dimensions measured at the surface and therefore considered pearlside as a strict physoclist (Kloser *et al.*, 2002; Fujino, T. *et al.*, 2009; Peña *et al.*, 2014; Peña and Calise, 2016). Furthermore, it remained unknown if pearlsides allow swimbladder gas to expand and compress with changes in depth in undisturbed conditions (Love *et al.*, 2004). Additionally, gas volume measurements at the surface are problematic due to the differences in pressure and temperature conditions between the surface and the depth of capture (Davison *et al.*, 2015b).

To address this issue, we simulated swimbladder backscattering response under different ranges of fish length, depth, tilt angle and swimbladder contraction rates. We then compared the simulated *TS* values to the experimental ones. The best model fit was achieved when a free ellipsoid was simulated (i.e. no volume compensation) with an incidence angle of 10º ± 5° (**Table 4.3**). These results support the hypothesis that fish

in the process of dying cannot compensate for the rapid pressure changes derived from capture. Therefore, the swimbladder volume seems to obey Boyle´s law (Godø *et al.*, 2009; Scoulding *et al.*, 2015; Proud *et al.*, 2018). Even if the physiological mechanisms lying behind these results may be more complex, it can now be assumed that the acoustic backscatter of captured pearlside must be modelled under a constant-mass assumption. Therefore, our modelling results support the hypothesis that the equivalent radius of the swimbladder at the mean depth of the trawls (84.5 m) would be 47% smaller than that measured at the surface (**Table 4.1**), which implies a 90% reduction of swimbladder volume.

There is still scope for increasing the knowledge about the behavior of pearlside swimbladder with depth. Our results support a lack of volume compensation during the trawl, but they do not shed any light about how the voluntary depth changes accomplished by this vertically migrant species affect its mean *TS* values. In this regard, further work should be done, measuring *TS* at different depths from submersible transducers such as the Wide-Band Autonomous Transceiver (WBAT) from Simrad (Kongsberg Maritime AS), approaching their distribution layers. One possible study would be to perform successive separated trawls of the higher and the lower part of a pearlside layer and comparing their mean *TS* values versus their body lengths.

The optimisation of the model parameters produced a mean tilt angle of 10° ± 5°. Therefore, one might conclude that the mean orientation of fish that best explains our data is -14° (± 9°) (obtained from subtracting the tilt angle of the swimbladder from the modelled optimal tilt angle). This would suggest that fish from the hauls used in this study were predominantly exhibiting a downwards swimming behaviour. However, mesopelagic species and in particular pearlside, can adopt a wide range of orientation angles along the diel cycle performing DVM (Bali and Aksnes, 1993; Godø *et al.*, 2009; Staby *et al.*, 2013). This behavior has been described in response to diverse hypothesised adaptive values (Staby *et al.*, 2013) including predator avoidance (Eggers, 1978; Hrabik *et al.*, 2006), optimal temperatures (Wurtsbaugh and Neverman, 1988) and improving feeding conditions (Neilson and Perry, 1990). Other factors that may induce variations of the tilt angle are time of day and time of year of data collection (Sawada, K. *et al.*, 1993), swimming behavior (Blaxter and Batty, 1990), schooling density (Foote, K.G.,

1980; Misund and Beltestad, 1996) and dispersion or position (Ona, 2003) in the water column. This suggests that the variability of data belonging to different trawls, as done in this study, might be greater than reflected here. However, as the effect that this variability has on the modelled *TS* increases with frequency and size, it is minimal at lower frequencies (Fujino, T. *et al.*, 2009; Scoulding *et al.*, 2015). This implies a minimal effect on the frequency typically used for biomass estimation (38 kHz).

5.3. Application of the TS values: estimation of biomass

For anchovy, despite the need for a precise *TS* value in the acoustic assessment of fish abundance, alongside the recommendation that an empirical *TS*-length data relationship be established whenever new data are collected (McClatchie, 2003), biomass estimates of this species in the Bay of Biscay have long been produced using *TS*-length relations from another species (herring) published more than three decades ago (ICES., 1982; Degnbol *et al.*, 1985). In response, this study has presented the first *TS* measurements for European anchovy at the frequency of 38 kHz used for assessment. The obtained b_{20} values at 38 kHz were 5-6 dB higher than those currently used by acoustic surveys in the assessment of European anchovy in the Bay of Biscay (Boyra *et al.*, 2013). Such values would represent a more than twofold decrease if applied to estimate the acoustic-based biomass of anchovy. However, the *TS* values were derived at a lower depth than is typical for anchovy during the daytime (i.e. the period at which acoustic surveys are conducted), especially for adults and larger juveniles that are subjected to nycthemeral migrations. Thus, given the expected decrease of *TS* with depth for anchovy and other physostomous species (Ona, 2003; Zhao *et al.*, 2008; Fässler *et al.*, 2009; Madirolas *et al.*, 2016), it is likely that the reduction in acoustic-based biomass will be somewhat lesser than that inferred solely from this work.

Therefore, further research is necessary to supplement the measurements obtained in this work at different depth ranges. The findings could then be combined with the present results to produce a thorough *TS*-length-depth relationship to update the acoustic-based assessment of this important species. This is a difficult objective to achieve using echosounders installed on a vessel, because it implies measuring the *TS*

during the day, when anchovies (specially adults) operate near the sea bottom (according to their nycthemeral migrations) and aggregate in schools, hampering the discrimination of single targets. One possible solution would involve the use of submersible echosounders inside the trawls (e.g., WBAT) at different trawl depths, hence allowing the determination of *TS*-length-depth relationships through the water column.

Regarding the biomass estimation of pearlside, this thesis provides for the first time, a *TS* versus length relationship. This is necessary and sufficient under the estimation procedure applied on the typical siwmbladder-bearing pelagic species, for whom the size of the swimbladder is larger than the acoustic wavelength hence belonging to the geometric region **Figure 5.1**.

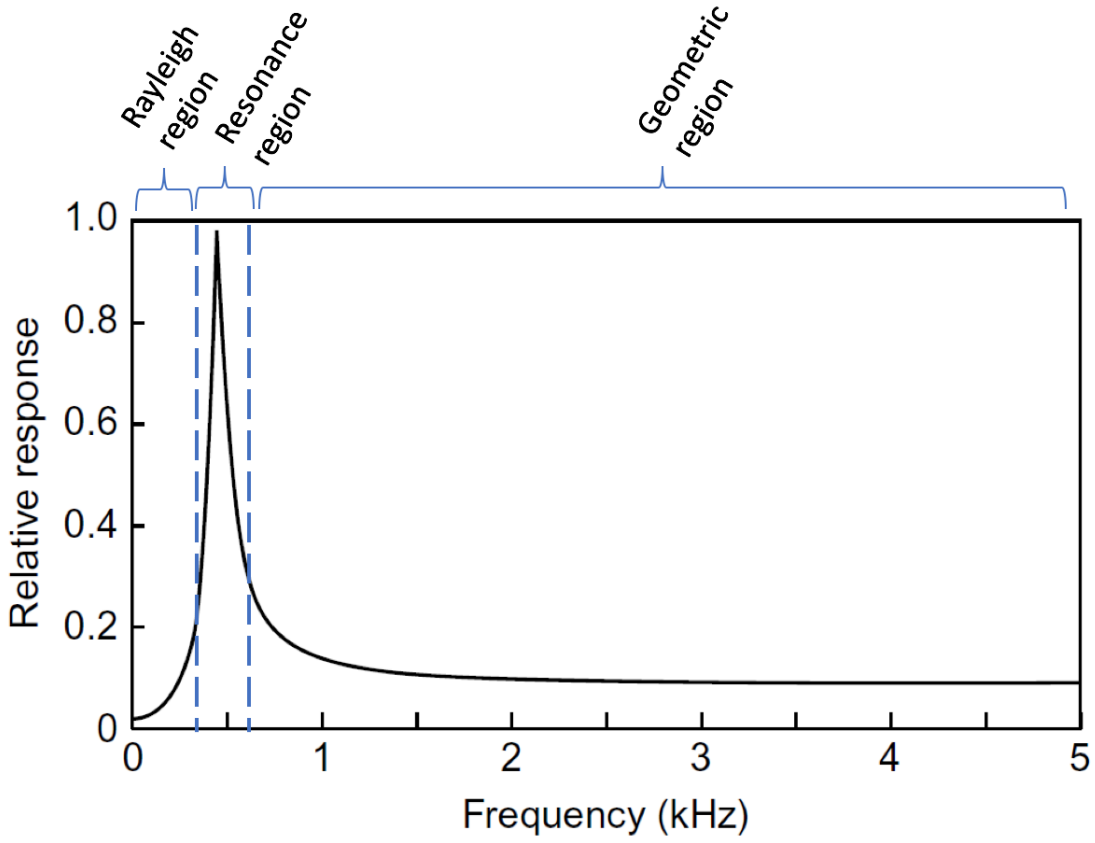

Figure 5.1 *Frequency dependence of scattering by a gas bubble. The intensity of the response has been normalised to 1 at resonance. It increases rapidly to a peak at the resonance frequency of the bubble, then it falls to a constant level at high frequencies (Simmonds and MacLennan, 2005).*

However, for pearlside, the particular range of sizes of the swimbladder plus the large range of distances to the transducer, cause its acoustic response to potentially cover a wider area of the frequency spectrum (from Rayleigh to the resonance and geometric regions), (**Figure 4.7**)hence causing a non-linear *TS* vs length relationship not present in (the normally larger) regular epipelagic species. This non-linearity, further complicated by potential changes of swimbladder wall elasticity and/or swimbladder volume with pressure (Davison *et al.*, 2015b), may induce bias on biomass estimations. To address it, instead of using one single *TS*-length (or *TS*-depth-length) relation for the whole water column, as it is done for small pelagics, biomass could be produced using different relations at different depth layers. Due to precisely the small size of their swimbladder and their long typical distance from the transducers, the exact shape and irregularities of the swimbladder are less important for small mesopelagic fishes such as pearlside, and thus, relatively reliable outcomes can be obtained from simple, idealized backscattering models as prolate-spheroid ones. Taking advantage of this aforementioned relative simplicity for modelling pearlside backscattering, empirical and modelled *TS*-length relationships could be combined to predict the *TS*-length relations at different depths, by modifying the empirical *TS* values using the model predictions. Then, biomass estimations could be produced using these measured and model-corrected *TS*-length relations per layer.

In sum, the results of this work have made an important improvement towards the assessment of these two species in such a different state of exploitation. Even if there is still much work to be done, I think that at least this thesis has contributed to outline the future research lines for both species, by providing some of the basic elements required to deliver absolute biomass estimations for them. Hopefully, we have also contributed to give one step further on the sustainable exploitation of these two important pelagic species.

5.4. Conclusions and thesis

The aim of this thesis was to provide the basic acoustic elements necessary to deliver unbiased abundance estimates of two small pelagic species in the Bay of Biscay. The objectives addressed to achieve this aim have delivered the following conclusions that have been divided per species:

For Muller´s pearlside the conclusions are:

- This thesis has provided the first *TS*-length relationships specific at six frequencies ranging from 18 to 200 kHz
- The swimbladder growth is positively related to the fish length, and is in agreement with the positive relationship between the *TS* and fish length.
- Theoretical simulations performed using the prolate spheroid approximation of the swimbladder using different contraction rates, were essential to understand the swimbladder volume changes during the trawling process.
- Even if it is considered a physoclist species, during the trawling process, the swimbladder volume is affected by Boyle´s law. Consequently, the actual swimbladder volume of pearlside at depth is smaller than the observed at the surface (i.e. X-ray images) and dependent on the depth of capture. This result has contributed to improve the basis of the backscattering theoretical modelling for pearlside.
- To overcome the non-linearity of TS-length relations affecting the biomass estimation of pearlside, abundance estimates should be given by combining theoretical and empirical *TS* measurements by depth layers.
- The swimbladder behaviour against depth variations needs further research to determine the detailed volume adaptation process.

For European anchovy the conclusions are:

- This thesis has provided the first *TS*-length relationships specific for European anchovy at the frequency used by assessment acoustic surveys (38 kHz) as well as the frequency response at typical frequencies (38, 120 and 200 kHz).
- The robustness of the *TS*-L values obtained in this work is supported by:
    - The wide range of sampled fish lengths that cover the seasonal mean size variation of the species along 7 years of study.
    - The significance of the linear relationship between TS and length and the consistency between *ex situ* and *in situ* data.
    - The consistency between theoretical and empirical results.
- Combining theoretical Methods of Fundamental Solutions (MFS) with the *ex situ* measurements was essential to reduce the bias associated to the short-range *TS* measurements, increasing the number of available data obtained from the *ex situ* experiments.
- The *TS*-length relationships used in the current acoustic surveys addressed for anchovy stock assessment, yield overestimated values for biomass. However, since the *TS*-length relationships obtained in this study, are valid only for the upper 25 meters of the water column, further research needs to be done on the *TS*-depth dependence before updating the currently used value for assessment.

Finally, considering these conclusions, the hypothesis has been confirmed, being the **thesis** that:

Acoustic data collected from *ex situ* and *in situ* experiments, subjected to cleaning, filtering and bias reduction methodologies, delivered robust species-specific *TS*-L relationships, that are essential for biomass estimation purposes. The use of acoustic backscattering theoretical models to interpret the empirical results, increases our understanding of the swimbladder behaviour under different conditions, essential to determine to what extent the empirical results can be used for biomass estimation purposes.

References

Anderson, T. R., Martin, A. P., Lampitt, R. S., Trueman, C. N., Henson, S. A., and Mayor, D. J. 2018. Quantifying carbon fluxes from primary production to mesopelagic fish using a simple food web model. ICES Journal of Marine Science, 76: 690–701.

Andreeva, I. B. 1964. Scattering of sound by air bladders of fish in deep sound-scattering ocean layers., 10: 20–24.

Bali, B. M., and Aksnes, D. L. 1993. Winter distribution and migration of the sound scattering layers, zooplankton and micronekton in Masfjorden, western Norway. Marine Ecology-Progress Series, 102: 35–35.

Ballón, M., Bertrand, A., Lebourges-Dhaussy, A., Gutiérrez, M., Ayón, P., Grados, D., and Gerlotto, F. 2011. Is there enough zooplankton to feed forage fish populations off Peru? An acoustic (positive) answer. Progress in Oceanography, 91: 360–381.

Barange, M., Hampton, I., and Soule, M. 1996. Empirical determination of in situ target strengths of three loosely aggregated pelagic fish species. ICES Journal of Marine Science: Journal du Conseil, 53: 225–232.

Barange, M., Bernal, M., Cercole, M., Cubillos, L., and Daskalov, G. 2009. de Moor (formerly Cunningham). CL, De Oliveira, JAA, Dickey-Collas, M., Gaughan, DJ, Hill, K., Jacobson, LD, Köster, FW, Massé, J., Ñiquen, M., Nishida, H., Oozeki, Y., Palomera, I., Saccardo, SA, Santojanni, A., Serra, R., Somarakis, S., Stratoudakis, Y., Uriarte, A., van der Lingen, CD, and A. Yatsu: 191–255.

Benoit-Bird, K. J., and Au, W. W. L. 2001. Target strength measurements of Hawaiian mesopelagic boundary community animals. The Journal of the Acoustical Society of America, 110: 812–819.

Blackman, S. S. 1986. Multiple Target Tracking with Radar Applications, Artech House, Massacheusetts.

Blaxter, J. H. S., and Batty, R. S. 1990. Swimbladder “behaviour” and target strength. Rapports et Proces-verbaux des Réunions du Conseil International pour l’Exploration de la Mer, 189: 233–244.

Blue, J. 1984. Physical calibration. Rapp. P.-v. Re’un. Cons. Int. Explor. Mer., 184: 19–24.

Boyra, G., Martínez, U., Cotano, U., Santos, M., Irigoien, X., and Uriarte, A. 2013. Acoustic surveys for juvenile anchovy in the Bay of Biscay: Abundance estimate as an indicator of the next year’s recruitment and spatial distribution patterns. ICES Journal of Marine Science, 70.

Boyra, G., Peña, M., Cotano, U., Irigoien, X., Rubio, A., and Nogueira, E. 2016. Spatial dynamics of juvenile anchovy in the Bay of Biscay. Fisheries Oceanography. http://doi.wiley.com/10.1111/fog.12170 (Accessed 12 July 2016).

Boyra, G., Moreno, G., Sobradillo, B., Pérez-Arjona, I., Sancristobal, I., Demer, D. A., and Handling editor: Purnima Ratilal. 2018. Target strength of skipjack tuna (Katsuwanus pelamis) associated with fish aggregating devices (FADs). ICES Journal of Marine Science, 75: 1790–1802.

Boyra, G., Moreno, G., Orue, B., Sobradillo, B., and Sancristobal, I. 2019. In situ target strength of bigeye tuna (Thunnus obesus) associated with fish aggregating devices. ICES Journal of Marine Science.

Cherel, Y., Ducatez, S., Fontaine, C., Richard, P., and Guinet, C. 2008. Stable isotopes reveal the trophic position and mesopelagic fish diet of female southern elephant seals breeding on the Kerguelen Islands. Marine Ecology Progress Series, 370: 239–247.

Conti, S., Demer, D., Soule, M., and Conti, J. 2005. An improved multiple-frequency method for measuring target strengths. ICES Journal of Marine Science, 62: 1636–1646.

Davison, P., Lara-Lopez, A., and Anthony Koslow, J. 2015a. Mesopelagic fish biomass in the southern California current ecosystem. Deep Sea Research Part II: Topical Studies in Oceanography, 112: 129–142.

Davison, P. C., Koslow, J. A., and Kloser, R. J. 2015b. Acoustic biomass estimation of mesopelagic fish: backscattering from individuals, populations, and communities. ICES Journal of Marine Science, 72: 1413–1424.

De Robertis, A., and Higginbottom, I. 2007. A post-processing technique to estimate the signal-to-noise ratio and remove echosounder background noise. ICES Journal of Marine Science: Journal du Conseil, 64: 1282–1291.

Degnbol, P., Lassen, H., and Staehr, K. J. 1985. In-situ determination of target strength of herring and sprat at 38 and 120 kHz. Dana, 5: 45–54.

Demer, D. A., Soule, M. A., and Hewitt, R. P. 1999. A multiple-frequency method for potentially improving the accuracy and precision of in situ target strength measurements. The Journal of the Acoustical Society of America, 105: 2359–2376.

Demer, D. a., Berger, L., Bernasconi, M., Bethke, E., Boswell, K. M., Chu, D., Domokos, R., *et al.* 2015. Calibration of acoustic instruments. ICES Cooperative Research Report, 326: 133.

Directorate-General for Maritime Affairs and Fisheries. 2018. Blue bioeconomy. Situation, report and perspectives. Director-General. http://www.eumofa.eu/documents/20178/84590/Blue+bioeconomy_Final.pdf (Accessed 18 July 2019).

Doray, M., Berger, L., Le Bouffant, N., Coail, J. Y., Vacherot, J. P., de La Bernardie, X., Morinière, P., *et al.* 2016. A method for controlled target strength measurements of pelagic fish, with application to European anchovy (\textit{Engraulis encrasicolus}). ICES Journal of Marine Science, 73: fsw084.

Echoview Software. 2013. . Echoview Software Pty Lt, Hobart, Tasmania, 7001, Australia.

Eggers, D. M. 1978. Limnetic feeding behavior of juvenile sockeye salmon in Lake Washington and predator avoidance 1. Limnology and Oceanography, 23: 1114–1125.

Fairweather, G., Karageorghis, A., and Martin, P. A. 2003. The method of fundamental solutions for scattering and radiation problems. Engineering Analysis with Boundary Elements, 27: 759–769.

Fässler, S. M. M., Fernandes, P. G., Semple, S. I. K., and Brierley, A. S. 2009. Depth-dependent swimbladder compression in herring Clupea harengus observed using magnetic resonance imaging. Journal of Fish Biology, 74: 296–303.

Fernandes, A., Masse, J., Iglesias, M., Diner, N., and Ona, E. 2006. The SIMFAMI project: species identification methods from acoustic multi-frequency information. Aberdeen, UK. 486 pp.

Fernandes, P. G., Copland, P., Garcia, R., Nicosevici, T., and Scoulding, B. 2016. Additional evidence for fisheries acoustics: small cameras and angling gear provide tilt angle distributions and other relevant data for mackerel surveys. ICES Journal of Marine Science, 73: 2009–2019.

Foote, K. G., and Francis, D. T. 2002. Comparing Kirchhoff-approximation and boundary-element models for computing gadoid target strengths. The Journal of the Acoustical Society of America, 111: 1644–1654.

Foote, K.G. 1980. Importance of the swimbladder in acoustic scattering by fish: A comparison of Gadoid and mackerel target strengths., 67: 2084–2089.

Foote K.G., Aglen A., and Nakken O. 1986. Measurement of fish target strength with a split-beam echo sounder, 80 (2).

Foote K.G., Knudsen, H. P., Vestnes, G., MacLennan, D.N., and Simmonds, E. J. 1987. Calibraton of acoustic instruments for fish density estimation: a practical guide. ICES Cooperative Research Report, 144. Copenhagen.

Francis, D. T., and Foote, K. G. 2003. Depth-dependent target strengths of gadoids by the boundary-element method. The Journal of the Acoustical Society of America, 114: 3136–3146.

Fujino, T., Sadayasu, K., Abe, K., Kidokoro, H., Tian, Y., Yasuma, H., and Miyashita, K. 2009. Swimbladder morphology and target strength of a mesopelagic fish, Maurolicus japonicus. Journal of marine acoustics society of Japan, 36: 241–249.

Furusawa, M. 1988. Prolate spheroidal models for predicting general trends of fish target strength. Journal of the Acoustic Society of Japan, 9.

Gartner, Jr., J. V. 1988. Escapement by fishes from midwater trawls:a case study using lanternfishes (Pisces:Myctophidae). Fish.Bull., 87: 213–222.

Gastauer, S., Scoulding, B., and Parsons, M. 2017. Estimates of variability of goldband snapper target strength and biomass in three fishing regions within the Northern Demersal Scalefish Fishery (Western Australia). Fisheries Research, 193: 250–262.

Gauthier, S., and Rose, G. A. 2001. Diagnostic tools for unbiased in situ target strength estimation. Canadian Journal of Fisheries and Aquatic Sciences, 58: 2149–2155.

Gjøsaeter, J., and Kawaguchi, K. 1980. A review of the world resources of mesopelagic fish. Food & Agriculture Org. http://books.google.com/books?hl=en&lr=&id=Zw0A_veImj8C&oi=fnd&pg=PA1&dq=%22been+intensified.+At+present,+it+seems+that+krill,+cephalopods+and+mesopelagic+fish%22+%22of+many+fish+families+will+fall+within+this+definition,+but+generally+the%22+%22fishing+fleet+of+the+U.S.S.R.+are+also+fishing+myctophids+off+West+Africa,+and+of+f%22+&ots=4FXe51iN74&sig=TCVOfeadUrS4yZ3TFJ8jENKxJDM (Accessed 27 September 2017).

Godø, O. R., Patel, R., and Pedersen, G. 2009. Diel migration and swimbladder resonance of small fish: some implications for analyses of multifrequency echo data. ICES Journal of Marine Science, 66: 1143–1148.

Godø, O. R., Handegard, N. O., Browman, H. I., Macaulay, G. J., Kaartvedt, S., Giske, J., Ona, E., *et al.* 2014. Marine ecosystem acoustics (MEA): quantifying processes in the sea at the spatio-temporal scales on which they occur. ICES Journal of Marine Science, 71: 2357–2369.

Gulland, J. A. 1983. Fish stock assessment: a manual of basic methods.

Gunderson, D. R. 1993. Surveys of fisheries resources. John Wiley & Sons.

Haslett, R. W. G. 1962. Determination of the acoustic backscattering patterns and cross sections of fish. British Journal of Applied Physics, 13: 349–357.

Heino, M., Porteiro, F. M., Sutton, T. T., Falkenhaug, T., Godø, O. R., and Piatkowski, U. 2011. Catchability of pelagic trawls for sampling deep-living nekton in the mid-North Atlantic. ICES Journal of Marine Science, 68: 377–389.

Henderson, M. J., and Horne, J. K. 2007. Comparison of in situ, ex situ, and backscatter model estimates of Pacific hake (Merluccius productus) target strength. Canadian Journal of Fisheries and Aquatic Sciences, 64: 1781–1794.

Hidalgo, M., and Browman, H. I. 2019. Contribution to the Themed Section:'Mesopelagic resources'.

Hodgson, W. C. 1950. Echo-Sounding and the Pelagic Fisheries, Fishery Investigations, Series II, Vol.

Hodgson, W. C., and Fridriksson, A. 1955. Report on echo-sounding and asdic for fishing purposes. Conseil permanent international pour l'exploration de la mer.

Horne, J. K. 2000. Acoustic approaches to remote species identification: a review. Fisheries oceanography, 9:4: 356–371.

Hrabik, T. R., Jensen, O. P., Martell, S. J. D., Walters, C. J., and Kitchell, J. F. 2006. Diel vertical migration in the Lake Superior pelagic community. I. Changes in vertical migration of coregonids in response to varying predation risk. Canadian Journal of Fisheries and Aquatic Sciences, 63: 2286–2295.

Ibaibarriaga, L., Fernández, C., Uriarte, A., and Roel, B. A. 2008. A two-stage biomass dynamic model for Bay of Biscay anchovy: a Bayesian approach. ICES Journal of Marine Science, 65: 191–205.

ICES. 1982. Report of the 1982 Planning Group on ICES-Coordinated Herring and Sprat Acoustic Surveys. ICES Document CM 1982/H: 04.

ICES. 2013. ICES WGACEGG REPORT 2013 Working Group on Acoustic and Egg Surveys for Sardine and Anchovy in ICES Areas VIII and IX (WGACEGG) By Correspondence and 25 – 29 November 2013. ICES CM, SSGESST:20: 131.

ICES. 2014. WOrking Group for the Bay of Biscay and the Iberian waters Ecoregion (WGBIE) 7-13 May 2014 Lisbon, Portugal. http://www.ices.dk/sites/pub/Publication%20Reports/Expert%20Group%20Report/acom/2014/WGBIE/01%20WGBIE%20report%202014.pdf (Accessed 18 July 2019).

ICES. 2015. Report of the Working Group on Southern Horse Mackerel, Anchovy and Sardine (WGHANSA). Lisbon, Portugal.

ICES. 2017. Report of the Working Group on Southern Horse Mackerel, Anchovy and Sardine (WGHANSA), 24–29 June 2017, Bilbao, Spain.

Irigoien, X., Klevjer, T. A., Røstad, A., Martinez, U., Boyra, G., Acuña, J. L., Bode, A., *et al.* 2014. Large mesopelagic fishes biomass and trophic efficiency in the open ocean. Nature Communications, 5. http://www.nature.com/doifinder/10.1038/ncomms4271 (Accessed 6 February 2018).

Itaya, K., Fujimori, Y., Shimizu, S., Komatsu, T., and Miura, T. 2007. Effect of towing speed and net mouth size on catch efficiency in framed midwater trawls. Fisheries Science, 73: 1007–1016.

Jech, J. M., Horne, J. K., Chu, D., Demer, D. A., Francis, D. T., Gorska, N., Jones, B., *et al.* 2015. Comparisons among ten models of acoustic backscattering used in aquatic ecosystem research. The Journal of the Acoustical Society of America, 138: 3742–3764.

Jennings, S., and Collingridge, K. 2015. Predicting Consumer Biomass, Size-Structure, Production, Catch Potential, Responses to Fishing and Associated Uncertainties in the World's Marine Ecosystems. PLOS ONE, 10: e0133794.

Kaartvedt, S., Staby, A., and Aksnes, D. 2012. Efficient trawl avoidance by mesopelagic fishes causes large underestimation of their biomass. Marine Ecology Progress Series, 456: 1–6.

Kang, D., and Hwang, D. 2003. Ex situ target strength of rockfish (Sebastes schlegeli) and red sea bream (Pagrus major) in the Northwest Pacific. ICES Journal of Marine Science, 60: 538–543.

Kang, D., Cho, S., Lee, C., Myoung, J.-G., and Na, J. 2009. Ex situ target-strength measurements of Japanese anchovy (Engraulis japonicus) in the coastal Northwest Pacific. ICES Journal of Marine Science, 66: 1219–1224.

Kimura, K. 1929. On the detection of fish-groups by an acoustic method. Journal of the Imperial Fisheries Institute, Tokyo, 24: 41–45.

Kloser, R. J., Ryan, T., Sakov, P., Williams, A., and Koslow, J. A. 2002. Species identification in deep water using multiple acoustic frequencies. Canadian Journal of Fisheries and Aquatic Sciences, 59: 1065–1077.

Kloser, R. J., Ryan, T. E., Young, J. W., and Lewis, M. E. 2009. Acoustic observations of micronekton fish on the scale of an ocean basin: potential and challenges. ICES Journal of Marine Science, 66: 998–1006.

Kloser, R. J., Ryan, T. E., Keith, G., and Gershwin, L. 2016. Deep-scattering layer, gas-bladder density, and size estimates using a two-frequency acoustic and optical probe. ICES Journal of Marine Science: Journal du Conseil, 73: 2037–2048.

Koslow, J. A., Kloser, R. J., and Williams, A. 1997. Pelagic biomass and community structure over the mid-continental slope off southeastern Australia based upon acoustic and midwater trawl sampling. Marine Ecology Progress Series: 21–35.

Latour, R. J., Brush, M. J., and Bonzek, C. F. 2003. Toward ecosystem-based fisheries management: strategies for multispecies modeling and associated data requirements. Fisheries, 28: 10–22.

Lezama-Ochoa, A., Ballón, M., Woillez, M., Grados, D., Irigoien, X., and Bertrand, A. 2011. Spatial patterns and scale-dependent relationships between macrozooplankton and fish in the Bay of Biscay: an acoustic study. Marine Ecology Progress Series, 439: 151–168.

Lilja, J., Marjomäki, T. J., Jurvelius, J., Rossi, T., and Heikkola, E. 2004. Simulation and experimental measurement of side-aspect target strength of Atlantic salmon (Salmo salar) at high frequency. Canadian Journal of Fisheries and Aquatic Sciences, 61: 2227–2236.

Love, R. H. 1971. Dorsal-aspect target strength of an individual fish. The Journal of the Acoustical Society of America, 49: 816–823.

Love, R. H. 1977. Target strength of an individual fish at any aspect. The Journal of the Acoustical Society of America, 62: 1397.

Love, R. H. 1978. Resonant acoustic scattering by swimbladder-bearing fish [a)]. The Journal of the Acoustical Society of America, 64: 571–580.

Love, R. H., Fisher, R. A., Wilson, M. A., and Nero, R. W. 2004. Unusual swimbladder behavior of fish in the Cariaco Trench. Deep Sea Research Part I: Oceanographic Research Papers, 51: 1–16.

Macaulay, G. J., Peña, H., Fässler, S. M., Pedersen, G., and Ona, E. 2013. Accuracy of the Kirchhoff-approximation and Kirchhoff-ray-mode fish swimbladder acoustic scattering models. PloS one, 8: e64055.

MacLennan, D., Fernandes, P. G., and Dalen, J. 2002. A consistent approach to definitions and symbols in fisheries acoustics. ICES Journal of Marine Science, 59: 365–369.

MacLennan, D. N., and Menz, A. 1996. Interpretation of in situ target-strength data. ICES Journal of Marine Science: Journal du Conseil, 53: 233–236.

Madirolas, A., Membiela, F. a., Gonzalez, J. D., Cabreira, A. G., dell'Erba, M., Prario, I. S., and Blanc, S. 2016. Acoustic target strength (TS) of argentine anchovy (*Engraulis anchoita*): the nighttime scattering layer. ICES Journal of Marine Science: Journal du Conseil: fsw185.

Madureira, L., Ward, P., and Atkinson, A. 1993. Differences in backscattering strength determined at 120 and 38 kHz for three species of Antarctic macroplankton. Marine Ecology Progress Series: 17–24.

Marshall N. B. 1960. Swimbladder Structure of Deep-Sea Fishes in Relation to Their Systematics and Biology. University Press, London, Cambridge. 121 pp.

Massé, J. 1996. Acoustic observations in the Bay of Biscay: schooling, vertical distribution, species assemblages and behaviour. Scientia Marina, 60: 227–234.

Massé, J., Duhamel, E., Petitgas, P., Doray, M., and Huret, M. 2018. Pelagic survey series for sardine and anchovy in ICES subareas 8 and 9 – Towards an ecosystem approach. Massé, J., Uriarte, A., Manuel Angélico, M., and Carrera, P. (Eds.). http://www.ices.dk/sites/pub/Publication%20Reports/Cooperative%20Research%20Report%20(CRR)/CRR%20332.pdf (Accessed 29 October 2019).

McClatchie, S. 2003. A requiem for the use of 20log10Length for acoustic target strength with special reference to deep-sea fishes. ICES Journal of Marine Science, 60: 419–428.

Medwin, H., and Clay, C. S. 1998. Fundamentals of acoustical oceanography. Applications of modern acoustics. Academic Press, Boston. 712 pp.

Misund, O. A., and Beltestad, A. K. 1996. Target-strength estimates of schooling herring and mackerel using the comparison method. ICES Journal of Marine Science, 53: 281–284.

Misund, O. A. 1999. Dynamics of pelagic fish distribution and behaviour: effects on fisheries and stock assessment. Fishing News Books.

Mitson, R., and Wood, R. 1961. An automatic method of counting fish echoes. ICES Journal of Marine Science, 26: 281–291.

Murase, H., Ichihara, M., Yasuma, H., Watanabe, H., Yonezaki, S., Nagashima, H., Kawahara, S., *et al.* 2009. Acoustic characterization of biological backscatterings in the Kuroshio-Oyashio inter-frontal zone and subarctic waters of the western North Pacific in spring. Fisheries Oceanography, 18: 386–401.

Murase, H., Kawabata, A., Kubota, H, Nakagami, M, Amakasu, K., Abe, K., Miyashita, K., *et al.* 2011. Effect of depth-dependent target strength on biomass estimation of japanese anchovy. Journal of Marine Science and Technology, 19: 267–272.

Nakken, O., and Olsen, K. 1977. Target strength measurements of fish. Ices.

Neilson, J. D., and Perry, R. I. 1990. Diel Vertical Migrations of Marine Fishes: an Obligate or Facultative Process? *In* Advances in Marine Biology, pp. 115–168. Ed. by J. H. S. Blaxter

and A. J. Southward. Academic Press. http://www.sciencedirect.com/science/article/pii/S006528810860200X.

Nichol, D. G., and Chilton, E. A. 2006. Recuperation and behaviour of Pacific cod after barotrauma. ICES Journal of Marine Science, 63: 83–94.

O'Driscoll, R. L., Gauthier, S., and Devine, J. A. 2009. Acoustic estimates of mesopelagic fish: as clear as day and night? ICES Journal of Marine Science, 66: 1310–1317.

Ona, E. 1990. Physiological factors causing natural variations in acoustic target strength of fish. Journal of the Marine Biological Association of the United Kingdom, 70: 107–127.

Ona, E., and Barange, M. 1999. Single target recognition. CRR, Methodology for Target Strength Measurement, 235. http://www.ices.dk/sites/pub/Publication%20Reports/Cooperative%20Research%20Report%20(CRR)/crr235/CRR235.pdf (Accessed 28 February 2017).

Ona, E. 2003. An expanded target-strength relationship for herring. ICES Journal of Marine Science, 60: 493–499.

Pakhomov, E., Yamamura, O., Advisory Panel on Micronekton Sampling Inter-calibration Experiment, and North Pacific Marine Science Organization. 2010. Report of the Advisory Panel on Micronekton Sampling Inter-calibration Experiment. North Pacific Marine Science Organization (PICES), Sidney, B.C.

Peltonen, H., and Balk, H. 2005. The acoustic target strength of herring (Clupea harengus L.) in the northern Baltic Sea. ICES Journal of Marine Science, 62: 803–808.

Peña, M., Olivar, M. P., Balbín, R., López-Jurado, J. L., Iglesias, M., Miquel, J., and Jech, J. M. 2014. Acoustic detection of mesopelagic fishes in scattering layers of the Balearic Sea (western Mediterranean). Canadian Journal of Fisheries and Aquatic Sciences, 71: 1186–1197.

Peña, M., and Calise, L. 2016. Use of SDWBA predictions for acoustic volume backscattering and the Self-Organizing Map to discern frequencies identifying Meganyctiphanes norvegica from mesopelagic fish species. Deep Sea Research Part I: Oceanographic Research Papers, 110: 50–64.

Peña, M. 2019. Mesopelagic fish avoidance from the vessel dynamic positioning system. ICES Journal of Marine Science. https://academic.oup.com/icesjms/advance-article/doi/10.1093/icesjms/fsy157/5181375 (Accessed 17 April 2019).

Pérez-Arjona, I., Godinho, L., and Espinosa, V. 2018. Numerical Simulation of Target Strength Measurements from Near to Far Field of Fish Using the Method of Fundamental Solutions. Acta Acustica united with Acustica, 104: 25–38.

Pikitch, E. K., Santora, C., Babcock, E. A., Bakun, A., Bonfil, R., Conover, D. O., Dayton, P., *et al.* 2004. Ecosystem-Based Fishery Management. Science, 305: 346–347.

Prario, I., Gonzalez, J., Madirolas, A., and Blanc, S. 2015. A prolate spheroidal approach for fish target strength estimation: modeling and measurements. Acta Acustica united with Acustica, 101: 928–940.

Prellezo, R. 2018. Exploring the economic viability of a mesopelagic fishery in the Bay of Biscay. ICES Journal of Marine Science, 76: 771–779.

Prosch, R.M, Hulley, P.A., and Cruickshank, R.A. 1989. Mesopelagic fish and some other forage species. *In* Oceans of Life off Southern Africa, Payne, A. I. L. and R. J. M. Crawford, pp. 130–135. Cape Town.

Proud, R., Cox, M. J., and Brierley, A. S. 2017. Biogeography of the Global Ocean's Mesopelagic Zone. Current Biology, 27: 113–119.

Proud, R., Handegard, N. O., Kloser, R. J., Cox, M. J., Brierley, A. S., and Handling editor: David Demer. 2018. From siphonophores to deep scattering layers: uncertainty ranges for the estimation of global mesopelagic fish biomass. ICES Journal of Marine Science. https://academic.oup.com/icesjms/advance-article/doi/10.1093/icesjms/fsy037/4978316 (Accessed 8 May 2018).

R: A language and environment for statistical computing. 2017. . R Core Team, Vienna, Austria.

Santos, M., Uriarte, A., Boyra, G., and Ibaibarriaga, L. 2018. Pelagic survey series for sardine and anchovy in ICES subareas 8 and 9 – Towards an ecosystem approach. Massé, J., Uriarte, A., Manuel Angélico, M., and Carrera, P. (Eds.). http://www.ices.dk/sites/pub/Publication%20Reports/Cooperative%20Research%20Report%20(CRR)/CRR%20332.pdf (Accessed 29 October 2019).

Sassa, C., Kawaguchi, K., Kinoshita, T., and Watanabe, C. 2002. Assemblages of vertical migratory mesopelagic fish in the transitional region of the western North Pacific. Fisheries Oceanography, 11: 193–204.

Savinykh, V.F., and Baytalyuk, A.A. 2010. New data on biology of pearlfish Maurolicus imperatorius (Sternopthychidae) from the Emperor Seamount Chain. Journal of Ichthyology, 50: 148–158.

Sawada, K., Furusawa, M., and Williamson, N. J. 1993. Conditions for the precise measurement of fish target strength in situ. Fish. Sci. (Tokyo), 20: 15–21.

Sawada, K., Furusawa, M., and Williamson, N. J. 1993. Conditions for the precise measurement of fish target strength in situ. The Journal of the Marine Acoustics Society of Japan, 20: 73–79.

Sawada, K., Takahashi, H., Abe, K., Ichii, T., Watanabe, K., and Takao, Y. 2009. Target-strength, length, and tilt-angle measurements of Pacific saury (Cololabis saira) and Japanese anchovy (Engraulis japonicus) using an acoustic-optical system. ICES Journal of Marine Science, 66: 1212–1218.

Scoulding, B., Chu, D., Ona, E., and Fernandes, P. G. 2015. Target strengths of two abundant mesopelagic fish species. The Journal of the Acoustical Society of America, 137: 989–1000.

Simmonds, E. J., and MacLennan, D. N. 2005. Fisheries acoustics: theory and practice. Fish and aquatic resources series. Blackwell Science, Oxford ; Ames, Iowa. 437 pp.

Simmonds, J. E., and Maclennan, D. N. 2005. Fisheries Acoustics Theory and Practice. Second Edition. Chapman & Hall, New York: 472pp.

Smith, A., Fulton, E., Hobday, A., Smith, D., and Shoulder, P. 2007. Scientific tools to support the practical implementation of ecosystem-based fisheries management. ICES Journal of Marine Science, 64: 633–639.

Soule, M., Barange, M., and Hampton, I. 1995. Evidence of bias in estimates of target strength obtained with a split-beam echo-sounder. ICES Journal of Marine Science: Journal du Conseil, 52: 139–144.

Soule, M., Hampton, I., and Barange, M. 1996. Potential improvements to current methods of recognizing single targets with a split-beam echo-sounder. ICES Journal of Marine Science: Journal du Conseil, 53: 237–243.

Soule, M. 1997. Performance of a new phase algorithm for discriminating between single and overlapping echoes in a split-beam echosounder. ICES Journal of Marine Science, 54: 934–938.

Springmann, M., Clark, M., Mason-D'Croz, D., Wiebe, K., Bodirsky, B. L., Lassaletta, L., de Vries, W., *et al.* 2018. Options for keeping the food system within environmental limits. Nature, 562: 519.

Staby, A., Srisomwong, J., and Rosland, R. 2013. Variation in DVM behaviour of juvenile and adult pearlside (*Maurolicus muelleri*) linked to feeding strategies and related predation risk. Fisheries Oceanography, 22: 90–101.

Strasberg, M. 1953. The pulsation frequency of nonspherical gas bubbles in liquids., 25: 536–537.

Sund, O. 1935. Echo sounding in fishery research. Nature, 135: 953.

Torgersen, T., and Kaartvedt, S. 2001. In situ swimming behaviour of individual mesopelagic fish studied by split-beam echo target tracking. ICES Journal of Marine Science, 58: 346–354.

Trenkel, V. M., Ressler, P. H., Jech, M., Giannoulaki, M., and Taylor, C. 2011. Underwater acoustics for ecosystem-based management: state of the science and proposals for ecosystem indicators. Marine Ecology Progress Series, 442: 285–301.

Tungate, Ds. 1958. Echo-sounder surveys in the autumn of 1956. HM Stationery Office.

Weimer, R., and Ehrenberg, J. 1975. Analysis of threshold-induced bias inherent in acoustic scattering cross-section estimates of individual fish. Journal of the Fisheries Board of Canada, 32: 2547–2551.

Weston, D. E. 1966. Sound propagation in the presence of bladder fish. *In* Underwater Acoustics, V. M. Albers, pp. 55–58. Plenum, New York.

WGACEGG. (n.d.). . http://www.ices.dk/community/groups/Pages/WGACEGG.aspx (Accessed 29 October 2019).

Whitehead, P.J.P, and Blaxter, J.H.B. 1989. Swimbladder form in the clupeoid fishes., 97: 299–372.

Williams, A., Koslow, J., Terauds, A., and Haskard, K. 2001. Feeding ecology of five fishes from the mid-slope micronekton community off southern Tasmania, Australia. Marine Biology, 139: 1177–1192.

Wood, A., Smith, F., and McGeachy, J. 1935. A magnetostriction echo depth-recorder. Institution of Electrical Engineers-Proceedings of the Wireless Section of the Institution, 10: 80–93.

Wurtsbaugh, W. A., and Neverman, D. 1988. Post-feeding thermotaxis and daily vertical migration in a larval fish. Nature, 333: 846–848.

Yasuma, H., Sawada, K., Takao, Y., Miyashita, K., and Aoki, I. 2009. Swimbladder condition and target strength of myctophid fish in the temperate zone of the Northwest Pacific. ICES Journal of Marine Science, 67: 135–144.

Ye, Z. 1997. Low-frequency acoustic scattering by gas-filled prolate spheroids in liquids. The Journal of the Acoustical Society of America, 101: 1945–1952.

Yoon, G-D., Shin, H-H., and Hwang, K-S. 1999. Target strength of fishes for estimating biomass - Distribution characteristics and target strength measurement of micronektonic fish, Maurolicus muelleri in the East Sea., 35: 404–409.

Zare, P., Kasatkina, S. M., Shibaev, S. V., and Fazli, H. 2017. In situ acoustic target strength of anchovy kilka (Clupeonella engrauliformis) in the Caspian Sea (Iran). Fisheries Research, 186: 311–318.

Zhao, X. 1996. Target strength of herring (Clupea harengus L.) measured by the split-beam tracking method. Department of Fisheries and Marine Biology: 103.

Zhao, X., Wang, Y., and Dai, F. 2008. Depth-dependent target strength of anchovy (Engraulis japonicus) measured in situ. ICES Journal of Marine Science, 65: 882–888.